ZINC GRANULOCYTES IN THE OYSTER, *OSTREA ANGASI*

By

DAVID G. LYTTON M.B., Ch.B., F.R.C.P.A.

Being a thesis submitted in part fulfilment
of the requirements for the degree
of Master of Environmental Studies
at the University of Tasmania.

DECEMBER, 1979

This thesis contains no material which has been accepted for the award of any other degree or diploma in any other university, and to the best of my knowledge contains no copy or paraphrase of material previously published or written by another person, except when due reference is made in the text.

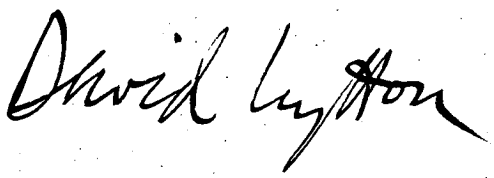

David Lytton,
University of Tasmania,

December, 1979.

ULRIKEI ANGO NIKOLAE

LIBERIS MEIS

QUI RES FUTURAS ILLUMINENT

ACKNOWLEDGEMENTS

I wish to thank the following people, who have helped in many ways to bring this project to fruition.

University Departments

(a)	Environmental Studies	Dr. Richard Jones, Director.
		Dr. John Todd, Supervisor.
(b)	Zoology	Dr. David Ritz, Supervisor.
		Dr. Yadviga Bick, Supervisor.
		Mr. Jerry Lim.
(c)	Pathology	Professor Roland Rodda
		Evelyn Trout, Electron Microscopist.
		Susan Dixon.
(d)	Clinical Photography	Mr. David Lees.
(e)	Central Science Laboratory	Mr. Wieslaw Jablonski, Microprobe Analyst.
		Mr. Alan Eastgate, Electronics Engineer.
(f)	Chemistry	Mr. John Kosmeyer.
(g)	Agricultural Science	Mr. Ralph Cruickshank.

State Government Departments

(a) Department of the Environment

Mr. Geoffrey Ayling, Senior Chemist.

Mr. Frank Brown, Chemist.

Mr. Bruce Hocking.

(b) Fisheries Development Authority
Marine Research Laboratory

Mr. Trevor Dix, Senior Marine Biologist.

Mr. John Thomson, Marine Chemist.

Commonwealth Scientific and Industrial Research Organisation (CSIRO)

(a) Division of Food Research, Hobart

Dr. June Olley, Director.

Mr. Stephen Thrower.

(b) Division of Mineralogy, Sydney

Mr. Lee Brunckhorst, Microprobe Analyst.

The Australian Museum, Sydney

Dr. Winston Ponder, Curator of Molluscs.

Electrolytic Zinc Co. of Australasia Ltd.

Environmental Services Division

Mr. Rodney Cooper.

Mr. David Langlois.

CONTENTS

	Page.
SYNOPSIS	1
INTRODUCTION	4
OBJECTIVES	9
LITERATURE REVIEW	
Specific metal bearing granulocytes	10
MATERIAL	
The oysters and sites of collection	19
METHODS	
Tissue fixation	23
Scanning electron microscopy-electron probe microanalysis	26
Transmission electron microscopy	27
Light microscopy	28
Histochemistry and histology	28
Atomic absorption spectrophotometry	31
RESULTS	
Light microscopy	32
Transmission electron microscopy	70
Correlative microscopy and X-ray analysis	88
DISCUSSION AND CONCLUSIONS	
Résumé of methods	111
Prospectus	118
Zinc granulocytes and pollution	119
REFERENCES	124
APPENDIX	
An ecological model of zinc accumulation in the oyster	128
Microorganisms and zinc uptake in the oyster	133
The function of the zinc granulocyte	135
References	137

SYNOPSIS

Man's activities impose an increasingly heavy burden of metals on the marine environment. An excess of the transitional element zinc, which is essential for life, is suspected of causing ecological disruption. Before stable zinc can be regarded as a pollutant, harm to marine organisms will have to be demonstrated.

Histochemical and physical methods of analysis have been applied to the tissues of the native oyster, Ostrea angasi to determine whether or not the accumulation of zinc is associated with any cytopathological effect or histological change.

Oysters were gathered from the south and east coasts of Tasmania and compared with specimens collected from sites in the Derwent Estuary, where commercially grown oysters containing up to 10% of their dry weight as zinc, had previously been responsible for cases of food poisoning.

Tissue was prepared for light and electron microscopy by fixation in glutaraldehyde saturated with hydrogen sulphide. The concentration of zinc in the visceral mass was determined by atomic absorption spectrophotometry and zinc in adjacent tissue located histochemically by the sulphide-silver and alkaline-dithizone techniques. Resin-embedded thin sections of the intestinal tract were examined in a transmission electron microscope and both thin and thick sections were analysed in a combined scanning electron

microscope-electron probe microanalyser.

Zinc was located intracellularly as electron dense granules 1 μm in diameter. In the scanning electron microscope these granules were electron reflective and appeared as bright spherules, which in the transmission electron microscope had a ring-like structure. The presence of zinc in these granules was confirmed by energy dispersive and wavelength dispersive systems of X-ray analysis.

Zinc-laden granulocytes were widely distributed throughout the connective tissue and vascular spaces and concentrated beneath the epithelia of the intestinal tract, palps, digestive diverticula, gills and mantle. The granulocytes were also conspicuous within these epithelia. There was no evidence of a pathological tissue reaction, although in some instances large collections of granulocytes beneath the intestinal epithelium were associated with abundant fibrous connective tissue.

The concentration of zinc in the visceral mass was the same order of magnitude (10^4 μg g dry weight^{-1}) in all specimens. Circumstantial evidence suggests that each specimen came from a 'high-zinc' environment, despite their wide geographical separation. Specimens would have to be obtained from a proven 'low-zinc' environment before definite conclusions can be drawn from the observed histological features.

The function of the zinc granulocyte is in debate. One school of thought claims that the cell is part of a

metal detoxification system, whereas others believe that the cell plays a physiological role in the cellular defence mechanism of the host against injury. The precise function of these cells will have to be established before definitive statements can be made about contamination of oyster tissue by zinc.

INTRODUCTION

Much of man's industrial activity is concerned with the extraction of metal elements from their native ore and their subsequent transformation into manufactured 'goods'. This process is amplified by the technique of mass production and the demands of a burgeoning world population. The industrial process is never 100% efficient and although most metals remain sequestered within man's economic system, a small percentage inevitably escapes into the environment. Ultimately it is the marine environment with its attendant organisms that bears the brunt of this burden.

Tasmania provides an ideal setting in which to investigate the relationship between one of these metals and the marine ecosystem. Zinc is mined as the ore sphalerite (ZnS) in the western part of the State and shipped to Hobart where it is refined to the pure metal by an electrolytic process (Middleton & Patterson, 1977). Zinc and other heavy metals are discharged as metallurgical waste into the Derwent River and the zinc refinery has for many years been the major source of zinc in the Derwent Estuary (Bloom & Ayling, 1977).

Oysters accumulate zinc (Phillips, 1977) although this was not so generally known when oyster leases were established in the Derwent Estuary in the late 1960's. The

Pacific oyster, Crassostrea gigas, was introduced into Tasmania from Japan in the late 1940's and it was this species, cultivated in Ralphs Bay (Fig.1) and marketed in 1970, that caused an outbreak of food poisoning in Hobart (Thrower & Eustace, 1973). People consuming the oysters complained of nausea and vomiting. At first a bacterial cause was suspected, but in 1973 Thrower & Eustace of the CSIRO Food Research Unit established that the symptoms were caused by high concentrations of zinc in the tissue, individual oysters containing up to 10% of their dry weight as zinc.

Squash preparations of oyster tissue, freeze-dried on glass slides were sent to the CSIRO Division of Mineralogy in Sydney and examined by electron probe micro-analysis (EPMA). Substantial amounts of zinc were detected throughout the soft tissue with the largest amount localized in the gills, heart, mantle and labial palps, a moderate amount in the hind gut and only a small amount in the adductor muscle (Brunckhorst, pers. comm.).

The numerical study of Ratkowsky et al., (1974), showed that for both the Pacific oyster Crassostrea gigas and the native oyster Ostrea angasi, those growing in Ralphs Bay and containing high concentrations of zinc, were larger than oysters having low zinc concentrations and growing in areas remote from urban centres and industrial activity.

The Ralphs Bay incident prompted a study of other commercial oyster beds in Tasmania and in 1974 Ayling of the Department of the Environment reported a correlation between the concentration of zinc in the Pacific oysters,

grown in the Tamar River, and the concentration of zinc in the sediment. He suggested that zinc was assimilated largely from ingested particles of sediment in suspension.

Alkaline phosphatase, a zinc metalloenzyme, was demonstrated in the oyster Crassostrea virginica by Wolfe (1970b), who concluded from dialysis experiments that zinc enzymes account for only a small portion of the total zinc in oysters. Coombs (1972) came to the same conclusion, but suggested that this apparent excess of dialysable zinc (95% of the total zinc) is a consequence of the high levels of calcium found in the tissues. He postulated a connection between zinc metabolism and shell formation. There is competition in the uptake of calcium and zinc in many species (Coombs, 1972) and this hypothesis is supported by the observation that the shells of the Ralphs Bay oysters had been abnormally soft (Thrower, pers. comm.).

Attempts were made to fractionate the zinc in the Ralphs Bay oysters and live specimens were sent to Dr. G. Nickless at the University of Bristol, who reported (1975) that he was unable to separate the zinc into discrete organic compounds by column chromatography, because the zinc load had 'swamped' his apparatus (Olley, pers. comm.).

My interest in environmental toxicology led me to ask the question: Is the high tissue concentration of zinc in the Ralphs Bay oysters associated with any histopathological reaction? Under the terms of the Tasmanian Environment Protection Act, 1973, a pollutant is any substance which causes contamination of the environment so as:

'to cause a condition that is detrimental or

hazardous or likely to be detrimental or hazardous to:-

(i) human health, safety, or welfare;

(ii) animals, plants, or microbes; or

(iii) property.'

The Ralphs Bay incident had established zinc as a pollutant in the first sense of the definition, namely its adverse effect on human health, however the role of zinc in human metabolism is not the concern of this thesis. The purpose of this study is to evaluate techniques for the assessment of zinc content and to see whether the zinc is acting as a pollutant, in the second sense of the definition, namely the demonstration of a detrimental effect on the tissues of the native oyster, Ostrea angasi. This requirement of demonstrating harm to organisms is echoed in the definition of marine pollution agreed upon in 1970 by the United Nations Group of Experts on the Scientific Aspects of Marine Pollution (GESAMP) as quoted by Barros and Johnston, (1974).

> The introduction by man, directly or indirectly, of substances or energy into the marine environment (including estuaries) resulting in such deleterious effects as harm to living resources (my emphasis) hazards to human health, hindrance to marine activities, including fishing, impairment of quality or use of sea water, and reduction of amenities.

A histological study of oysters obtained from high and low zinc environments would indicate whether or not the accumulation of zinc in excess was associated with damage

to the tissue. It was considered that an electron and light microscope correlation of oyster tissue combined with electron probe X-ray analysis would answer this question.

Following discussions with Stephen Thrower in November 1978, the sensitivity of the X-ray analytical system was evaluated on the original Ralphs Bay tissue homogenate, that had been kept frozen since 1972.

The original X-ray analysis of the freeze-dried material on glass slides carried out in 1972-73 could not be correlated with light microscopy, because the squash preparations had disrupted cell morphology. My discussions in January 1979, in Sydney, with Lee Brunckhorst who had done the original analysis, convinced me of the need to combine conventional microscopy with X-ray analysis.

It was apparent that the scope of the project would be limited both by the sophisticated techniques required in the preparation of tissue, and by course work commitments in the Lent term. These constraints limited the number of samples that could be examined by correlative microscopy, but would allow the efficacy of the techniques to be assessed. Unfortunately the small number of samples precluded definitive statements on the relative pollution at the proposed collection sites.

OBJECTIVES

1. To evaluate the different methods of analysis employed in this study.

2. To confirm the presence of zinc by correlating histochemical techniques with X-ray analysis of the tissue.

3. To estimate the concentration of zinc in the tissue by atomic absorption spectrophotometry.

4. To investigate the localization and distribution of zinc in the tissues of the native oyster, Ostrea angasi.

5. To compare the histological appearances of oysters obtained from the Derwent Estuary with those gathered from localities remote from man's industrial and domestic activities.

6. To examine the fine structure of any zinc found by transmission and scanning electron microscopy.

7. To establish any abnormal tissue reaction associated with the presence of zinc in oyster tissue.

LITERATURE REVIEW

Specific metal bearing granulocytes

Over the last century the concept has emerged of a population of cells within the oyster that contain within their cytoplasm a homogeneous collection of metallic granules. The function of these cells is the subject of debate. One school of thought maintains that these cells are part of the normal defence mechanism of the oyster (Ruddell & Rains, 1975), while a second school regards the same cells as part of the mechanism whereby the oyster rids itself of excess metal (George *et al.*, 1978). It is of some value to trace the development of these ideas.

Multicellular organisms require a defence against foreign material introduced into their tissue, whether this be inorganic material or pathogenic microorganisms. The primary defence mechanism in both vertebrates and invertebrates consists of a population of motile cells that can migrate through the tissue and phagocytose the foreign material (Metschnikoff, 1884).

These amoeboid cells were observed on the surface of the gill epithelium in the oyster *Ostrea edulis*, by Sir Ray Lankester in 1885. At first he supposed these 'secretion-cells' to be independent amoeboid organisms,

but the same cells were observed within the gill epithelium, labial palps and interlamellar space. Lankester was studying 'green-gilled' oysters that had ingested the diatom Navicula ostrearia, containing the blue pigment "Marennin". He established the phagocytic properties of these amoeboid cells by demonstrating the pigment within the amoeboid cells. He noted the occurrence of the diatom in the intestine of the oyster and assumed that the pigment had been absorbed from the gut.

Drew (1910) in his study of lamellibranch 'blood-corpuscles' described these amoeboid cells as 'amoebocytes' and differentiated them into two distinct cell types according to their staining properties. The majority of the amoebocytes contained eosinophilic granules, whereas a small percentage were agranular and basophilic. Drew, working with Cardium norvegicum, showed that these two cell types had different functions. The eosinophilic granulocytes phagocytosed bacteria, whereas no phagocytic action was observed on the part of the basophils.

In the same year Drew & De Morgan (1910), working with the lamellibranch Pecten maximus, showed that the inflammatory reaction in lamellibranchs is essentially the same as that in vertebrates. A homograft of infected gill tissue, transplanted into the adductor

muscle, elicited an acute inflammatory response characterized by the infiltration of leucocytes, which phagocytosed the bacteria and necrotic debris. The lesion was eventually repaired by the formation of fibrous tissue.

The migratory pathway of these amoebocytes was delineated by Stauber (1950). Particles of India ink, injected into the ventricle of the oyster, Ostrea virginica, were phagocytosed by the amoebocytes and distributed to all parts of the organism. The ink-laden amoebocytes were eliminated through the epithelia of the alimentary tract, digestive diverticula, labial palps, mantle, heart and pericardium into lumina from which they were voided. The epithelia of gonads, nephridia and shell-forming mantle were not routes of emigration.

Tripp (1960) repeated these experiments with live microorganisms. Injected yeast cells and bacterial spores were disposed of in the same way as carbon particles. Within five days most of the phagocytosed bacteria were removed from the oyster by the amoebocytes emigrating through the epithelia of the gut and mantle.

The metal content of these granular amoebocytes was first established in the American oyster, Crassostrea virginica, by Boyce & Herdman in 1897. They described a disease characterized by a leucocytosis in which large numbers of leucocytes appeared on the mantle surface.

They wrote:

> 'These cells are granular and amoeboid. The granules do not give any definite reaction with the aniline stains ..... We find them in masses in the heart, in both auricle and ventricle, in the vessels....in the lacunar spaces of the connective tissue of the mantle and other organs and also in the more solid parts of the tissues wandering amongst the other cells, wedged into the epithelium and coming out in great numbers on the surface of the body.'

These accumulations of leucocytes on the surface of the body, and especially on the mantle produced a green discolouration, not to be confused with Lankester's 'green-gilled' oysters.

Boyce & Herdman demonstrated the presence of copper in these granules by treating the sections of tissue with acidified potassium ferrocyanide, which produced a red-brown precipitate of cupric ferrocyanide on the granules. They also converted the copper in the granules to cupric sulphide by immersing alcohol-fixed sections in a solution of ammonium-hydrogen sulphide. The 'corpuscles' (presumably granules) stained dark yellow-brown.

The authors were at a loss to explain the aetiology of the 'green leucocytosis' but made the interesting

observation:

> 'We are not prepared to state whether copper in the food can bring about the condition, but certainly we have abundant evidence to show that it can occur where no copper mines or other evident sources of copper are present.'

The role of the amoebocyte in metal detoxification was suggested by Orton (1923) in his investigation of an unusual mortality among oysters in English oyster beds during 1920 and 1921. He examined the metal content of the European oyster, Ostrea edulis, obtained from Mylor Bank, Falmouth. The principal river draining into the area is the River Carnon, which runs through heavily mineralized Devonian rocks, worked since Roman times for tin (as cassiterite) and copper (as sulphide) but which also contains arsenic (as arsenopyrite), zinc (as sphalerite) and lead (as galena). Thornton et al., (1975), showed metal contamination of sediments in tributaries draining the mineralized areas with peak values up to 13,000 $\mu g\ g^{-1}$ Zn and 2,900 $\mu g\ g^{-1}$ Cu. Water draining the mines had peak values of 29,600 $\mu g\ l^{-1}$ Zn and 1,900 $\mu g\ l^{-1}$ Cu.

Orton (1923) showed that the 'blood-cells' (amoebocytes) taken from the Mylor Bank oysters contained far more zinc and copper than oysters analysed as a whole and he concluded that the blood-cells were concerned

in the segregation and excretion of metals; the cells leaving the body of the oyster and carrying the metals with them.

Ruddell (1971) established that wound repair in the Pacific oyster, Crassostrea gigas was mediated by several types of amoebocytes. The oysters were healthy at the time of collection and he wrote:

> 'Immediately after making a small incision in the oyster mantle, amoebocytes from surrounding tissues migrated into the wound area, filling up the wound with a plug of amoebocytes. After an initial lag period of 48 to 72 hours, epithelial cells began migrating over the amoebocyte plug. Agranular phagocytic amoebocytes comprised the greater portion of the cells in the plug and were observed to modulate or differentiate into fibroblasts by 120 to 144 hours after wounding. Two other amoebocyte types, both nonphagocytic and granular, were observed invading oyster wounds. A basophilic granular amoebocyte invaded the wound area in large numbers; many of these cells became swollen on arriving at the wound site. A third amoebocyte type, an acidophilic granular cell, also invaded the wound area.'

Histochemical studies of the two types of granulocytes revealed that the basophil granules were zinc positive

and the acidophil granules copper positive (Ruddell, 1971).

In a later paper Ruddell & Rains, (1975) reported that, in response to both physical and chemical injury, oyster basophils release zinc into the surrounding tissue, from their granules, thereby playing a role in the inflammatory reaction. Basophilic granules of both Pacific and American oysters yielded positive reactions for phenolics (Ruddell, unpublished results) and it was suggested that the granules serve as antimetabolites against microorganisms.

Ruddell & Rains (1975) were of the opinion that the zinc in the granulocyte had a physiological function as part of the oyster's normal defence mechanism and postulated that oysters living under non-optimal conditions, for example in polluted waters, might be stimulated to shed their zinc granulocytes at a different rate to oysters living under more optimal conditions. They collected Pacific oysters from three geographically related areas near San Francisco; one area was undeveloped, a second was surrounded by dairy lands and the third area was heavily polluted by industrial and municipal waste.

The mantles of the oysters from the 'dirty' environment contained higher concentrations of zinc and larger numbers of basophils per unit area of tissue when compared with oysters from the 'cleaner' environments. They were also able to show that the oyster basophils contain a large proportion of the oyster's zinc; the estimated concentration of zinc in the cell being 6% of the dry weight. They concluded that:

'Until the mechanisms governing the turnover of oyster basophils are fully elucidated, one should not ascribe large amounts of zinc and copper in oysters to the effects of mining or industrial pollution.'

Ruddell had shown that specific metals are segregated into distinct types of granular amoebocytes. George et al., (1978) confirmed these findings and their Type A and B amoebocytes correspond to Ruddell's granular acidophils and basophils respectively. They were working with 'green-sick' oysters, 'contaminated' with copper and zinc and obtained from Falmouth, the same area from which Orton (1923) had obtained his oysters; a marine environment known for its high levels of copper and zinc (Thornton et al., 1975).

George et al., (1978), using the techniques of transmission electron microscopy and electron probe microanalysis, examined the fine structure of the zinc and copper granules and found that the Type A cell contained copper in membrane-limited vesicles 0.8 μm in diameter. The Type B cell contained zinc in the form of amorphous, round, electron-dense granules, 0.5 to 1.0 μm in diameter, which were also surrounded by a membrane.

They calculated that the individual cell types may contain as much as 13,000 μg g wet weight^{-1}Cu and 25,000 μg g wet weight^{-1}Zn. Assuming an 80% water content for the cell, the latter concentration (12% dry weight Zn)

is similar to that calculated by Ruddell.

The sequestration of specific metals into separate amoebocytes raises the question - how are the granules formed? George *et al.*, (1978) maintained that the granules were formed by the selective uptake, from the serum, of zinc and copper into the respective amoebocytes, to maintain honeostasis in the extracellular fluid in the face of high levels of zinc and copper in the external environment. If this hypothesis is correct each cell would have to have specific surface receptors and cytoplasmic ligands for complexing the metals inside the cell.

MATERIAL

The oysters and sites of collection

The native mud oyster Ostrea angasi was selected because of its wide distribution around the Tasmanian coastline (Macpherson & Gabriel, 1962). Oysters were collected from three distinct areas on the coastline of South-Eastern Tasmania (Fig. 1.). The first two collection sites were in the marine zone of the Derwent Estuary and close to the urban centre of Hobart. The third site at Little Swanport on the east coast is remote from urbanization, in an area developed agriculturally. The fourth site on Bruny Island is remote from both industrial and agricultural activity.

The largest specimens from each site were collected, however the specimens within the Derwent Estuary were scanty and smaller so that it was not possible to obtain oysters of a uniform size.

Site 1. Ralphs Bay

Ralphs Bay is a shallow diverticulum off the main channel of the Derwent Estuary, with a depth of only 3 m. A specimen was collected from the low-water mark along the southern shore. The commercial oyster lease had been situated on the west side of the bay. Very few live specimens were seen, although there were large numbers of opened shells along the beach.

Fig. 1. A map of South-Eastern Tasmania and adjoining waters, indicating the four collection sites referred to in the text.

1 RALPHS BAY
2 CRAYFISH POINT
3 LIMEKILN POINT
4 MICKEYS BAY

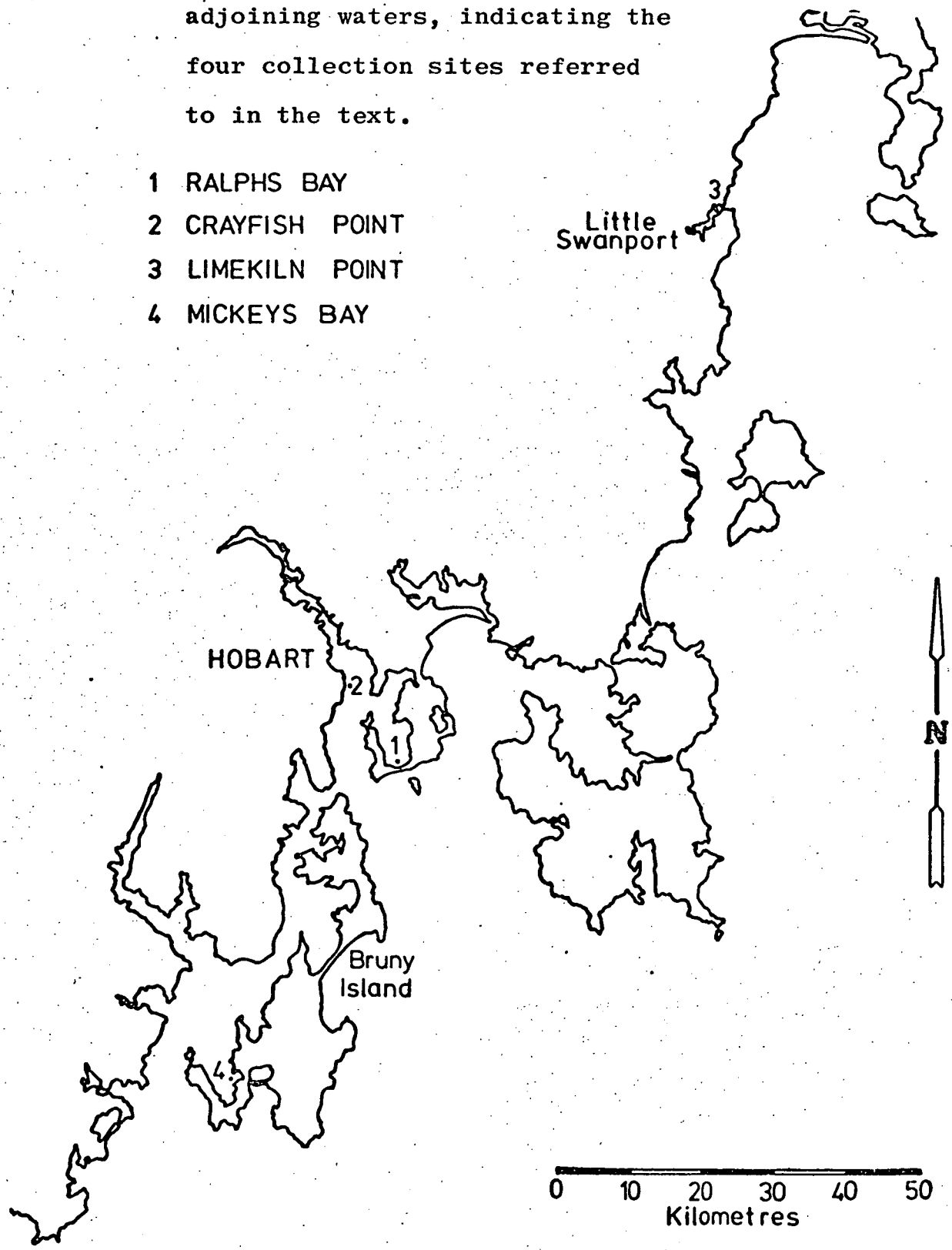

Site 2. Crayfish Point

Crayfish Point is situated in the main channel of the Derwent Estuary, which has a maximum depth in this region of 24 m. A specimen was collected from the sandy bottom by diving to a depth of 3 m. Live specimens were difficult to find, but empty shells, that had been prised open, were attached to the rocks.

Site 3. Limekiln Point

Little Swanport is a narrow inlet 5 km long and 100 m across at the mouth. It receives water from the Little Swanport River that arises in undeveloped hinterland. The land surrounding the inlet has been turned over to pasture. Human settlement is sparse and there are only about a dozen houses in the hamlet of Little Swanport. There were many large oysters amongst the seaweed on a sandy bottom. Oysters were attached to each other in clumps and could be found up to the sandbar that separated the inlet from the sea. A specimen was collected without difficulty in the fast flowing main channel close to the mouth of the inlet at Limekiln Point.

Site 4. Mickeys Bay

Mickeys Bay on the west coast of Bruny Island and facing the D'Entrecasteaux Channel, is exposed to waters from the Tasman Sea. Water draining into the bay comes

from uncleared land. The beach is unspoilt, access being by rough track and there was a profusion of oyster shells on the beach. A sand shelf extended seawards some 200 m before shelving down steeply. Ostrea angasi was the dominant species on this slope and a mature specimen was selected from a depth of 3 m.

The initial site was selected because it was felt that a high level of zinc would be found in the oyster tissue. Subsequent sites were selected in the hope that zinc levels in the tissue would be lower.

METHODS

One oyster from each collection site, hereafter referred to as (O1), (O2), (O3) & (O4), was brought to the laboratory in a damp sack and prepared for analysis within 24 h of collection. The visceral mass (Plate 1.) was cut transversely into adjacent blocks of tissue (A & B) 4 mm thick. Block (A) was prepared for correlative microscopy/X-ray analysis; block (B) for atomic absorption spectrophotometry (AAS) as outlined in Fig. 2.

Block (A) was examined by:

1. Transmission electron microscopy (TEM)
2. Scanning electron microscopy (SEM)
3. Light microscopy (LM)

After examination in their respective modes of microscopy, sections were analysed by electron probe microanalysis (EPMA), using energy dispersive (EDAX) and wavelength dispersive systems of X-ray analysis. Sections were re-examined microscopically after X-ray analysis to confirm the location of the area analysed.

Tissue fixation

Block (A) was removed from the live oyster and fixed immediately in cold glutaraldehyde saturated with hydrogen sulphide (Pihl & Falkmer, 1967). Shortly before use, H_2S generated from Kipp's apparatus, was bubbled through

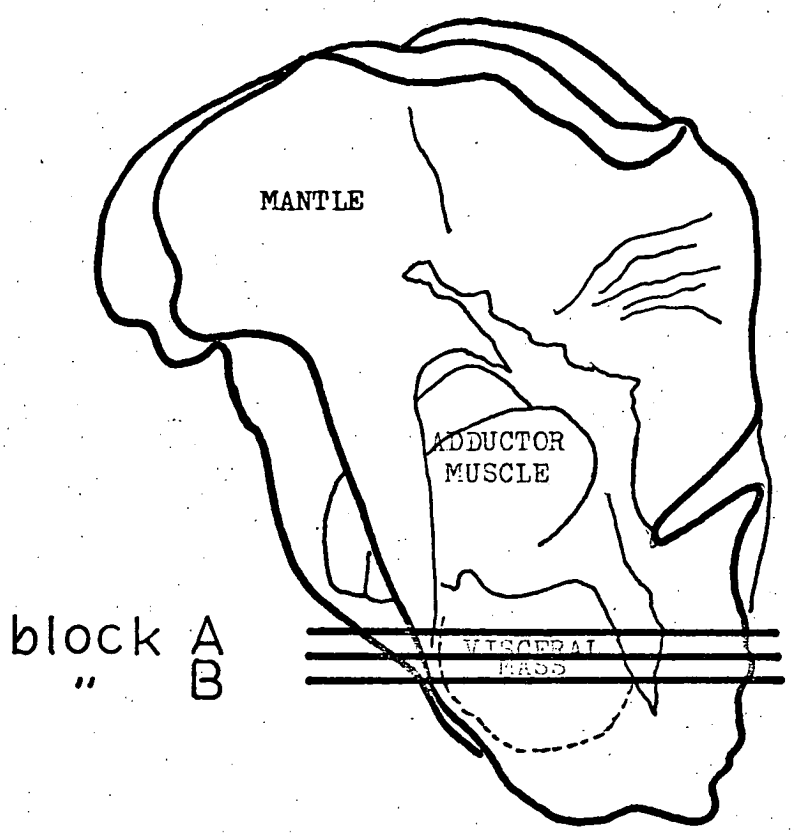

PLATE I. Photograph of (03) showing the line of sectioning through the visceral mass. Mag. X 1.5

FIG. 2. CORRELATIVE MICROSCOPY AND X-RAY ANALYSIS

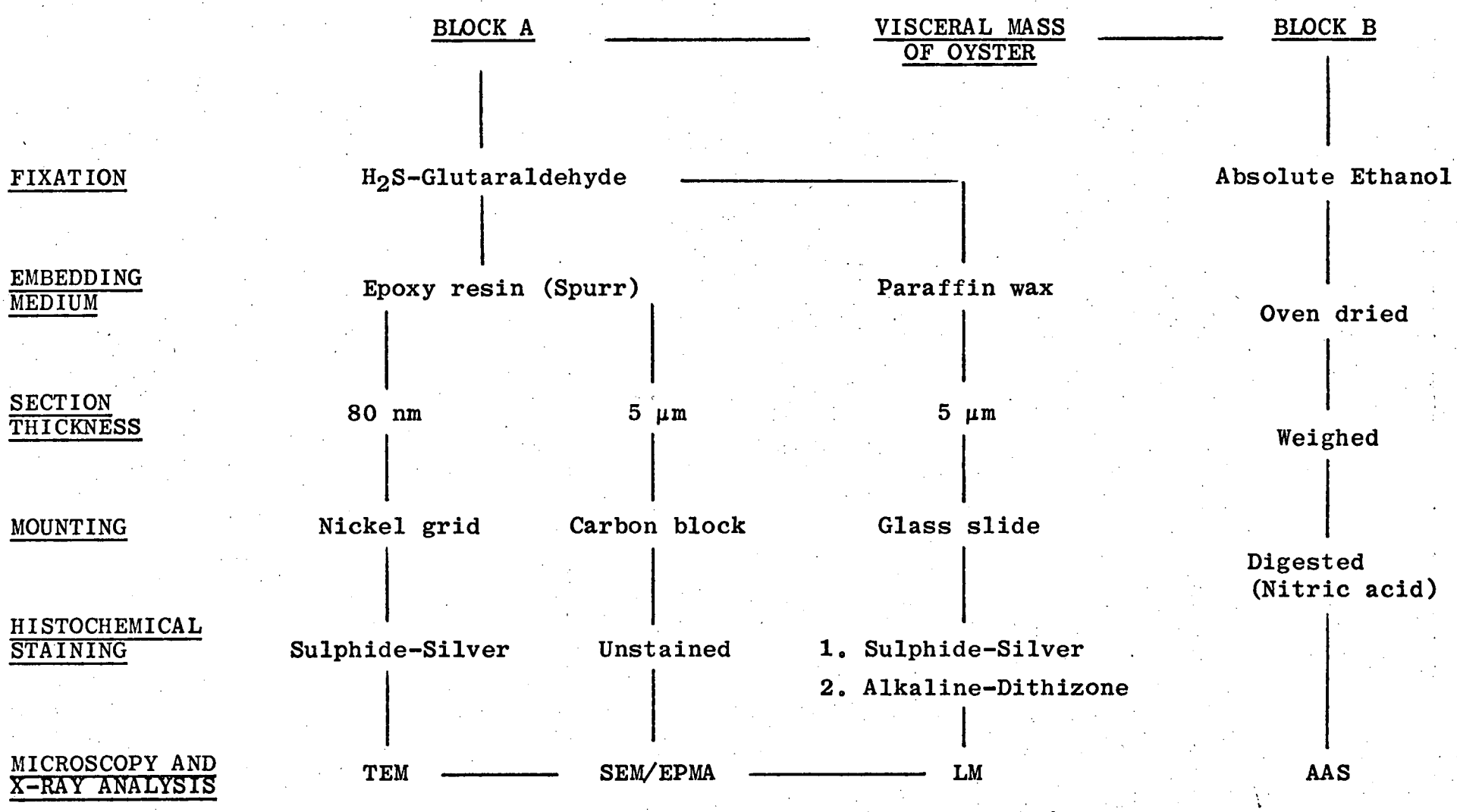

a 3% solution of glutaraldehyde in 0.067 M phosphate buffer at pH 7.4. After half an hour a white flocculent precipitate formed, at which time the fixative was judged to be saturated with the gas.

After 2 h fixation a small block of tissue (A_1) 2 mm^3 was cut from the parent block (A) on the face adjoining Block (B). Block (A_1), consisting of mid-gut epithelium and subjacent tissue, was transferred to phosphate buffered saline (pH 7.4) for 24 h prior to dehydration for SEM & TEM. The remainder of Block (A) was left in the fixative for 24 h before dehydration for LM.

SEM/EPMA examination

Block (A_1) was dehydrated in a graded series of ethanol, embedded in Spurr low-viscosity epoxy resin and cured overnight. 5 µm sections were cut with freshly prepared glass knives on a LKB Ultrotome III and dried onto a clean carbon block. The section was coated with 20-30 nm carbon and examined in a JEOL JXA-50A scanning electron microscope-electron probe microanalyser. The SEM was calibrated on polystyrene, monodispersed, latex spheres with a diameter of 1.25 µm (std.dev. = 0.02). EDAX was calibrated on a Cu standard using L_α/K_α ratio. Operating conditions varied according to the sample, but were usually in the range 15-25 kV and 2-6 X 10^{-9}A. The topography of the section was determined at low

magnification using the secondary electron image and areas of interest examined at high magnification with the back-scattered electron image. Individual cells suspected of containing heavy metals were analysed by EDAX in either the scanning or spot mode. Individual granules were analysed in the spot mode.

X-ray mapping was carried out by setting either EDAX or WDX spectrometers on the appropriate emission line of the element concerned.

TEM examination

Serial sections of Block (A_1), cut at 80 nm, were placed on Formvar coated nickel grids and stained (O2) by the sulphide-silver method (Timm, 1958) as described for ultrastructural cytochemistry by Pihl & Falkmer, 1967. Stained and unstained sections were examined in a Hitachi HS-7S transmission electron microscope operating at 50 kV and 35 x 10^{-6}A.

N.B. (i) (O1) was prepared for TEM/SEM/EPMA by fixation in 5% glutaraldehyde (in 0.1 M cacodylate buffer), post-fixed in OsO_4 and mounted on a copper grid. After TEM the grid was transferred to the SEM/EPMA for X-ray analysis.

(ii) Silver stained thin sections of (O2) were examined in the TEM post X-ray analysis.

LM examination

Block (A), fixed for 24 h in H_2S-saturated glutaraldehyde, was dehydrated in a graded series of ethanol, cleared, embedded in paraffin wax and cut at 5 μm. Serial sections of paraffin wax and epoxy resin embedded material, stained by a variety of techniques (see below), were examined in an Olympus Vanox light microscope, with photographic attachment. The instrument was calibrated by photographing a Leitz micrometer slide (10 μm grating) at the same magnification as the tissue. Photographic records were kept using Agfacolor 35 for transparencies and Kodacolor II for prints.

N.B. (i) Paraffin embedded 5 μm unstained sections of (O2) were examined in the SEM/EPMA, stained, and re-examined in the LM.

(ii) Stained sections of (O2) were examined in the LM before and after SEM/EPMA.

(iii) (O1) was prepared for LM by fixation in Histochemistry and histology (unbuffered 10% formalin.

Serial sections of tissue embedded in paraffin wax were stained by the following methods:

(a) Haematoxylin and eosin (H&E)

Sections were deparaffinised in xylene, taken to water through a graded series of ethanol and stained for four minutes in Harris's alum haematoxylin. After differentiation and blueing, sections were counter-stained in aqueous eosin, dehydrated in ethanol, cleared in xylene and mounted in D.P.X.

(b) Masson's trichrome technique

The procedure adopted was as described by Culling, 1974.

(c) Alkaline dithizone method for zinc

The method employed was based on the work of Timm (1960) and Midorikawa & Eder (1962). Sections, fixed in H_2S-glutaraldehyde, were deparaffinised in xylene and absolute ethanol and:

(i) Transferred to an ammoniacal solution of dithizone (pH 8.0-9.5) for 30 minutes at 55°C.

(ii) Rinsed in distilled water and counterstained lightly with haematoxylin without differentiation.

(iii) Rinsed briefly in distilled water and mounted in glycerine jelly.

The dithizone solution was made up just before use according to the method of Midorikawa & Eder (1962).

(d) Sulphide-silver method for heavy metals

The method used was based on the work of Timm (1958) and Pihl & Falkmer (1967). It was applied to thin and thick sections of epoxy resin embedded tissue as well as to sections of tissue embedded in paraffin wax. The principle of the method is the conversion of the heavy metals into insoluble sulphides during fixation with H_2S-glutaraldehyde. Heavy metal sulphides are argyrophilic (Timm, 1958) and serve as points of condensation when developed with silver nitrate in a colloidal suspension of hydroquinone.

This process is analogous to photographic development.

The development solution was made up as recommended by Pihl & Falkmer (1967), but development was carried out in daylight under microscopic control as originally stipulated by Timm. Generally speaking development started to appear within minutes and was quite intense by 10 minutes.

The development solution was stored in the refrigerator for a few days before use to develop colloidal properties and could be stored for a month under these conditions without loss of its properties. Immediately before use 1 ml of a 10% solution of $AgNO_3$ was thoroughly mixed for 30 s with 10 ml of developer.

Paraffin embedded sections were taken to water and the developer laid on the surface of the slide. After development the slide was rinsed in distilled water, counterstained with safranin, dehydrated, cleared and mounted in D.P.X. Epoxy embedded thick sections, stained with 1% toluidine blue in 5% borax, were treated in the same way. Thin sections on Formvar coated nickel grids were inverted onto a drop of developer on a glass slide.

(e) Rubeanic acid method for copper

Paraffin sections of (02) were stained for copper as described by Pearse (1972).

(f) Perls' method for ferric iron

Paraffin sections of (02) were stained for ferric iron as described by Pearse (1972).

(g) Controls

Rat tissue was processed in parallel with oyster tissue.

Atomic absorption spectrophotometry

The concentration of zinc and cadmium in block (B) was estimated by AAS using a Pye-Unicam, SP 1900 instrument, operated in accordance with the manufacturer's instructions and under the supervision of officers of the Department of the Environment. Tissue was prepared for AAS by the method described by Ayling (1974). Analytical grade chemicals were used and glassware was washed before use in 5% Decon 90, a non-ionic detergent and rinsed in deionized water. This was followed by a wash in 10% nitric acid and a final rinse in deionized water.

Block (B) was removed from the ethanol fixative with stainless steel forceps and cut into small pieces (2 mm^3), which were dried in an oven for 16 h at 105°C. After weighing, the dry tissue was digested in 2 ml concentrated nitric acid and made up to 5 ml with deionized water.

N.B. Block (B) of (01) was preserved in cacodylate buffer before preparation for AAS and both wet and dry weights were determined.

RESULTS

Zinc was detected in high concentrations within the visceral mass of each oyster obtained from the four widely separated localities. From Table 1. it can be seen that the concentration of zinc was the same order of magnitude (10^4 µg g dry weight^{-1}) in all four samples, although the oyster from Ralphs Bay contained twice the concentration of zinc in its visceral mass.

Zinc was located intracellularly and its presence confirmed in each instance by both histochemical and X-ray analyses.

Light microscopy

The distribution of zinc was essentially the same in all specimens and predominantly associated with the intestinal tract (Plates 2 & 3).

Initial observations on (01), which had been fixed in formalin and stained with H & E, revealed a cellular infiltrate within the peri-intestinal connective tissue, the cells having an amphoteric cytoplasm suspected of containing zinc. A serial section, left overnight in H_2S-glutaraldehyde and developed the next day by the sulphide-silver method, confirmed the presence of heavy metals (Plates 3 & 4). Further serial sections, stained with dithizone, showed magenta deposits of zinc within the cytoplasm of these cells (Plate 5).

TABLE I. OSTREA ANGASI: ANALYSES OF VISCERAL MASS

Location	Site No.	Date of Collection	Diameter of shell (cm)	EPMA for Zn	Dithizone reaction	$\mu g\ Zn\ g\ dry\ wt^{-1}$	$\mu g\ Cd\ g\ dry\ wt^{-1}$
Derwent Estuary							
Ralphs Bay	1	3.3.79	6	pos.	pos.	32,800	55
Crayfish Point	2	2.8.79	8	pos.	pos.	16,200	25
Little Swanport							
Limekiln Point	3	2.9.79	12	pos.	pos.	13,600	14
Bruny Island							
Mickeys Bay	4	1.10.79	12	pos.	pos.	17,700	13

Pos. = Positive

N.B. Cadmium concentration shown here for comparison but not discussed in text.

Cells containing heavy metal (01), as revealed by the sulphide-silver technique, extended throughout the vascular spaces of the connective tissue up to the epithelium of the mantle (Plate 6). Clusters of these cells were also present in the interlamellar space of the gill (Plate 7).

The intracellular deposit of zinc was amorphous in tissue that had been fixed in formalin. However when tissue from (02) was fixed in H_2S-glutaraldehyde, the difference in appearance was quite striking. Routine H & E staining now showed innumerable cells containing brown deposits of zinc sulphide which were refractile and took up neither the haematoxylin nor the eosin. The cells containing this material were distributed in the mantle (Plate 8), gill (Plate 9) and peri-intestinal tissue (Plate 10).

Examination under the oil immersion lens showed that these zinc-laden cells were packed with spherical granules, which were remarkably uniform in size, measuring 1 μm in diameter. Their staining characteristics are illustrated in Plates 11 to 14 and summarized in Table 2.

The majority of the zinc granulocytes were situated within the vascular spaces of the connective tissue, but they were also present in the intestinal and mantle epithelia (Plates 15, 16 and 17).

TABLE II. HISTOCHEMICAL PROPERTIES OF ZINC GRANULES IN PARAFFIN AND RESIN EMBEDDED TISSUE FIXED IN H_2S-GLUTARALDEHYDE

Histochemical Test	Result
Haematoxylin + Eosin	Brown, refractile, sphere 1 μm diameter
Sulphide-silver	Positive (black)
Alkaline dithizone	Positive (magenta)
Masson's trichrome	Amphoteric
Toluidine blue	Variable
Rubeanic acid	Negative
Perls' reaction	Negative

Extracellular deposits of heavy metal were observed in the lumen of the stomach (01) as shown in Plate 18, with smaller particles, 2-3 μm in diameter, adherent to the cilia on the surface of the mid-gut epithelium (Plate 19).

Intact zinc granulocytes were seen in the lumen of the mid-gut (Plates 20 to 27) associated with sloughed intestinal epithelium. Ponder has suggested (pers. comm.) that this may be a preparation artefact. Block (B) was removed from the live oyster before Block (A) and during the vivisection fragments of epithelium may have been sucked into Block (A) by the vigorous beating action of the intestinal cilia.

Zinc granulocytes were distributed through the full thickness of the visceral mass (Plates 28 & 29), but not seen in the gonad tissue. Small numbers of zinc granulocytes were seen within the epithelium of the digestive diverticula and they were conspicuous on the outer surface of the mantle; presumptive evidence of their excretion.

Fibrous tissue was associated with accumulations of zinc granulocytes in the peri-intestinal connective tissue, particularly in the stomach wall (Plate 31) and to a lesser extent in the mid-gut (Plates 32 & 33). This was not a constant association and the fibrous tissue may be within normal limits rather than a pathological tissue reaction.

PLATE 2. LM (01). Mid-gut showing the subepithelial infiltrate of cells laden with heavy metals. Metal deposits can also be seen within the epithelium and lumen of the gut. Gonad on left free of deposits.
Formalin fixation: Section treated with H_2S-glutaraldehyde and developed by the sulphide-silver method.
Safranin counterstain.
Mag. X 100.

PLATE 3. LM (04). Mid-gut, Cf. Plate 2. Note the similar distribution of heavy metals. The basement membrane is also taking up the silver. The epithelium of the digestive diverticula (bottom) is free of heavy metals as is the gonad (upper left).
Fixed and stained as in Plate 2.
Mag. X 100.

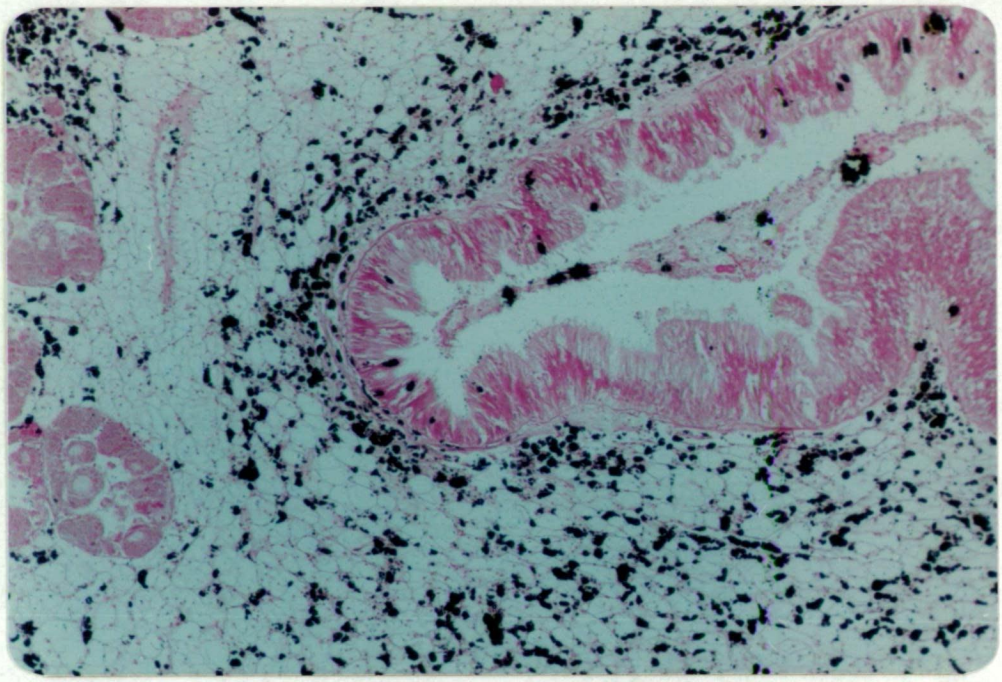

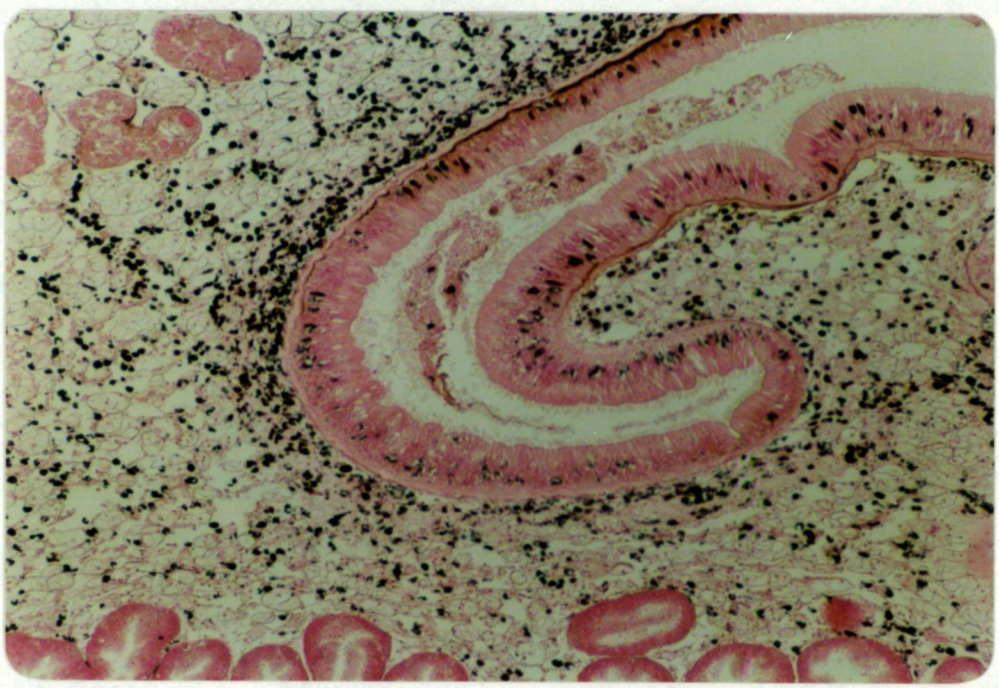

PLATE 4. LM (01). Mid-gut, same field as Plate 2. at higher magnification. Note particles of heavy metal, 30 μm in diameter in the lumen. Intracellular deposits of heavy metal are clustered beneath the basement membrane, with occasional cells in the epithelium.
Mag. X 200.

Plate 5. LM (01). Stomach showing dithizone positive material within cells situated predominantly in the connective tissue beneath the epithelium.
Haematoxylin counterstain.
Mag. X 200.

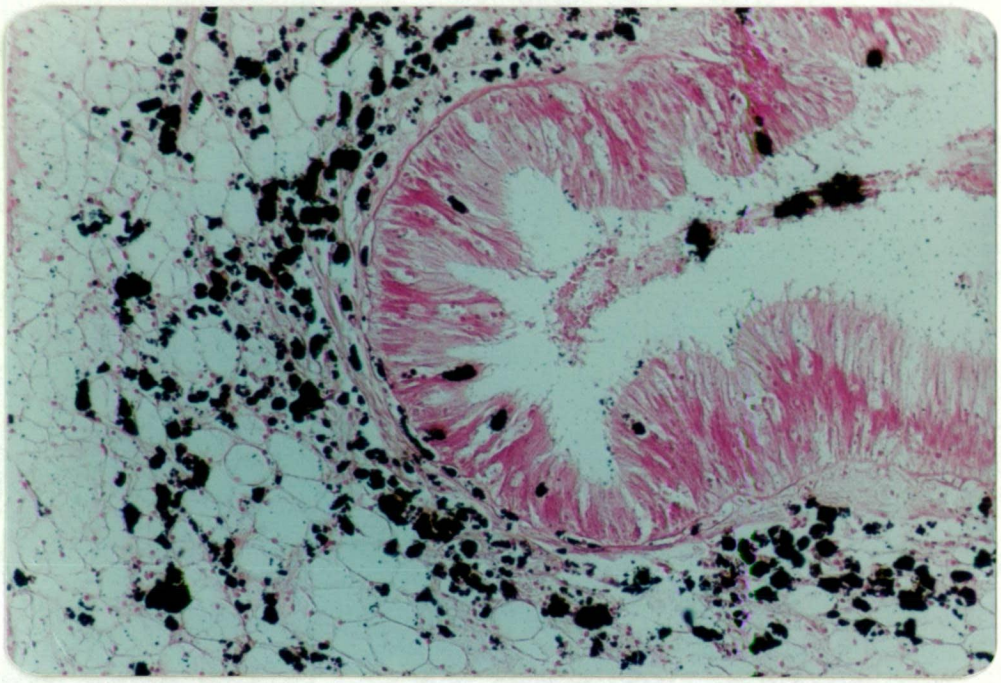

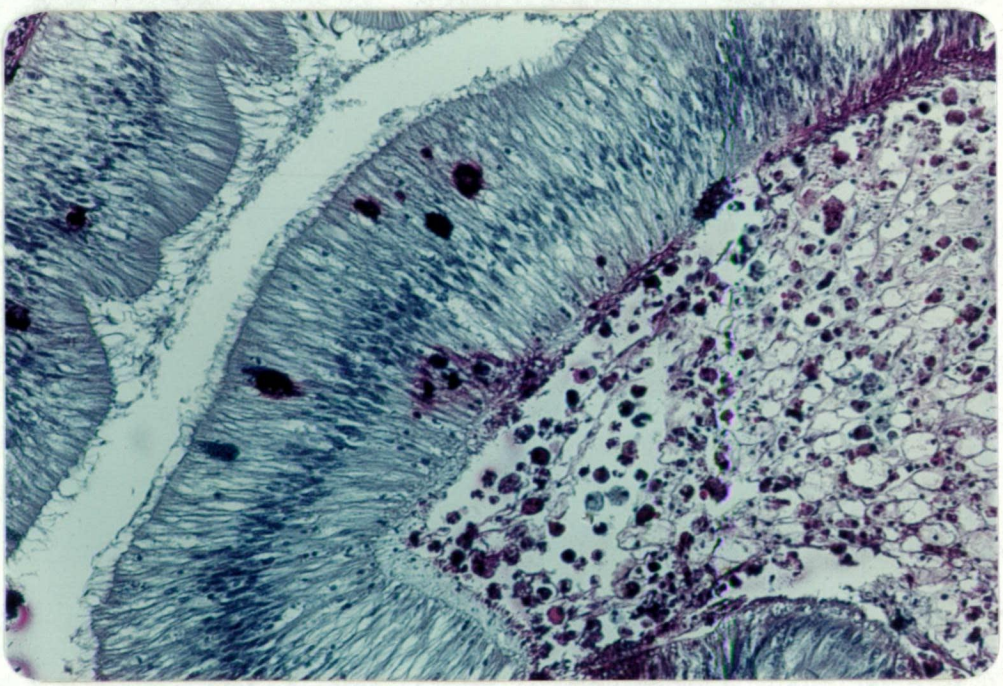

PLATE 6. LM (01). Showing widespread, predominantly intracellular, deposition of heavy metal in the connective tissue, subjacent to the epithelium of the mantle. The deposit forms heavy metal 'lakes' in some areas.
Formalin fixation. Sulphide-silver technique on section exposed to H_2S-glutaraldehyde.
Safranin counterstain.
Mag. X 100.

PLATE 7. LM(01). Cross section of gill showing heavy metal deposits in the interlamellar space. Heavy metal has also been deposited on the chitinous supporting rods.
Preparation as in Plate 6.
Mag. X 100.

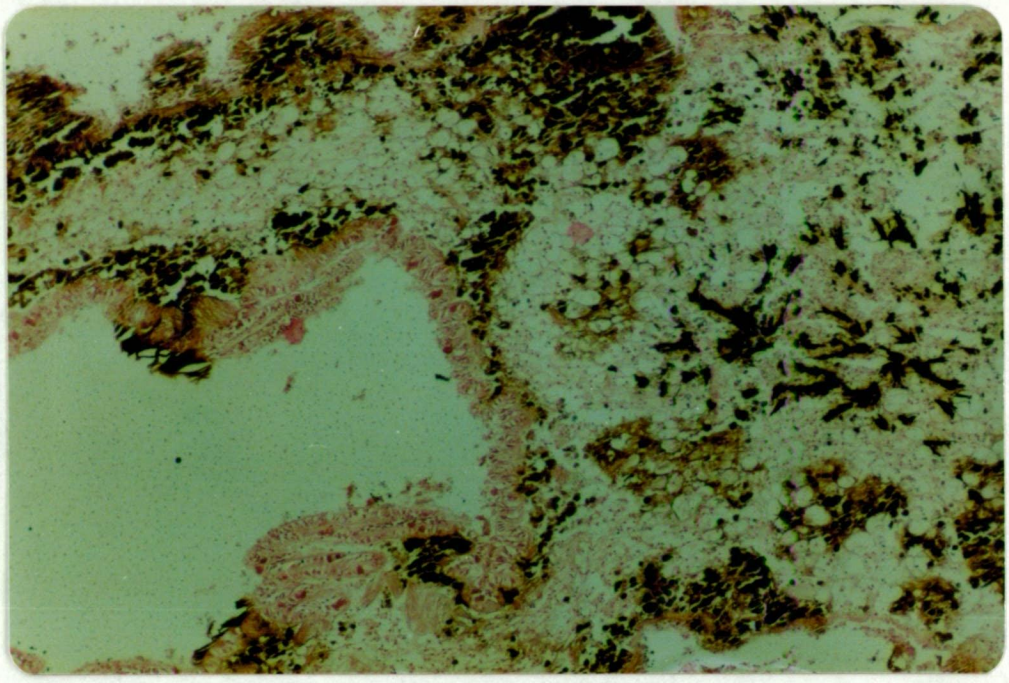

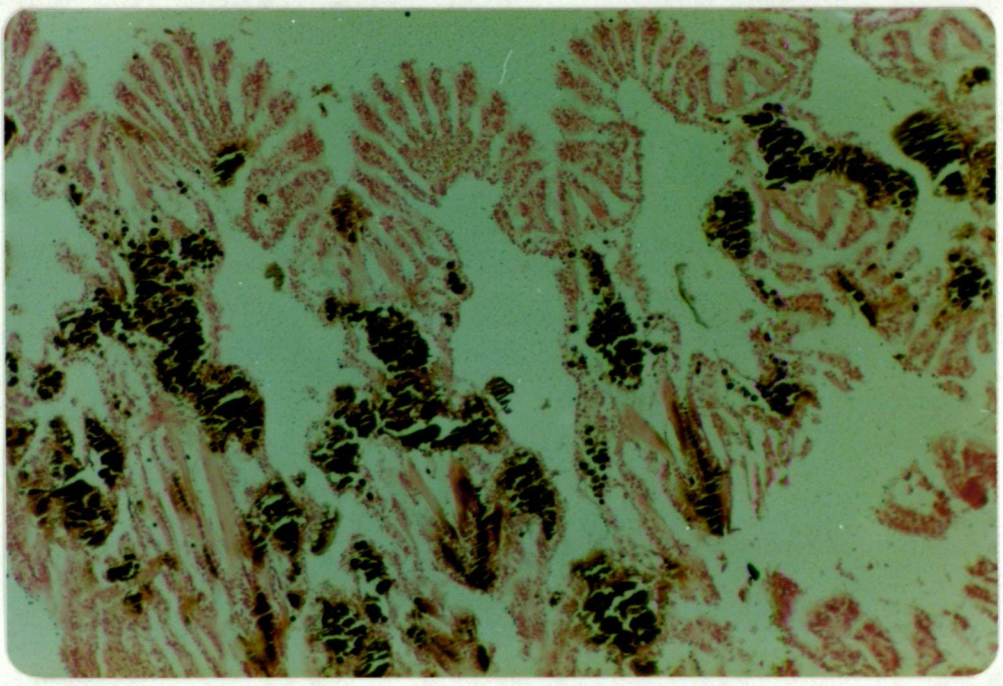

PLATE 8. LM (02). Section through mantle showing brown, unstained intracellular deposits of zinc sulphide in the connective tissue. Cf. Plate 6.
Fixation: H_2S-glutaraldehyde.
Stain: H & E.
Mag. X 100.

PLATE 9. LM (02). Longitudinal section of gill. The zinc sulphide has the same distribution as in (01), Cf. Plate 7.
Fixation and stain as in Plate 8.
Mag. X 100.

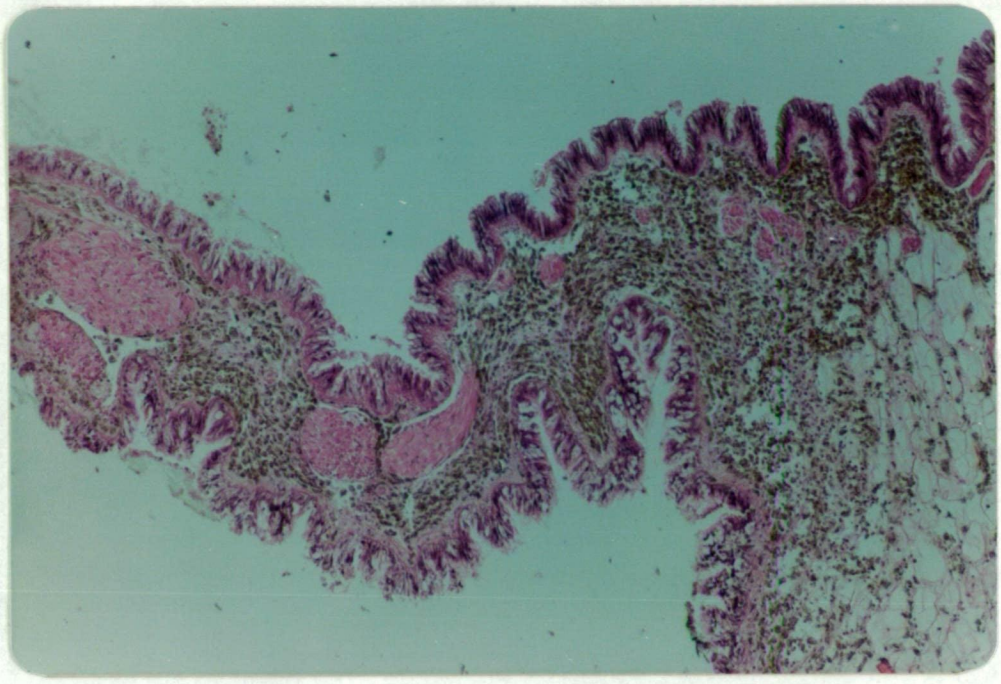

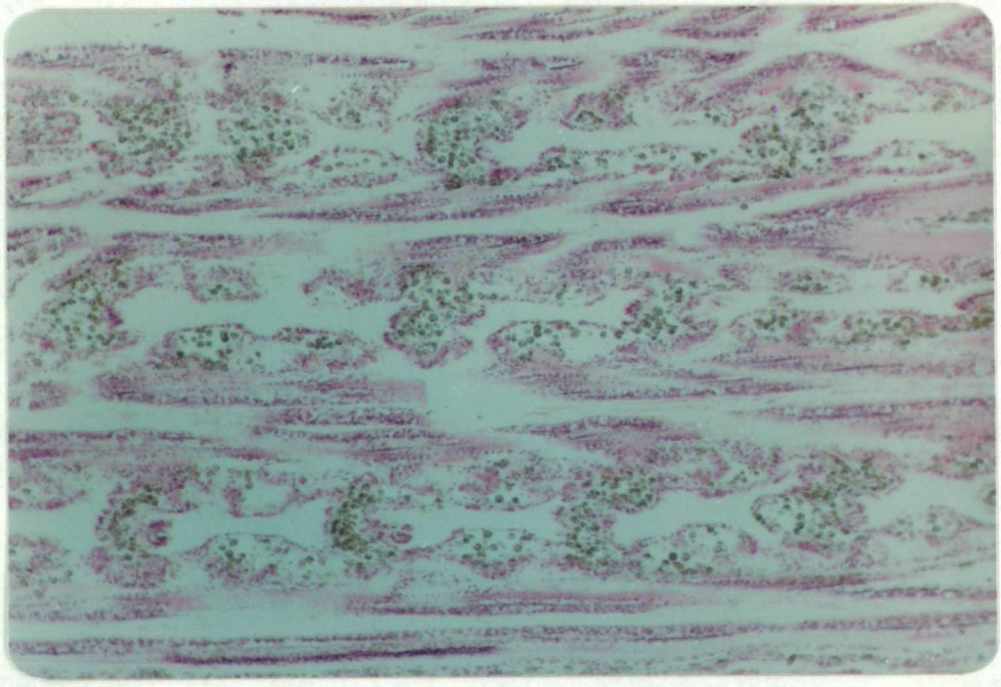

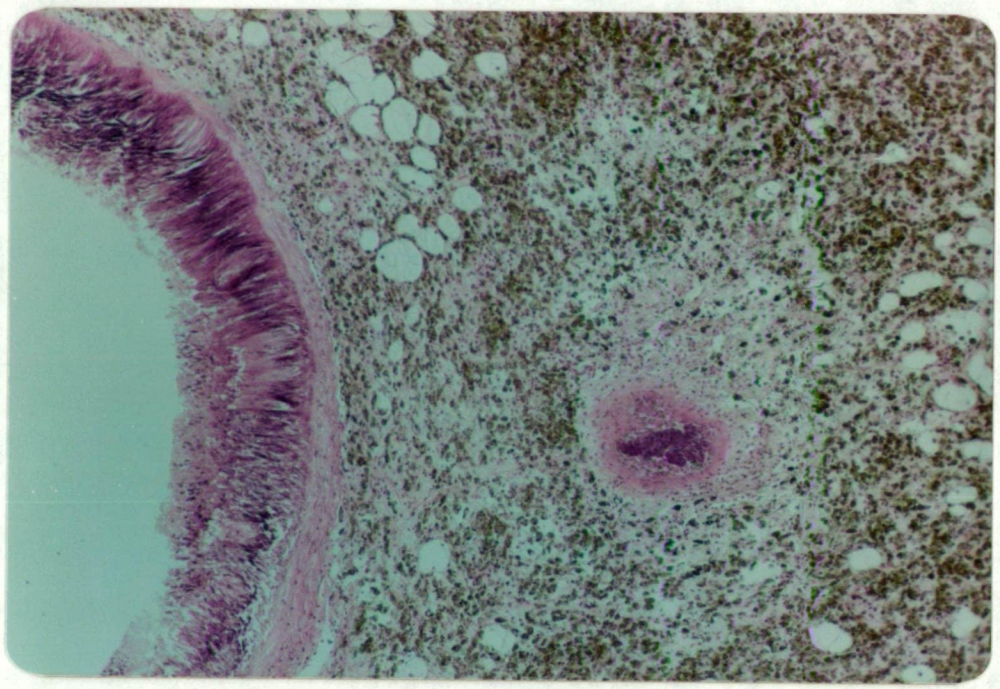

PLATE 10. LM (02). Transverse section of stomach wall showing extensive intracellular deposition of zinc sulphide throughout the peri-intestinal connective tissue.
Fixation and stain as in Plates 8 & 9.
Mag. X 100.

PLATE 11. LM (02). Zinc granulocytes in the vascular space beneath the gill epithelium. The cells are variable in shape, some having pointed ends. Others have burst releasing their granules into the extracellular fluid (ECF). The cells are distended by the refractile spherules pushing the nucleus to one side.
Fixation: H_2S-glutaraldehyde.
Stain: H & E.
Mag. X 1000.

PLATE 12. LM (04). Zinc granulocytes beneath the basement membrane of the mid-gut. The granules are mostly intracellular, but some are free in the ECF, presumably released from disrupted cells.
Fixation: H_2S-glutaraldehyde.
Stain: Sulphide-silver, safranin.
Mag. X 1000.

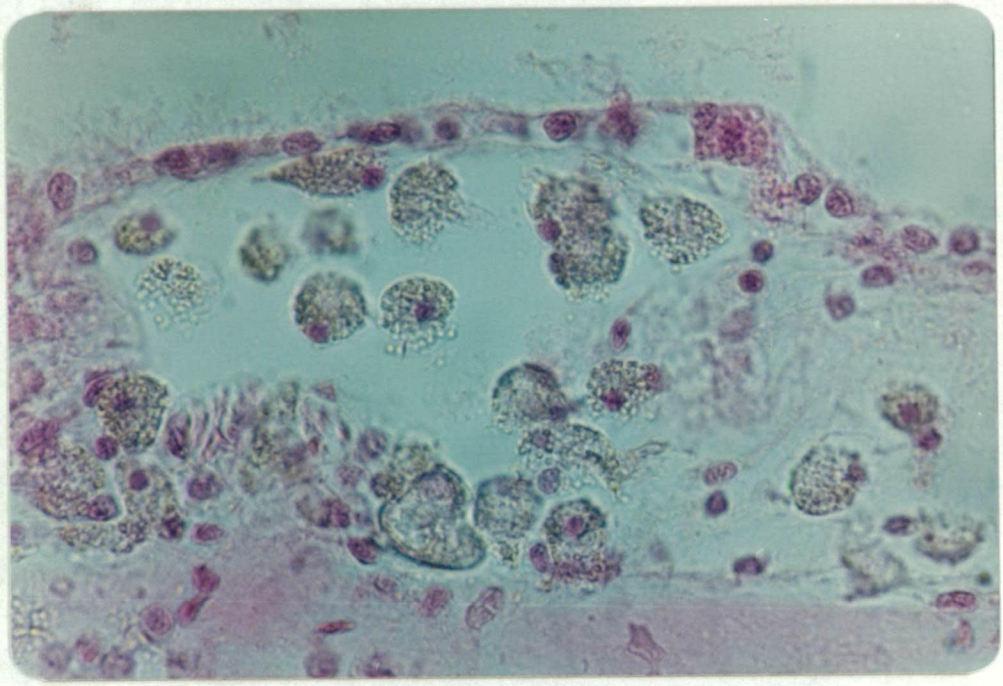

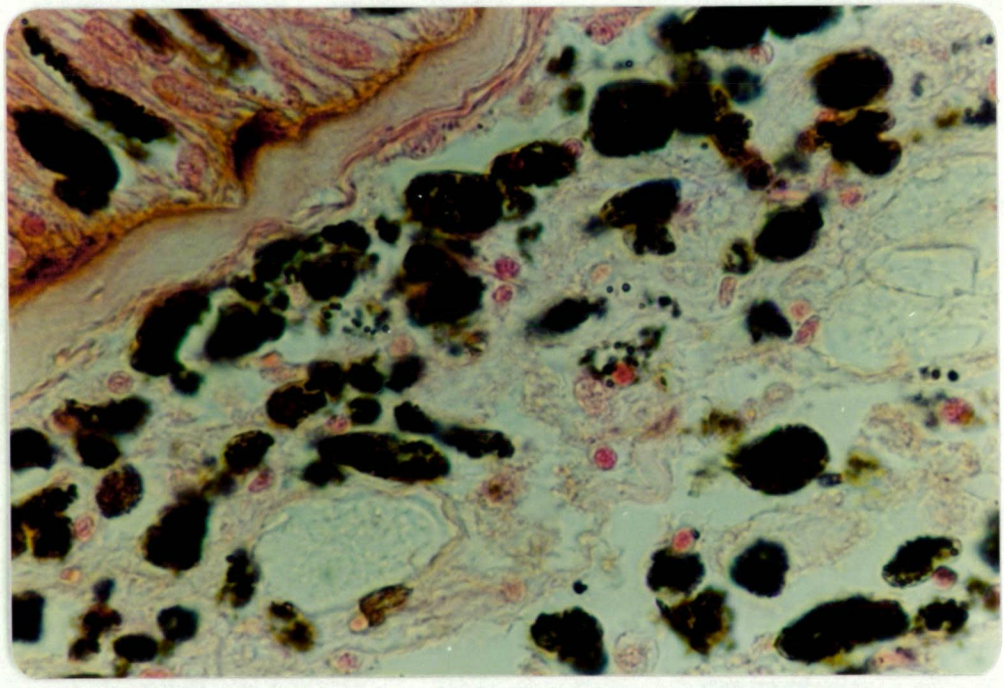

PLATE 13. LM (04). A cluster of zinc granulocytes lying in a vascular space within the peri-intestinal connective tissue. Some granulocytes are disrupted and have released granules into the ECF. The large vacuolated cells are the glycogen and fat storage cells of Leydig.

Fixation: H_2S-glutaraldehyde.

Stain: Alkaline dithizone, haematoxylin.

Mag. X 1000.

PLATE 14. LM (04). Zinc granulocytes clustered beneath the epithelium of the mid-gut. The The granules are amphoteric but appear to have taken up Weigert's iron haematoxylin.

Fixation: H_2S-glutaraldehyde.

Stain: Masson's trichrome (with aniline blue).

Mag. X 1000.

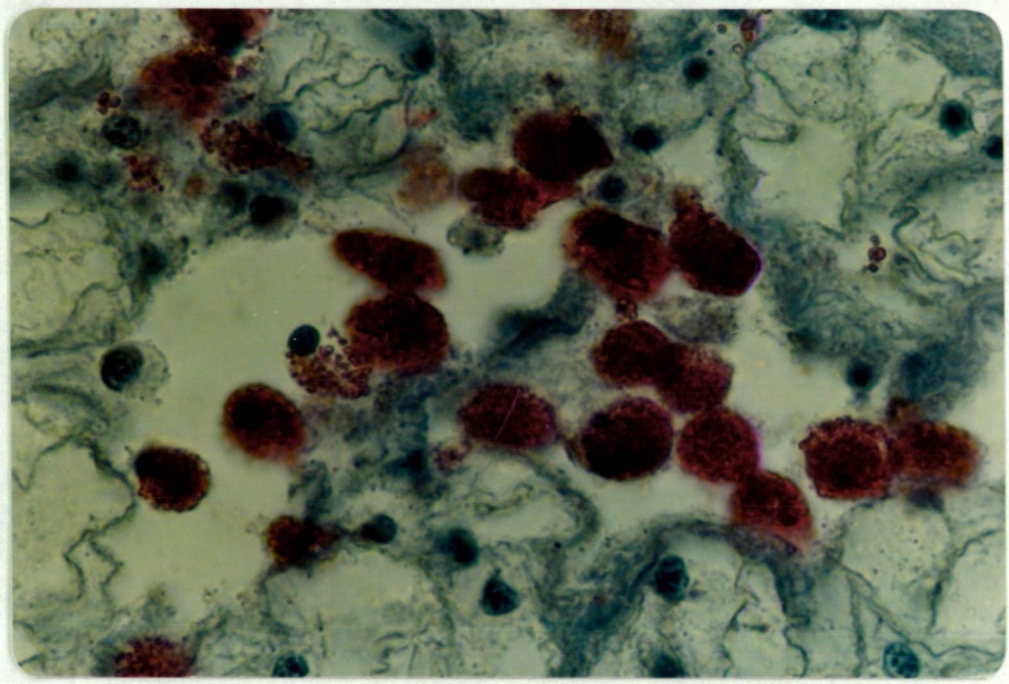

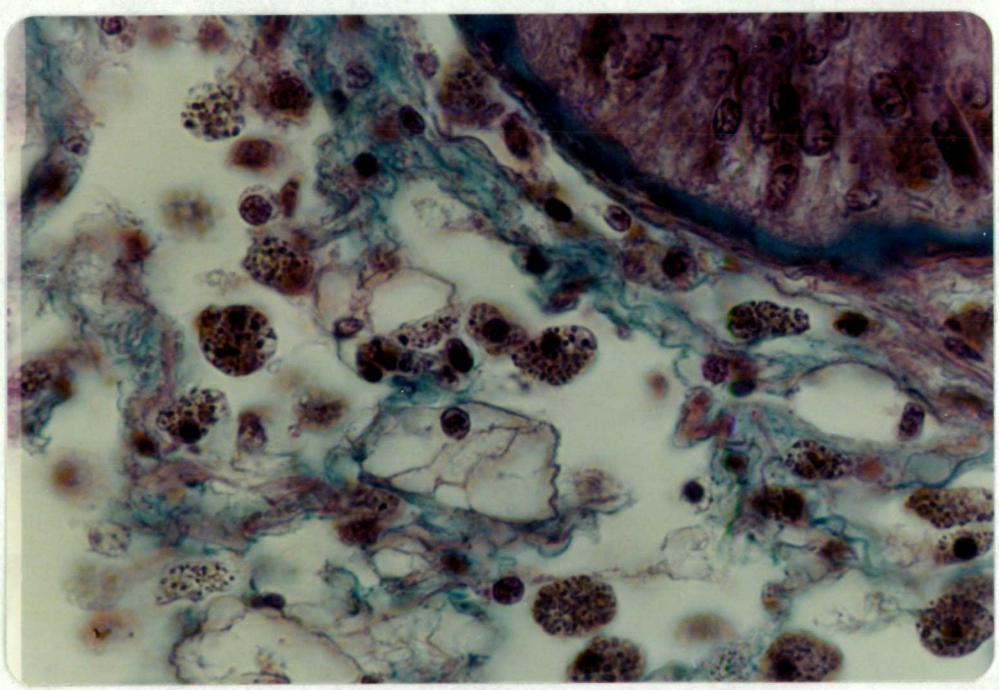

PLATE 15. LM (01). Zinc granulocytes in the epithelium of the mid-gut. Note the indistinct morphology due to the preservation of the tissue in formalin; the zinc appears as an amorphous mass.
Stain: Sulphide-silver, safranin.
Mag. X 1000.

PLATE 16. LM (04). Same region as previous plate. Zinc granulocytes are in the epithelium and beneath the basement membrane, in which zinc is deposited on the epithelial aspect. Note better preservation of cellular morphology in the H_2S-glutaraldehyde preserved material.
Stain: Sulphide-silver, safranin.
Mag. X 1000.

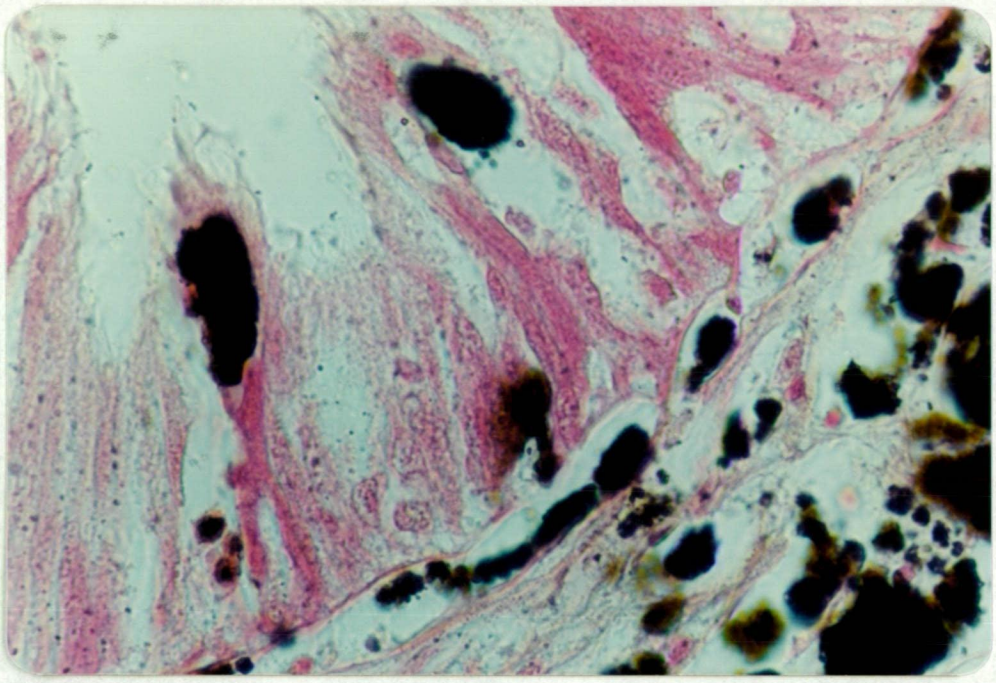

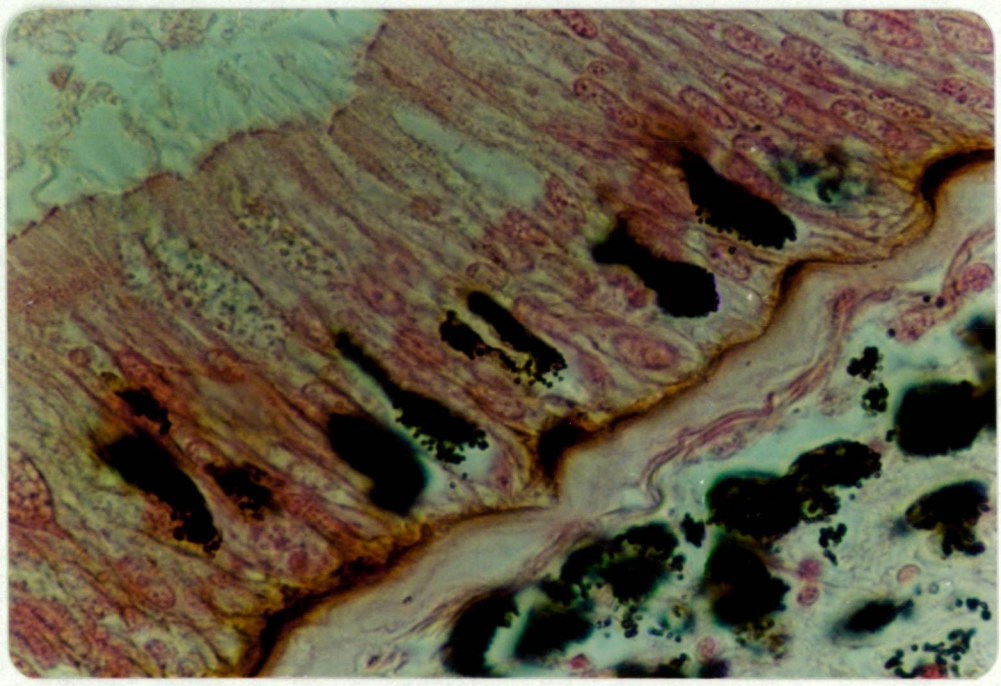

PLATE 17(a) LM (02). A zinc granulocyte is in the mantle epithelium. Other cells, exhibiting variable morphology are present in the subepithelial vascular space.
Fixation: H_2S-glutaraldehyde
Stain: H & E.
Mag. X 1000

PLATE 17(b) LM (02). Zinc granulocyte within mantle epithelium. Large numbers of similar cells are clustered beneath the basement membrane.
Fixation and stain as in 17(a).
Mag. X 1000.

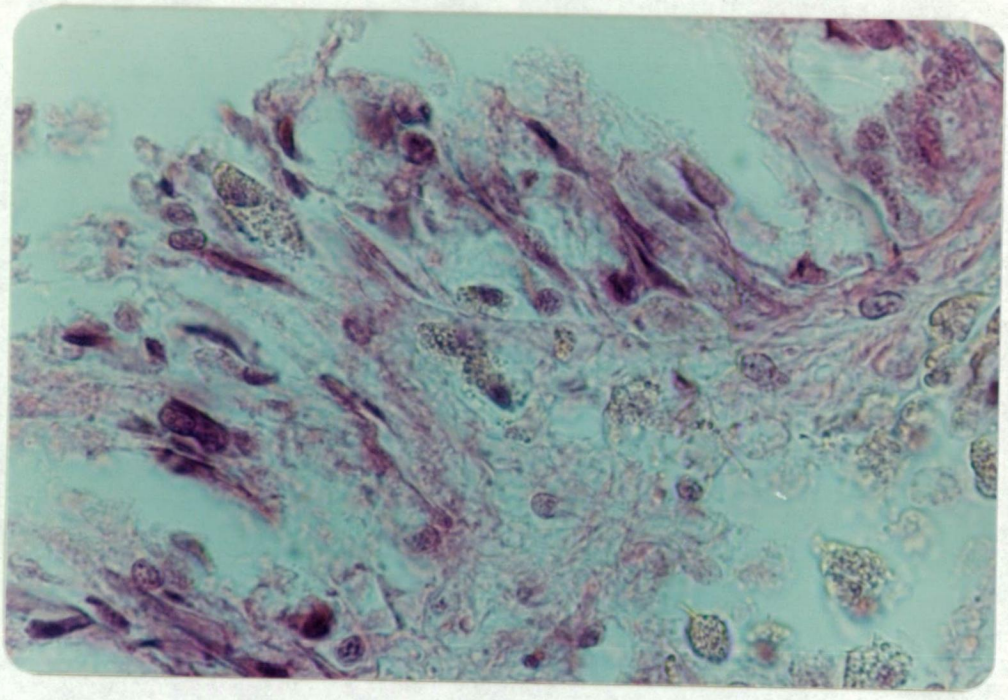

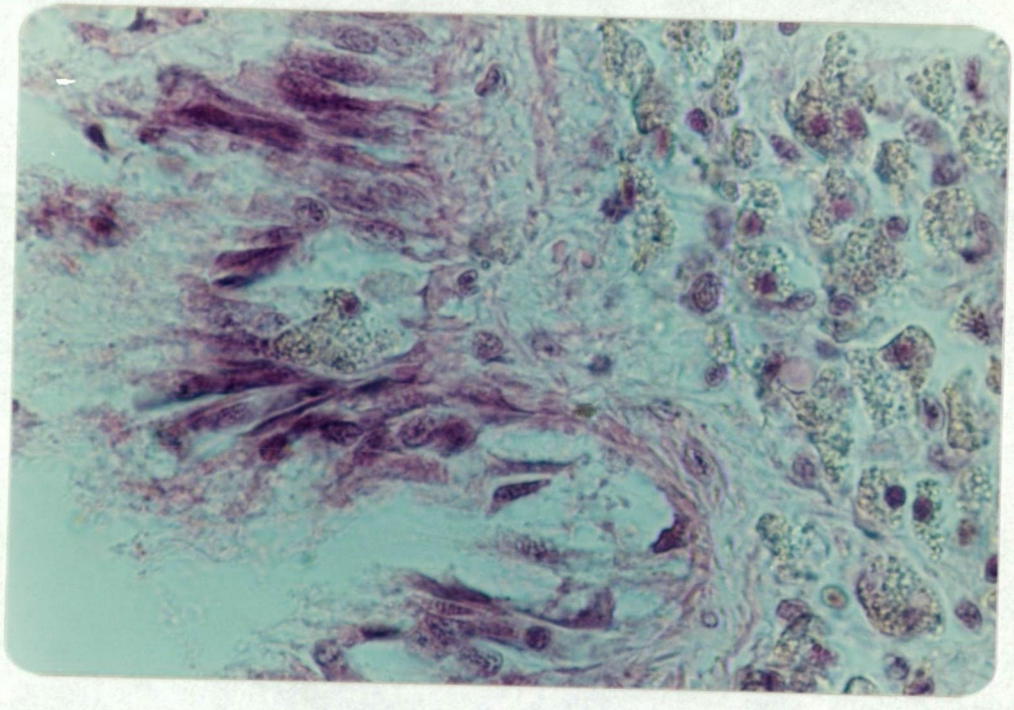

PLATE 18. LM (01). Large extracellular deposits of heavy metal within the lumen of the stomach, some of which are adherent to the epithelial surface. Note the 'lakes' of heavy metal within the epithelium and subjacent tissue. Zinc granulocytes are seen traversing the epithelium (bottom left).
Fixation: Formalin.
Stain: Sulphide-silver, safranin.
Mag. X 100.

PLATE 19. LM (01). Mid-gut showing small particles of heavy metal, 2-3 μm in diameter, adherent to the cilia. The fine stippling within the epithelium may be an artefact.
Fixation and stain as in Plate 18.
Mag. X 1000.

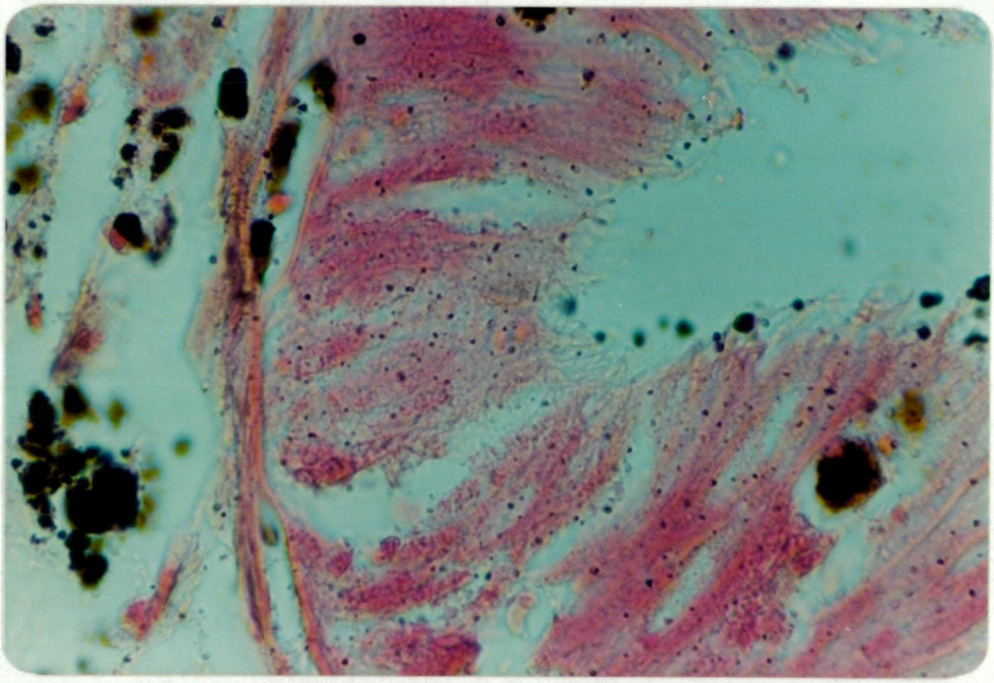

PLATE 20. LM (04). Zinc granulocytes, associated with epithelial cell debris, are present in the lumen of the mid-gut. Large numbers of zinc granulocytes are seen beneath the basement membrane with considerable numbers within the epithelium itself. Gonad (bottom right).

Fixation: H_2S-glutaraldehyde.

Stain: Sulphide-silver, safranin.

Mag. X 200.

PLATE 21. LM (04). Serial section stained with dithizone and counterstained with haematoxylin. Note the intact zinc granulocyte in the lumen of the gut and the zinc deposited on the epithelial aspect of the basement membrane.

Mag. X 200.

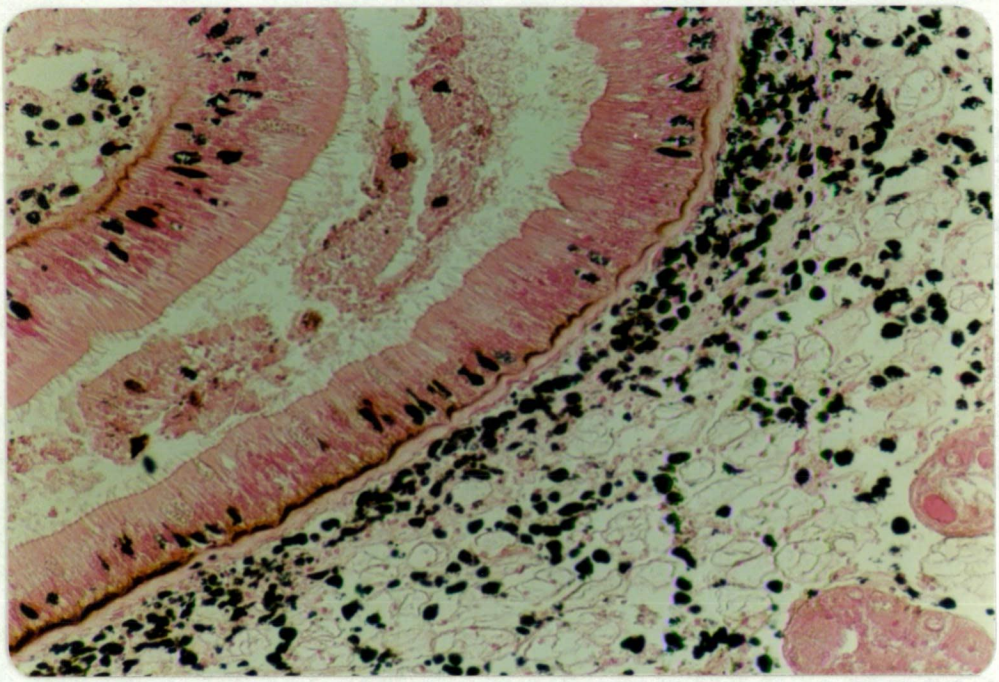

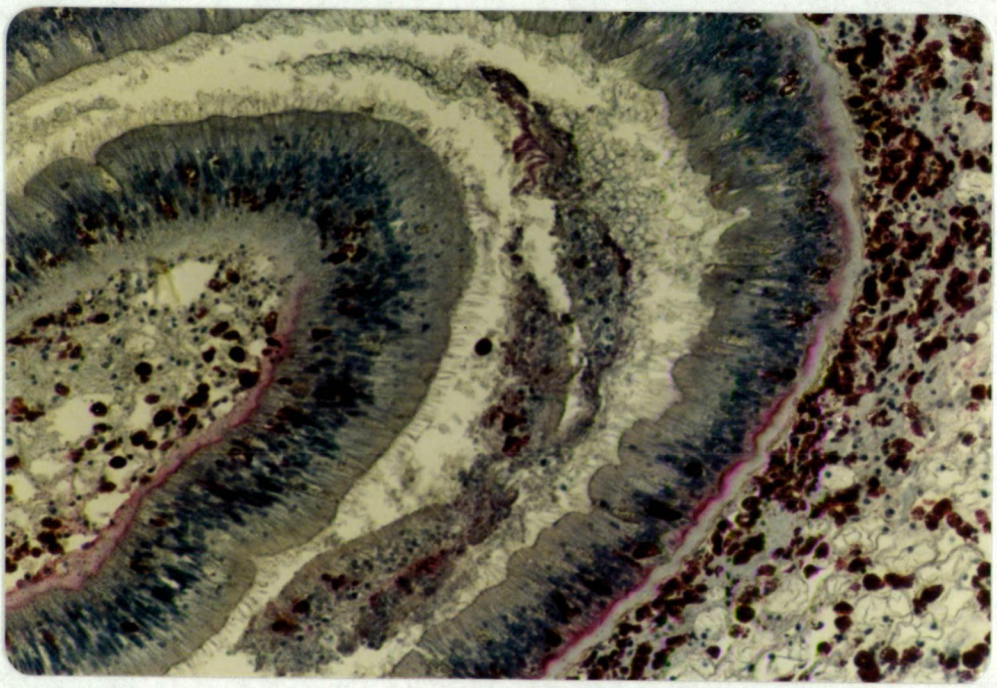

PLATE 22. LM (04). Intact zinc granules in lumen of mid-gut; same field as Plate 20.
Mag. X 400.

PLATE 23. LM (04). Intact zinc granulocyte in lumen of mid-gut; same field as Plate 21.
Mag. X 400.

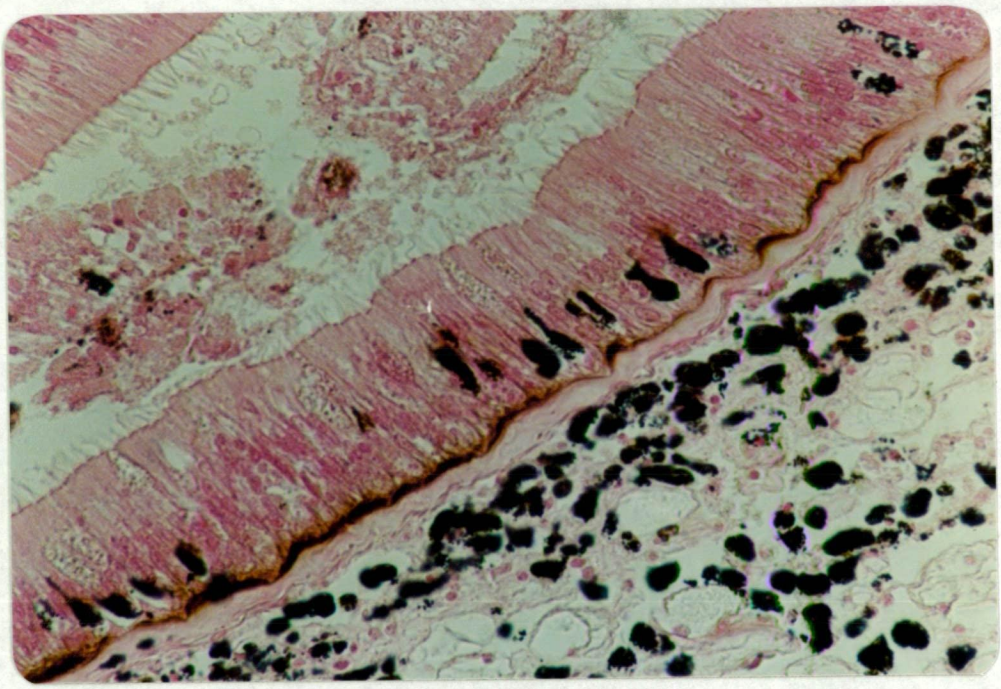

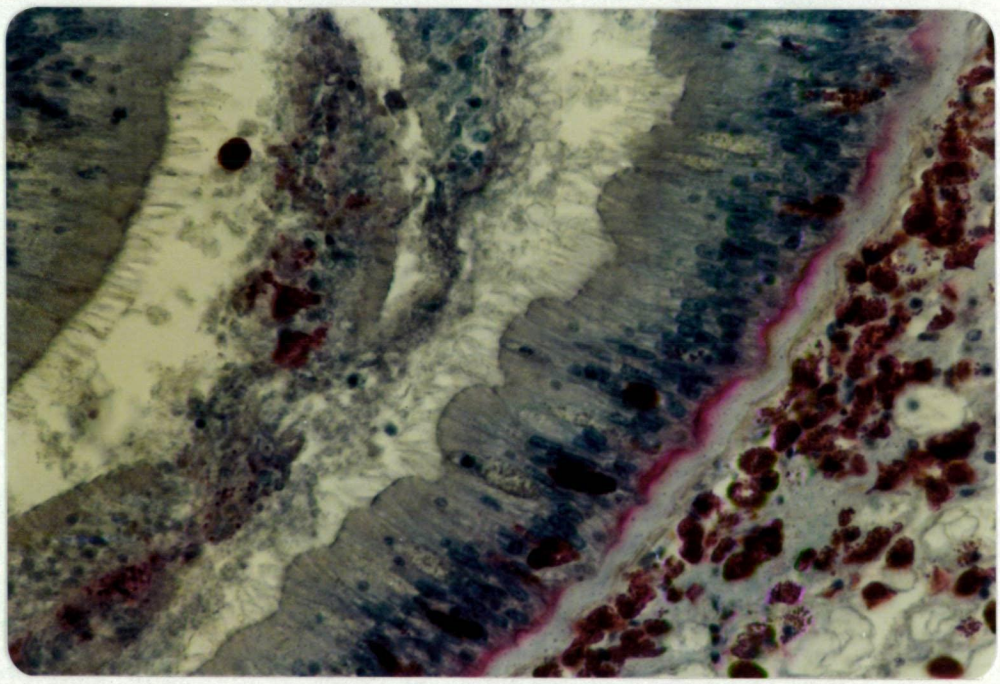

PLATE 24. LM (04). Lumen of mid-gut. Serial section of Plate 20, showing intact and disrupted zinc granulocytes associated with sloughed intestinal epithelium.
Stain: H & E.
Mag. X 1000.

PLATE 25. LM (04). Lumen of mid-gut showing intact zinc granules and cell detail of the sloughed epithelium. The ciliated epithelial borders of the mid-gut are visible (top left and bottom right).
Same field as Plate 20.
Mag. X 1000.

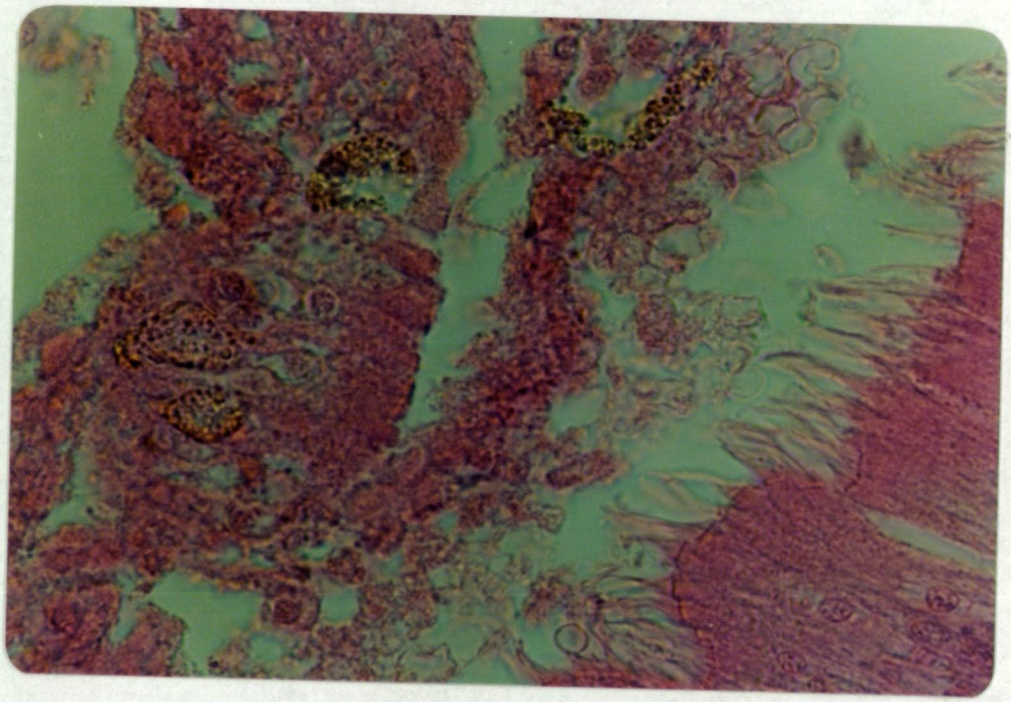

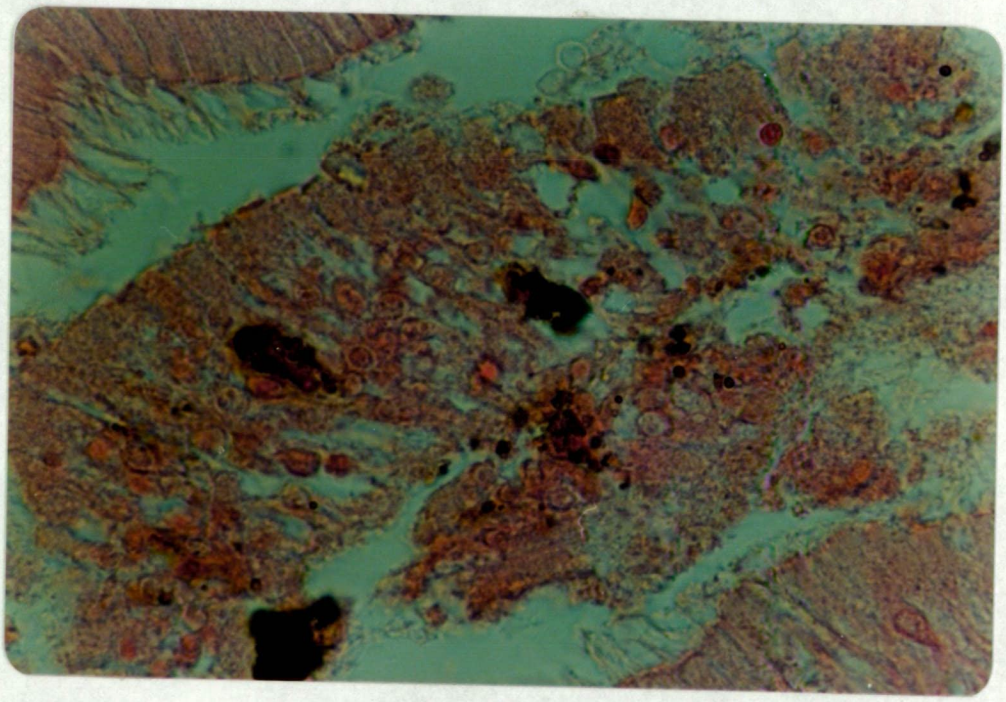

PLATE 26. LM (04). Detail of Plate 23.
Mag. X 1000.

PLATE 27. LM (04). Detail of Plate 23, showing cell morphology of the zinc granulocytes within the epithelium.
Mag. X 1000.

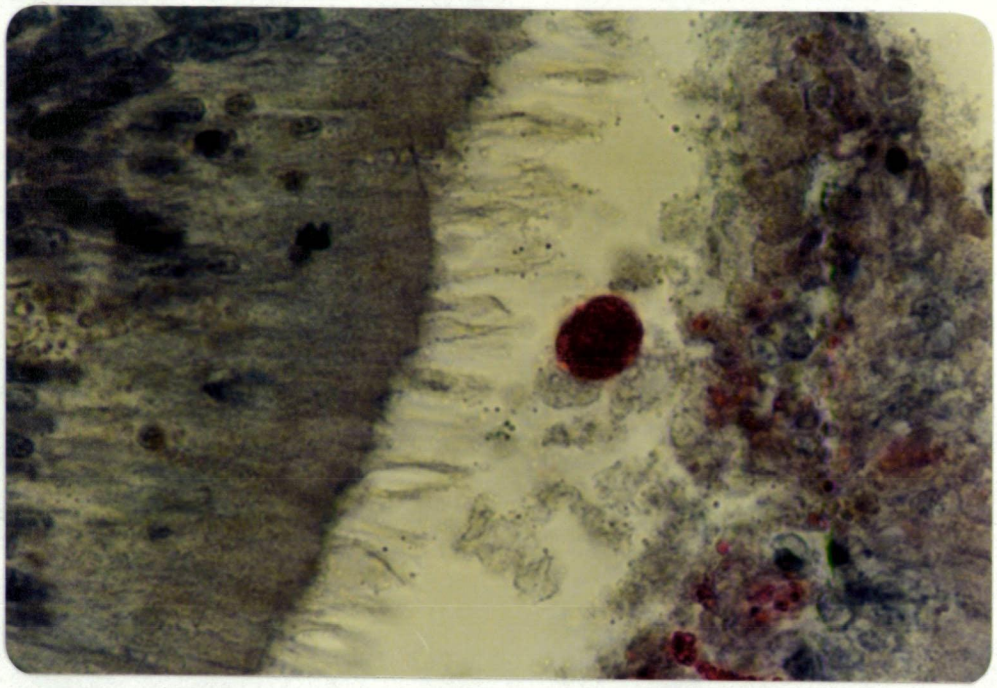

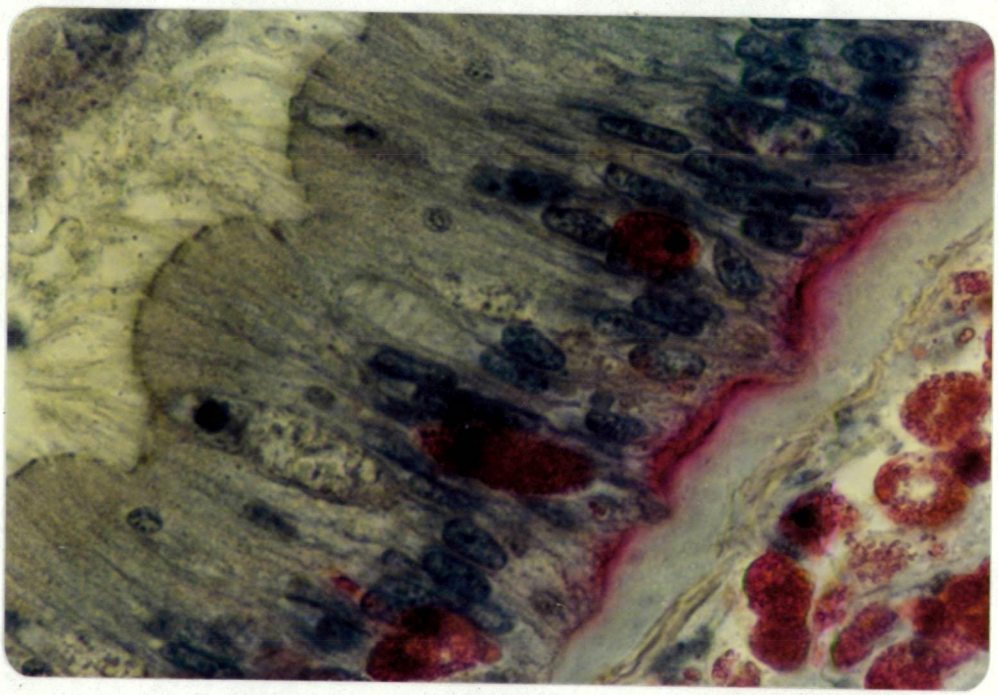

PLATE 28. LM (04). Continuation of field to the right of Plate 20. Zinc granulocytes within the vascular connective tissue, but not in the parenchyma of the gonad.
Mag. X 200.

PLATE 29. LM (04). Continuation of field to the right of Plate 28., showing the relationship of zinc granulocytes to the gonad. Edge of visceral mass (bottom right).
Mag. X 200.

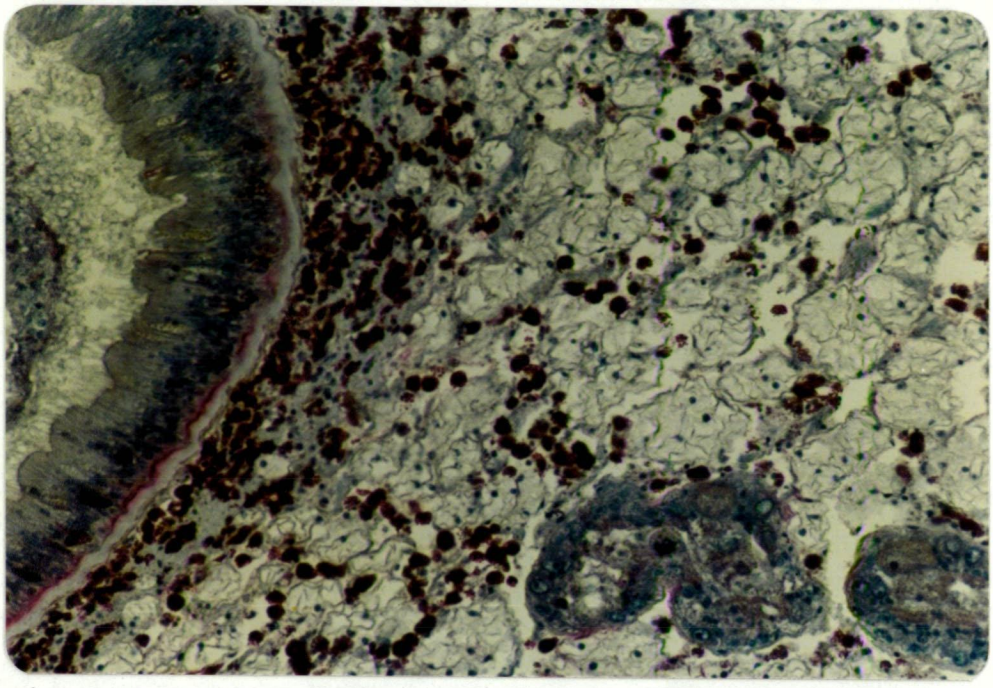

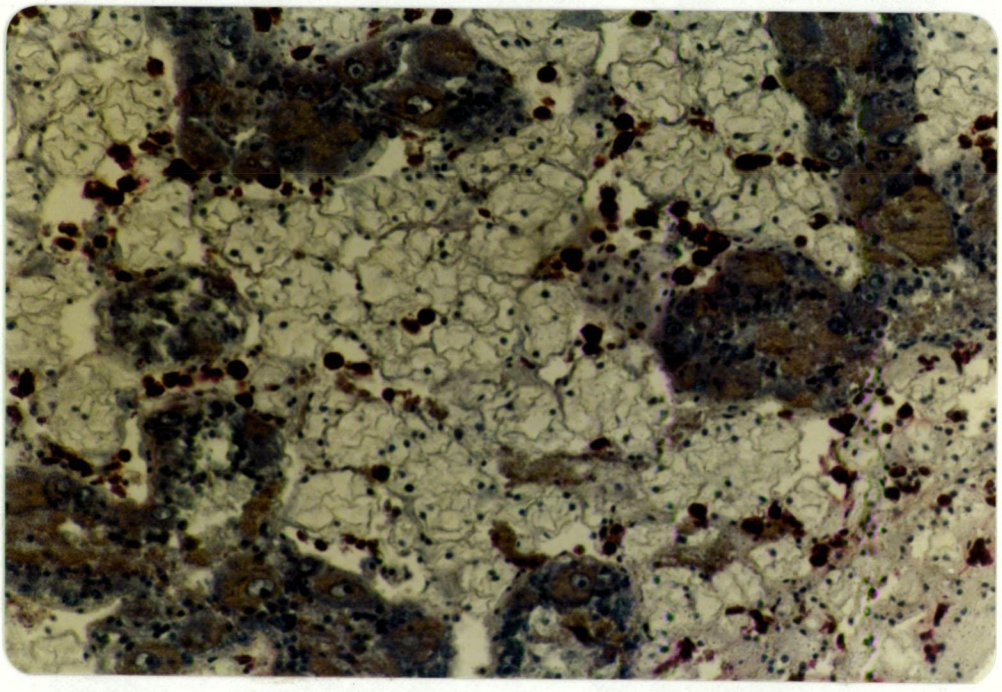

PLATE 30. LM (04). Intestinal tract and digestive diverticula showing the distribution of zinc granulocytes. Note that zinc granulocytes are situated beneath and within the epithelium of the digestive diverticula.

Fixation: H_2S-glutaraldehyde.

Stain: Alkaline dithizone, haematoxylin.

Mag. X 100.

PLATE 31. LM (04). Stomach wall. Note the abundant fibrous connective tissue beneath the conspicious basement membrane. Occasional smooth muscle fibres are seen (upper centre).

Fixation: H_2S-glutaraldehyde.

Stain: Masson's trichrome.

Mag. X 100.

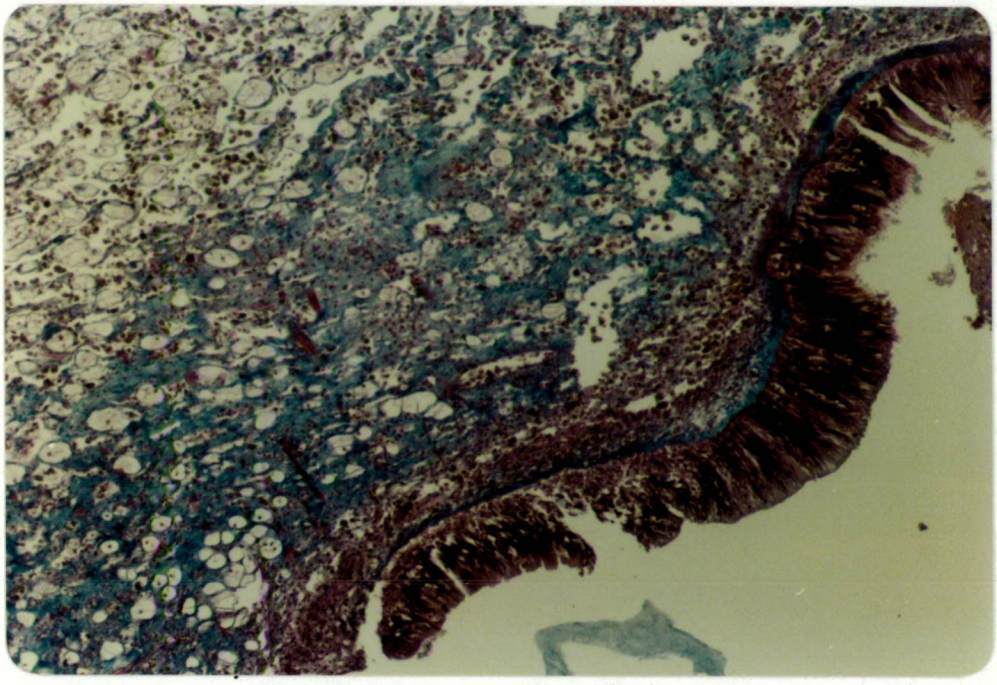

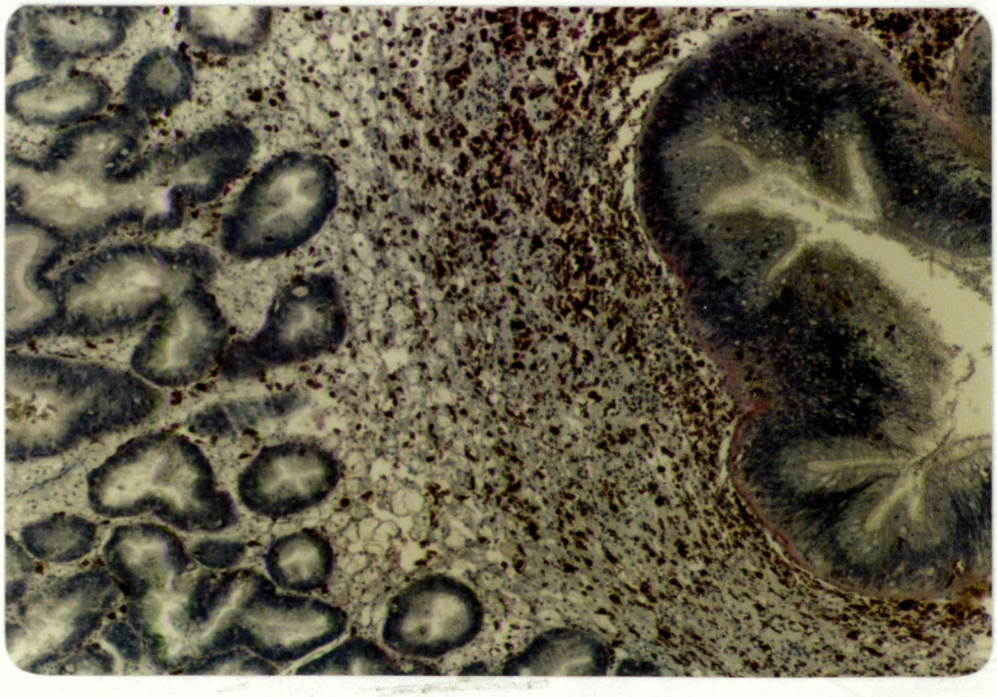

PLATE 32. LM (04). Serial section of Plates 21 to 27 showing the extent of the fibrous connective tissue surrounding the mid-gut.
Fixation: H_2S-glutaraldehyde.
Stain: Masson's trichrome.
Mag. X 100.

PLATE 33. LM (04). Centre of field in previous Plate (32.), showing the zinc granulocytes interspersed amongst the bands of fibrous tissue.
Fixation: H_2S-glutaraldehyde.
Stain: Masson's trichrome.
Mag. X 100.

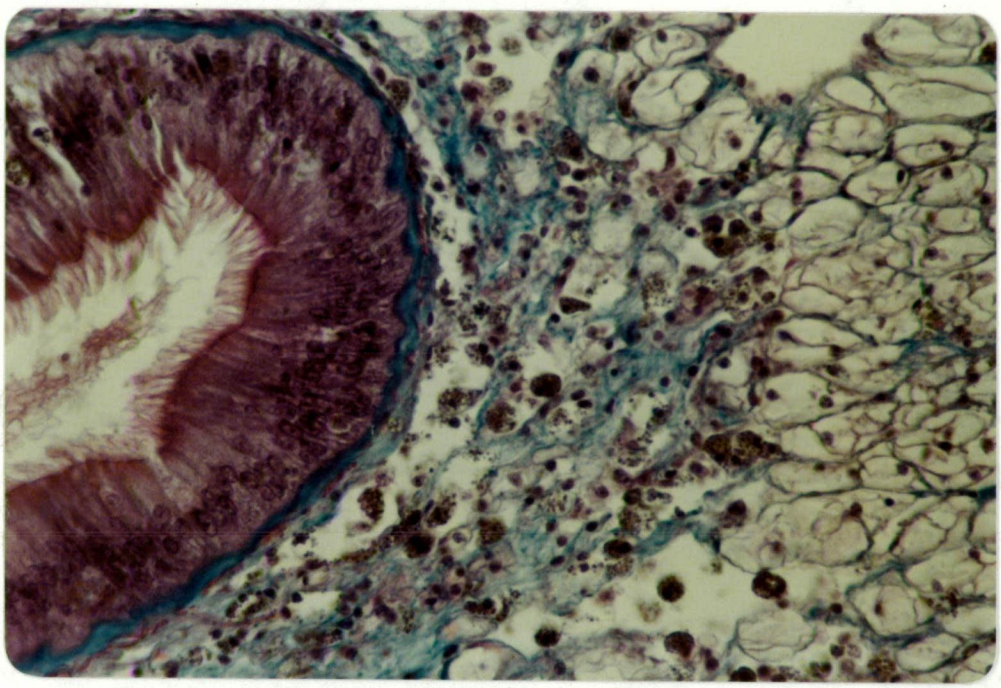

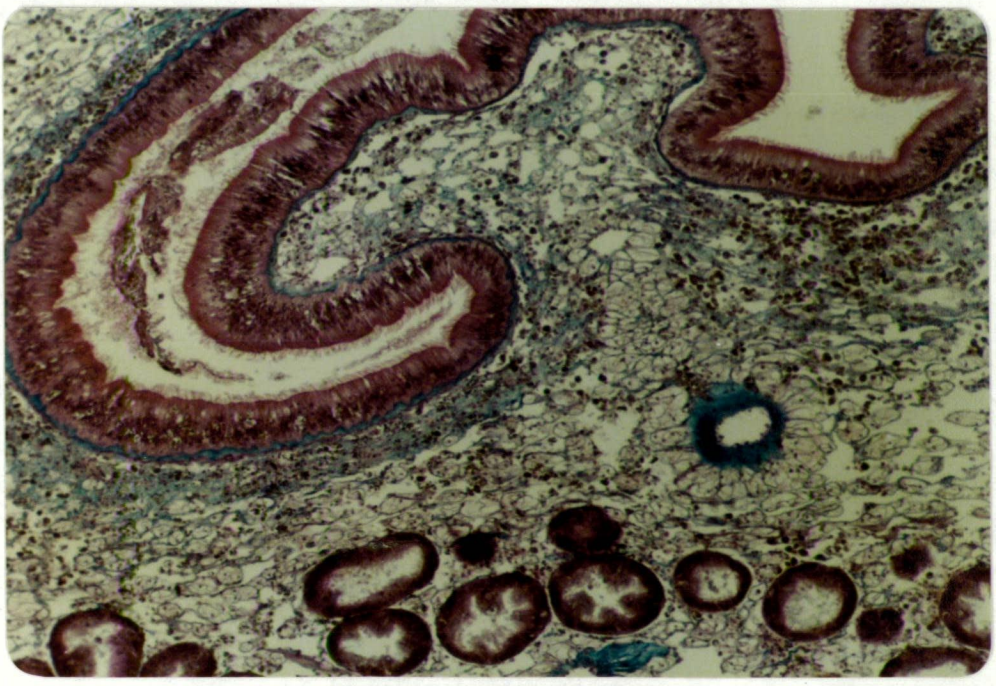

Transmission electron microscopy

The fine structure of the zinc granulocyte was examined by TEM. The method of preparing tissue for TEM determined the morphology of the granulocyte, just as it had done for LM.

Initially tissue (01) was fixed in glutaraldehyde, unsaturated with H_2S, and post-fixed in OsO_4. The zinc granulocytes in the subepithelial connective tissue of the intestinal tract were packed with numerous electron-dense granules (Plate 34). It was not possible to differentiate the electron-density contributed by the zinc from that produced by the adventitious metals osmium (acting as a stain) and arsenic (in the cacodylate buffer).

The granules were spherical with a maximum diameter of 1 μm and were mostly homogeneous, although some had a 'feathery' appearance (Plate 35). Granules were present intra- and extra-cellularly, those within the cell being enclosed within membranous vesicles. Many of the granulocytes were degenerate (Plate 36) with pyknotic nuclei and cytoplasm devoid of organelles. Some cells had lysed (Plate 37) and released their granules into the ECF, where they were lying unenclosed by a membrane and surrounded by empty vesicles.

Adventitious metals were eliminated from subsequent experiments by examining unstained tissue that had been fixed with H_2S-glutaraldehyde in phosphate buffer.

Electron-dense objects in the TEM now represented metals present *in vivo*.

The structure of the zinc granule after H_2S saturation was quite different, the TEM appearance corresponding to the 'hard' translucent spherules in the LM. The granules no longer had a homogeneous or 'feathery' appearance, but consisted of ring-like structures with an electron-dense periphery and electron-lucent core (Plate 38).

The cell membrane had been 'etched' by the precipitated zinc sulphide and many of the granules had 'tails' that spiraled out from the parent 'body' (Plate 39), suggesting that the granules had been formed by the accretion of smaller particles. As before many of the granulocytes were degenerate and granules were free in the ECF (Plate 40).

The granulocytes varied considerably in their morphology, some having 'bristle-like pseudopodia' (Takatsuki, 1934), formed by fusion of the cell membrane with zinc sulphide (Plate 41). When the sulphide-silver technique was applied to thin sections, silver 'grains' were deposited on the argyrophilic zinc sulphide granules (Plate 42).

TEM of the intestinal epithelium (03) revealed intracellular particles of zinc sulphide that differed from the granules observed in the subepithelial connective tissue of (01) and (02). The particles

varied in size and shape (Plate 43), many of them less than 0.5 μm in diameter and may have been taken up from the gut lumen by phagocytic cells.

The problems of:

(i) differing morphology of the zinc granule and

(ii) migration pathway of the zinc granulocyte, were investigated by TEM of the mid-gut epithelium (04). Zinc granulocytes were observed in the epithelium (Plate 44), and the basement membrane was stippled with a fine deposit of zinc (Plates 45 & 46) on its epithelial aspect (cf. Plate 27). Extracellular zinc granules were seen beneath the basement membrane (Plate 46) together with zinc granulocytes (Plate 47 & 48) having the same morphology as those observed within the epithelium, and presumably about to emigrate into the gut lumen.

PLATE 34. TEM (01). Zinc granulocytes in the subepithelial connective tissue of the intestinal tract. Individual granules are homogeneous and uniform in size with a diameter not exceeding 1 μm. Intracellular granules are enclosed within membranous vesicles. Extracellular granules are not enclosed by a membrane and lie free in the ECF together with empty vesicles.

'White-holes' are artefacts produced by granules being torn out of the embedding medium during sectioning.

Fixation: Glutaraldehyde in cacodylate buffer.

Block stained with OsO_4 only.

Mag. X 10,000.

Poor contrast due to the omission of other heavy metal staining (i.e. uranyl acetate and lead citrate).

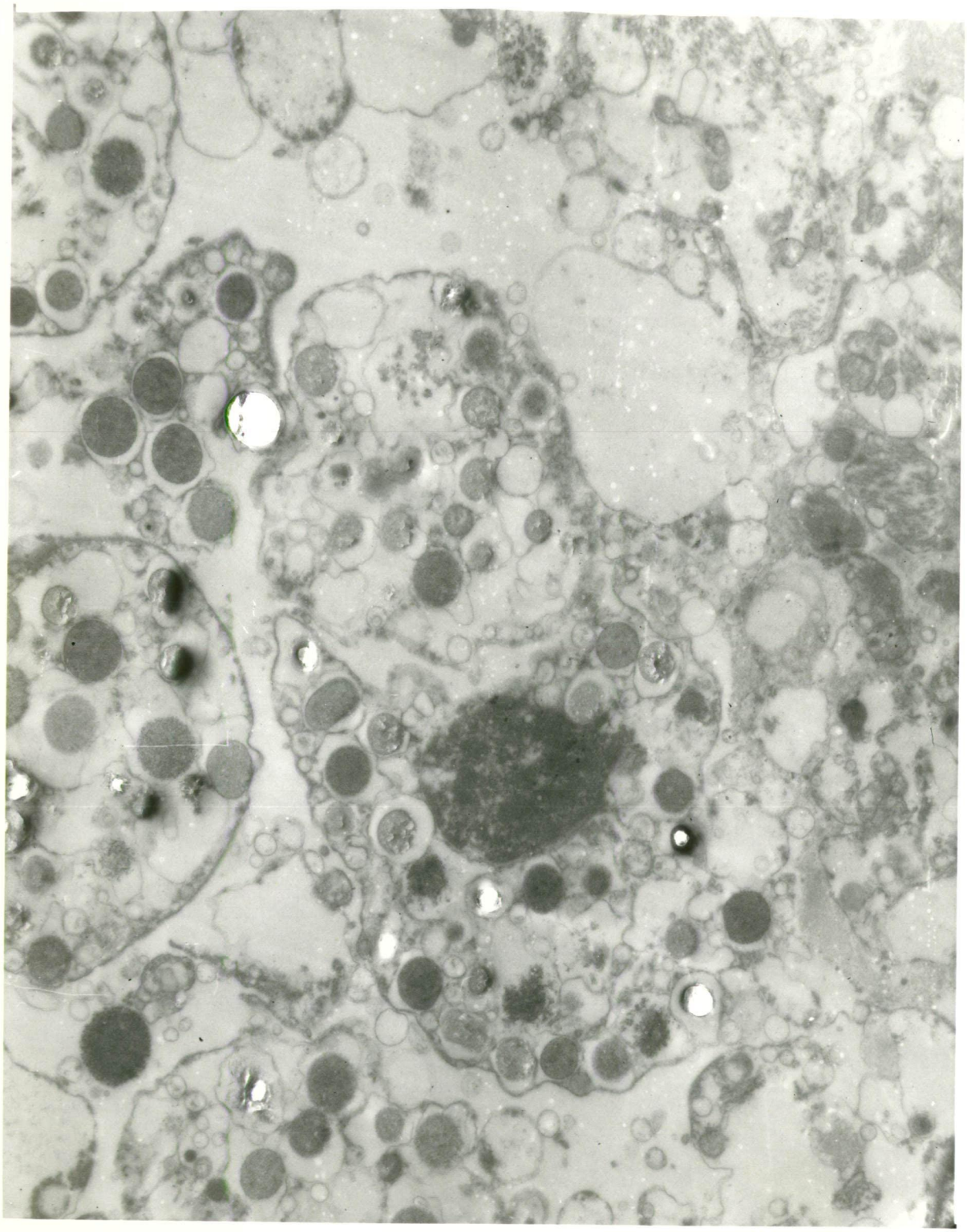

PLATE 35. TEM (01). Field adjacent to Plate 34. There is evidence of cytopathology. Zinc granules and empty vesicles are scattered through the ECF. A band of collagen runs down the field (left of centre) and the adjacent zinc granulocyte is degenerate, with a pyknotic nucleus and a disrupted cell membrane. Normal metabolic organelles are absent. Note the 'feathery' appearance of some of the granules.

Fixation: Glutaraldehyde in cacodylate buffer.

Block stained with OsO_4 only.

Mag. X 10,000.

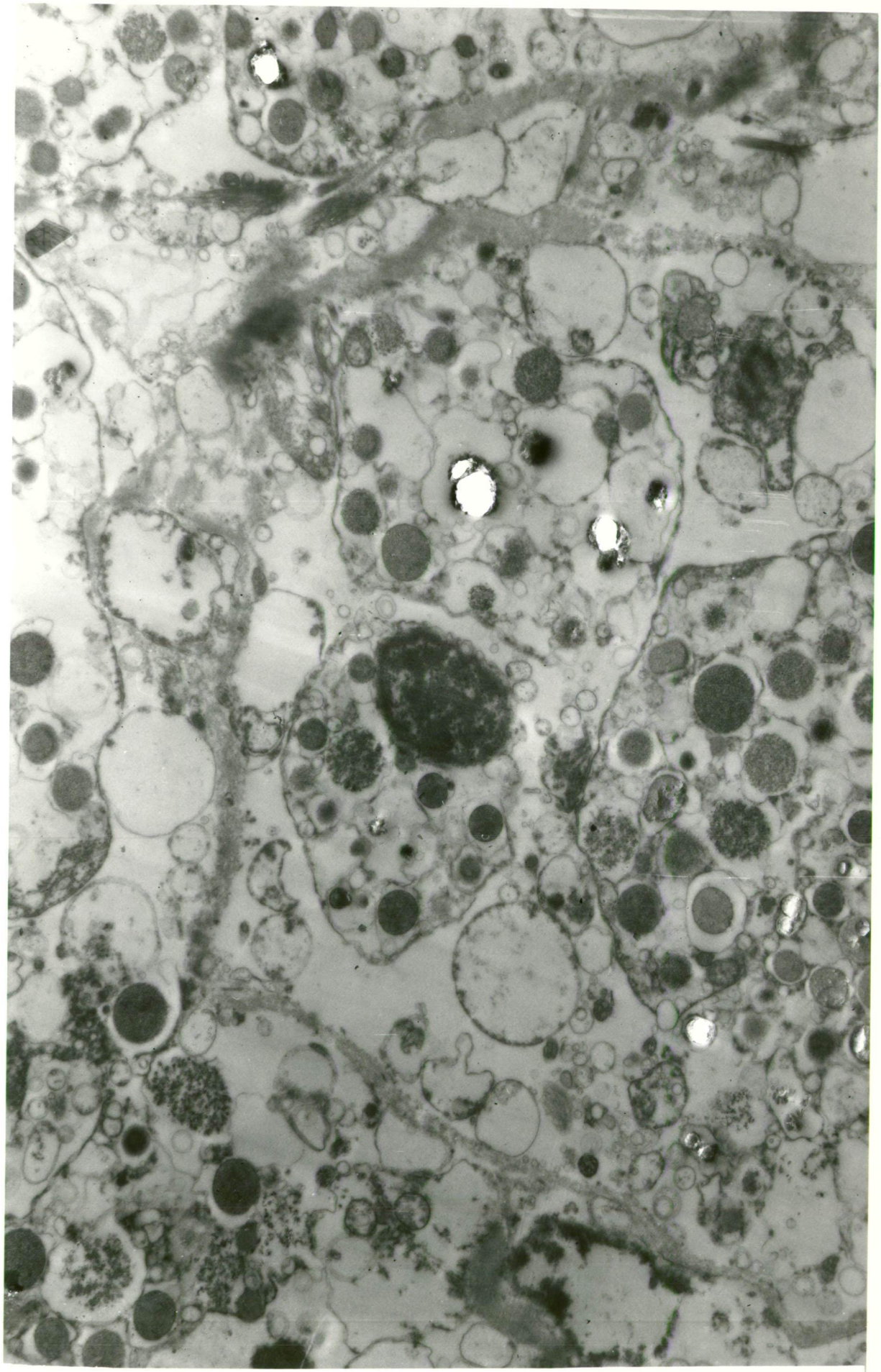

PLATE 36. TEM (01). Field adjacent to Plate 35. A group of moribund zinc granulcoytes, surrounded by collagen fibres. The cell (top) is on the point of lysis with swollen cytoplasm. The cell (bottom), with a pyknotic nucleus, is distended with vesicles containing zinc granules.
Fixation: Glutaraldehyde in cacodylate buffer.
Block stained with OsO_4 only.
Mag. X 10,000.

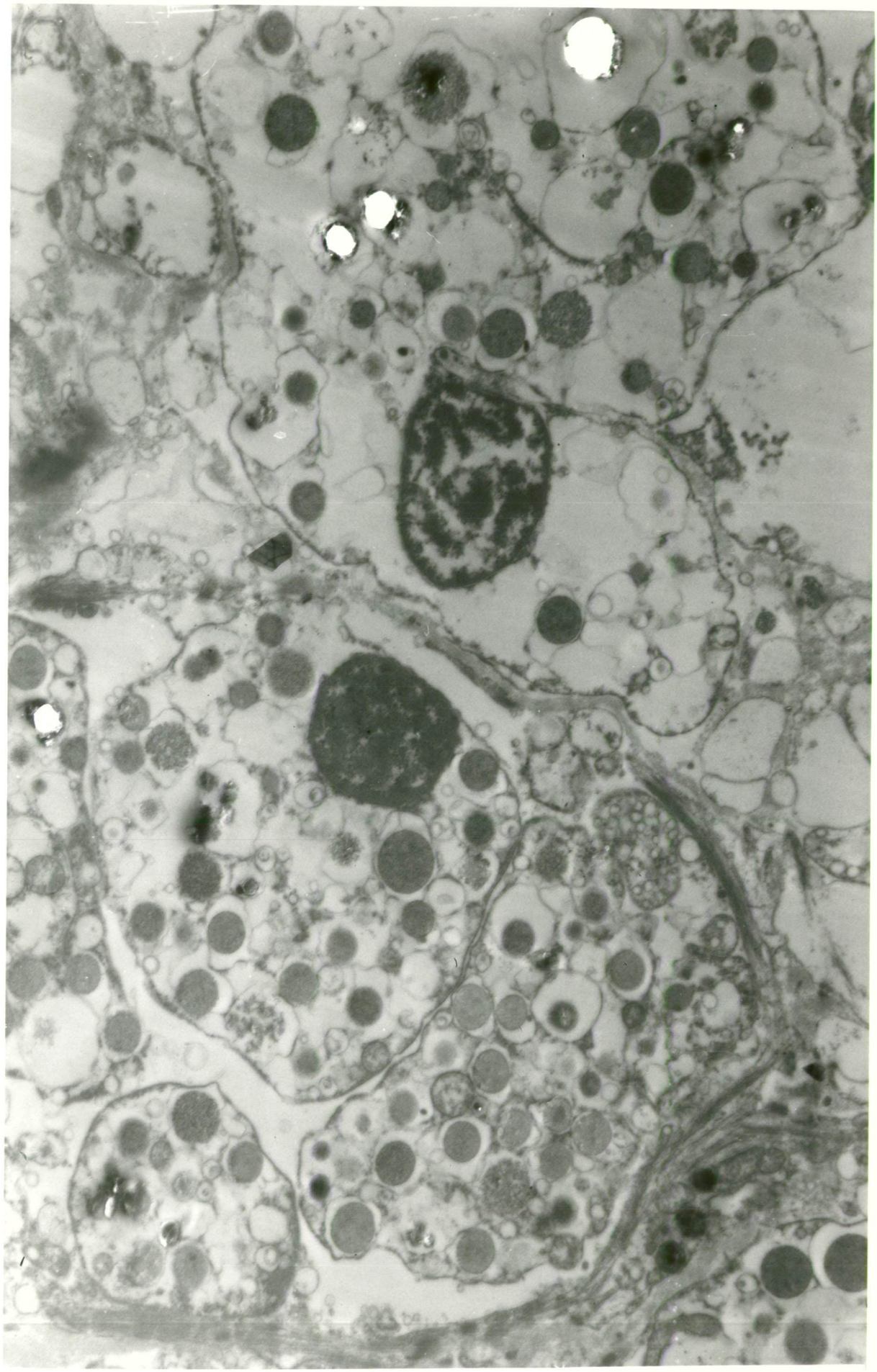

PLATE 37. TEM (01). Field adjacent to Plate 36. This zinc granulocyte has undergone lysis, releasing its granules into the ECF, where there are a number of empty vesicles.

Fixation: Glutaraldehyde in cacodylate buffer.

Block stained with OsO_4 only.

Mag. X 10,000.

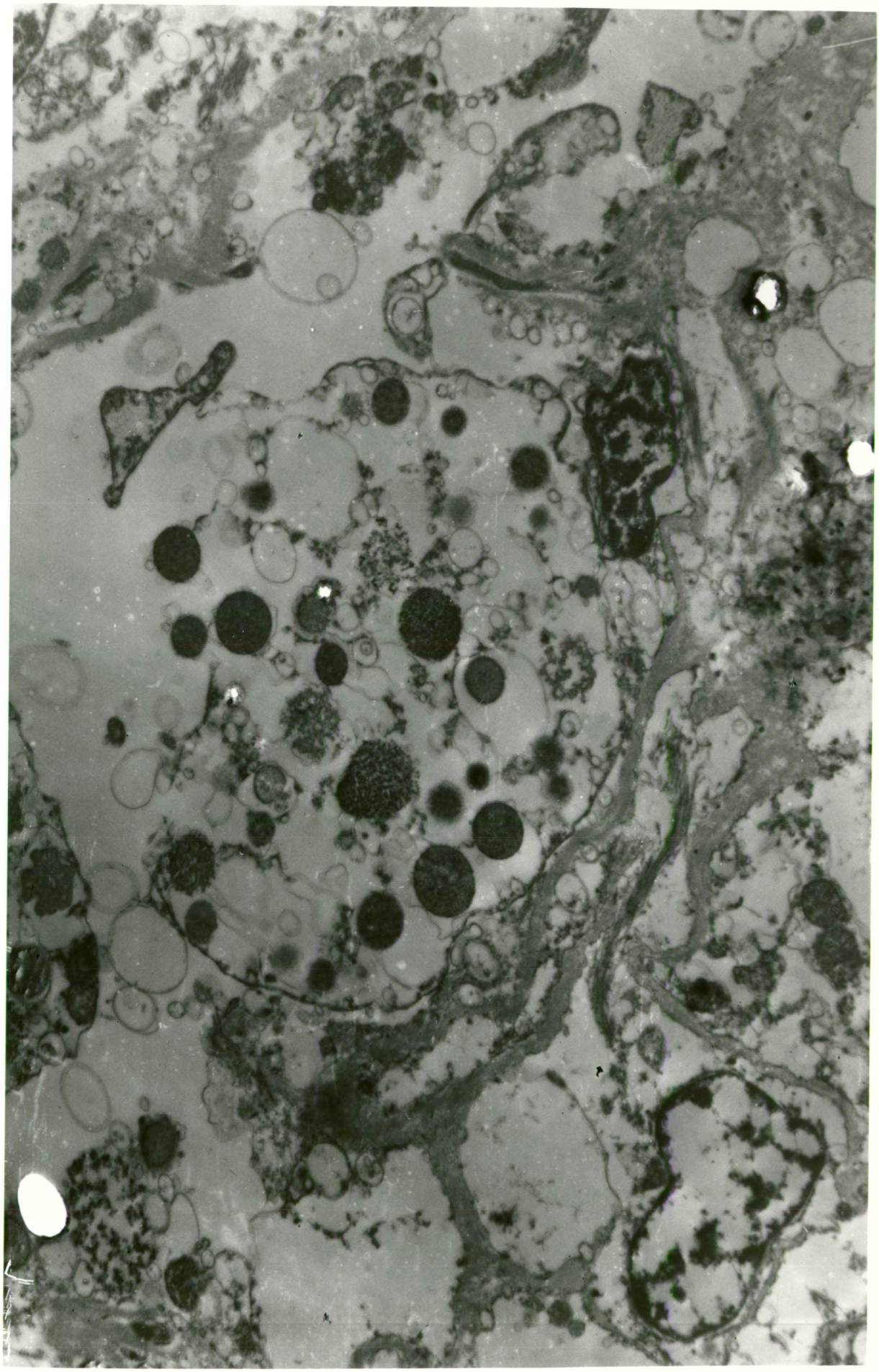

PLATE 38. TEM (02). Zinc granulocyte in the subepithelial connective tissue of the intestinal tract. The whole cell has been 'etched' by the precipitated zinc sulphide. The granules have an electron-dense periphery, surrounding an electron-lucent core. They are enclosed in membranous vesicles, some of which are empty and one (left) is releasing a granule into the ECF.

Fixation: H_2S-glutaraldehyde.

Unstained.

Mag. X 20,000.

PLATE 39. TEM (02). Field adjacent to Plate 38. The nucleus of the zinc granulocyte is clearly seen, although the section is unstained. The cell membrane has been 'etched' by the precipitated zinc sulphide. The granules vary in appearance, some of them having 'tails' that spiral out from the parent 'body'. This suggests that the granules may be formed by the accretion of smaller particles.
Fixation: H_2S-glutaraldehyde.
Mag. X 20,000.
Unstained.

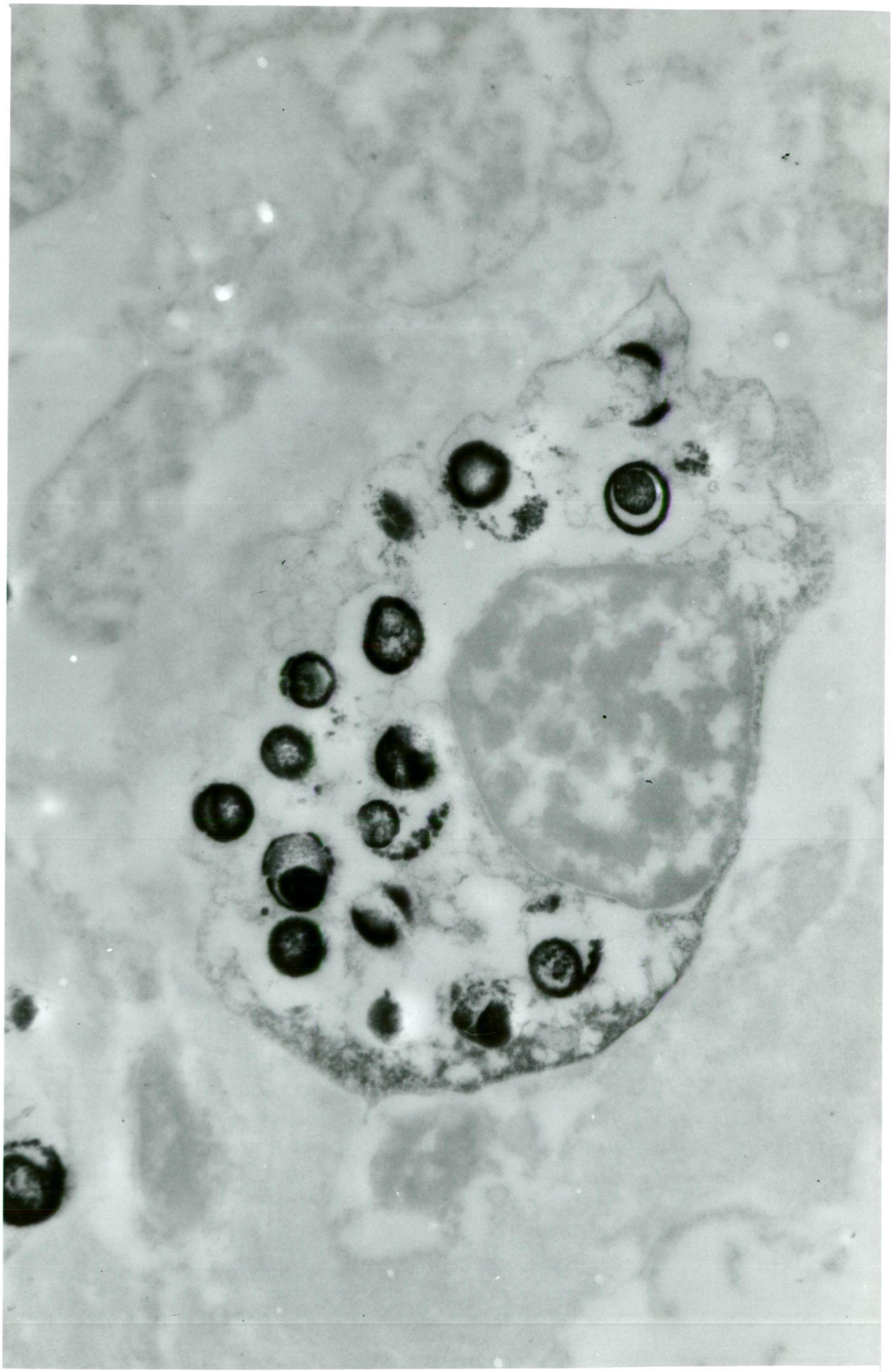

PLATE 40. TEM (02). Field adjacent to Plate 39.
Zinc granulocyte with a degenerate nucleus.
The granules vary in structure and some
appear to be free in the ECF.
Fixation: H_2S-glutaraldehyde.
Unstained.
Mag. X 20,000.

PLATE 41. TEM (02). Field adjacent to Plate 40.
Two zinc granulocytes showing the variation in their cellular morphology. The cell membrane is often protruded into a 'bristle-like pseudopodium', which is formed by the zinc sulphide fusing the cell membrane (cf. Plate 11.).
Fixation: H_2S-glutaraldehyde.
Unstained.
Mag. X 20,000.

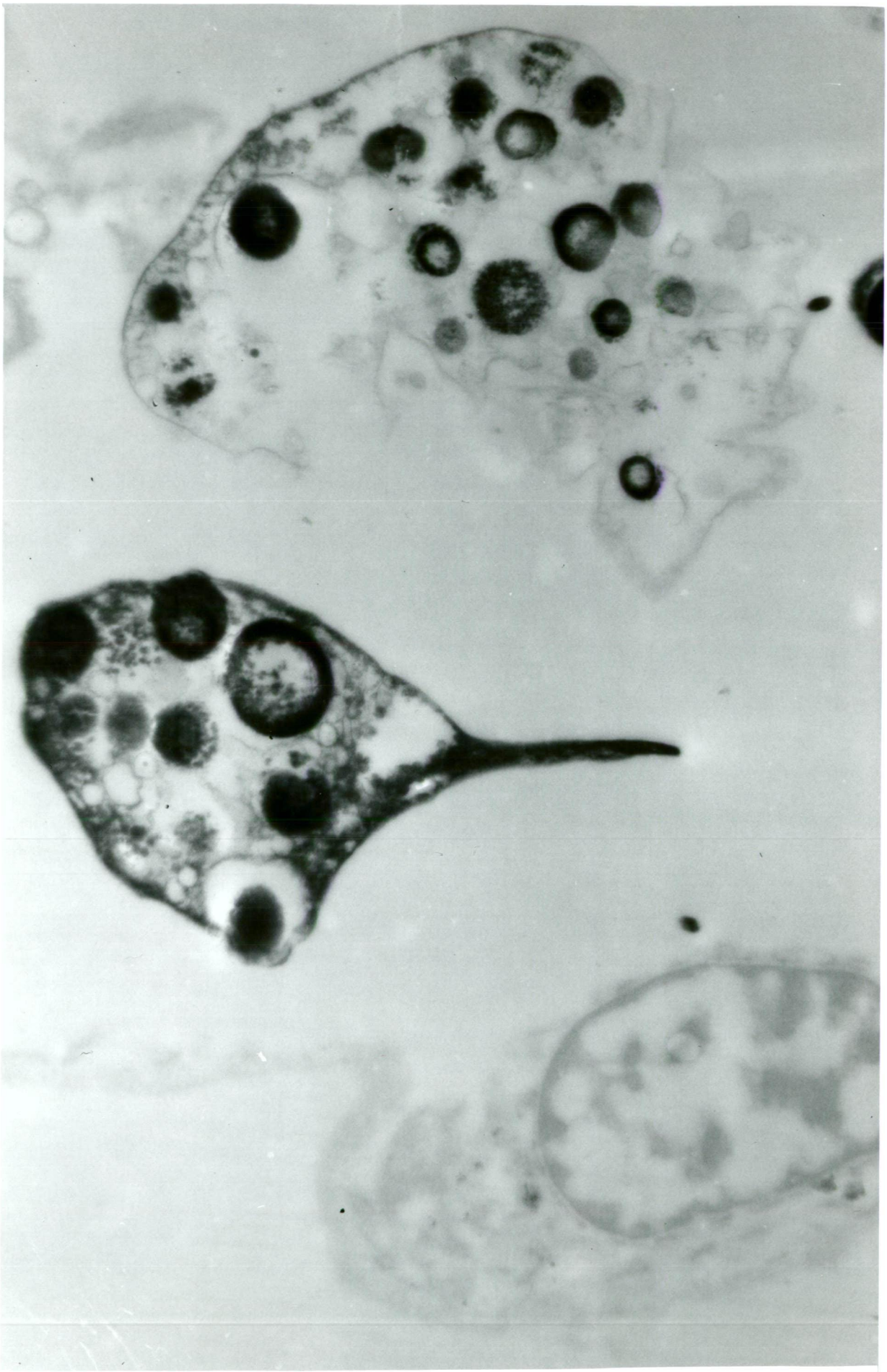

PLATE 42. TEM (02). 80 nm section through the cytoplasm of a zinc granulocyte developed by the sulphide-silver technique. Note the very electron-dense silver 'grains' (100 nm diameter) deposited on the zinc sulphide granules (1 μm diameter). The zinc sulphide granules are less electron-dense than the silver 'grains' and the 'signet-ring' appearance of the former is noticeable.

Fixation: H_2S-glutaraldehyde.

Stain: Sulphide-silver.

Mag. X 50,000.

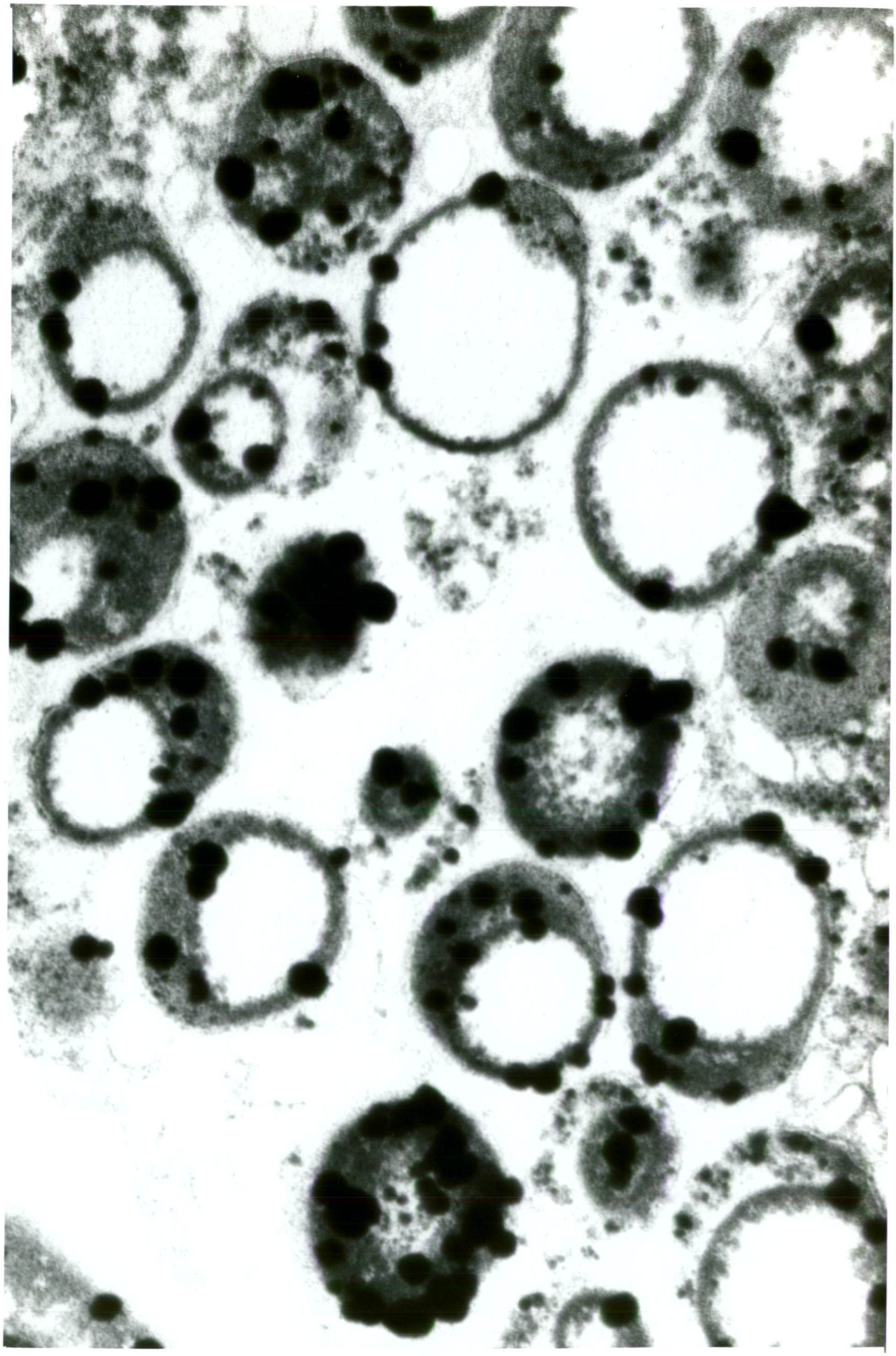

PLATE 43. TEM montage (03). Intestinal epithelium with basement membrane (bottom). Electron-dense particles of zinc are situated intracellularly. The particles vary in size and shape, many of them less than 0.5 μm in diameter. They differ from the intracellular zinc granules in the subepithelial connective tissue and may have been taken up from the gut lumen by phagocytic cells.

Fixation: H_2S-glutaraldehyde.

Unstained.

Mag. X 6,700.

PLATE 44. TEM (04). Mid-gut epithelium. Zinc granulocyte, similar to that in (02), traversing the epithelium. It is laden with granules, although some vesicles contain only a fine rim of zinc. Presumably the cell is emigrating into the lumen.

Fixation: H_2S-glutaraldehyde.

Unstained.

Mag. X 10,000.

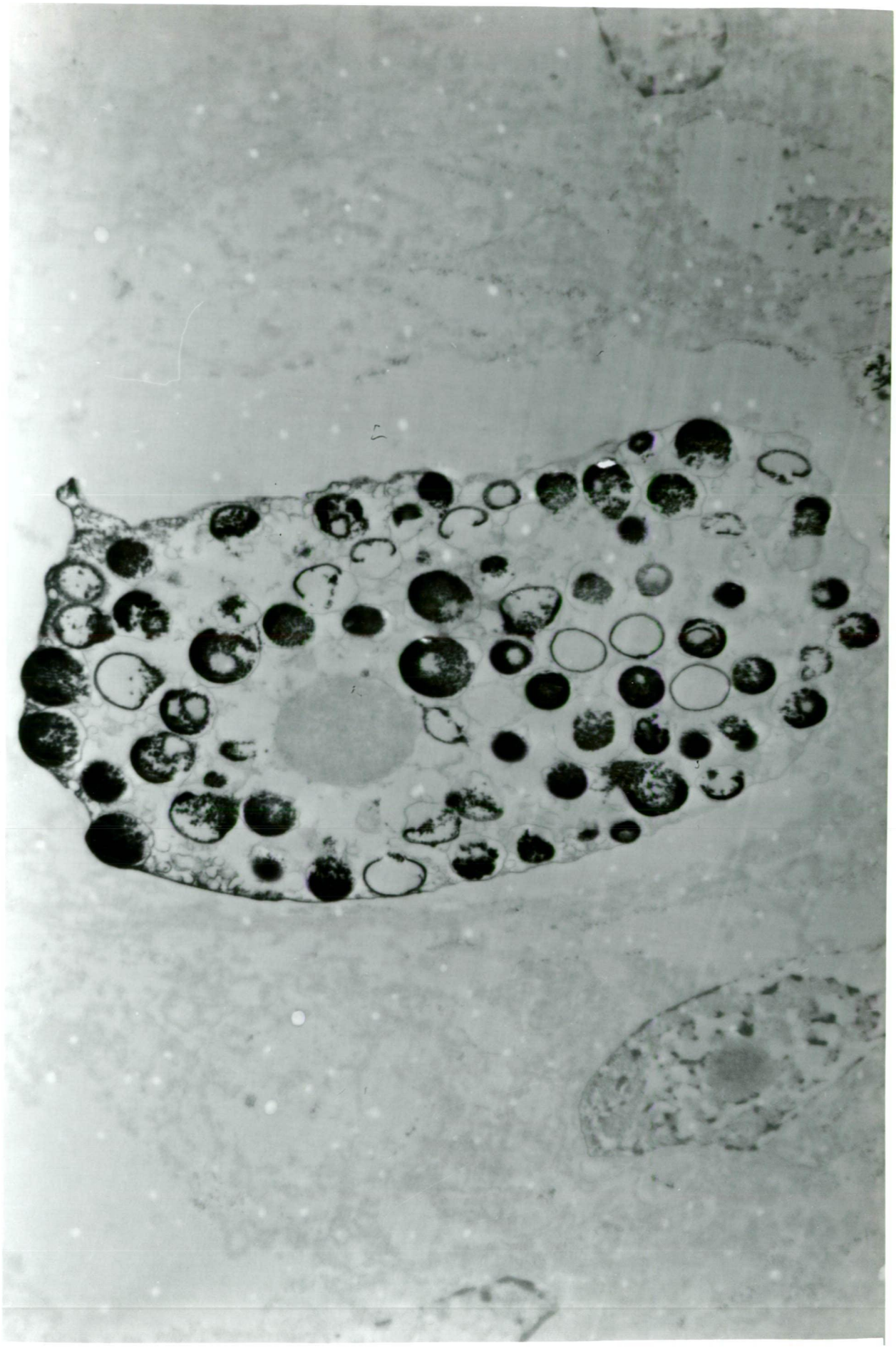

PLATE 45. TEM (04). Consecutive field to Plate 44. Base of mid-gut epithelium. Note the fine stippling of zinc on the epithelial aspect of the basement membrane (bottom right). Cf. Plate 27.

Fixation: H_2S-glutaraldehyde.

Unstained.

Mag. X 10,000.

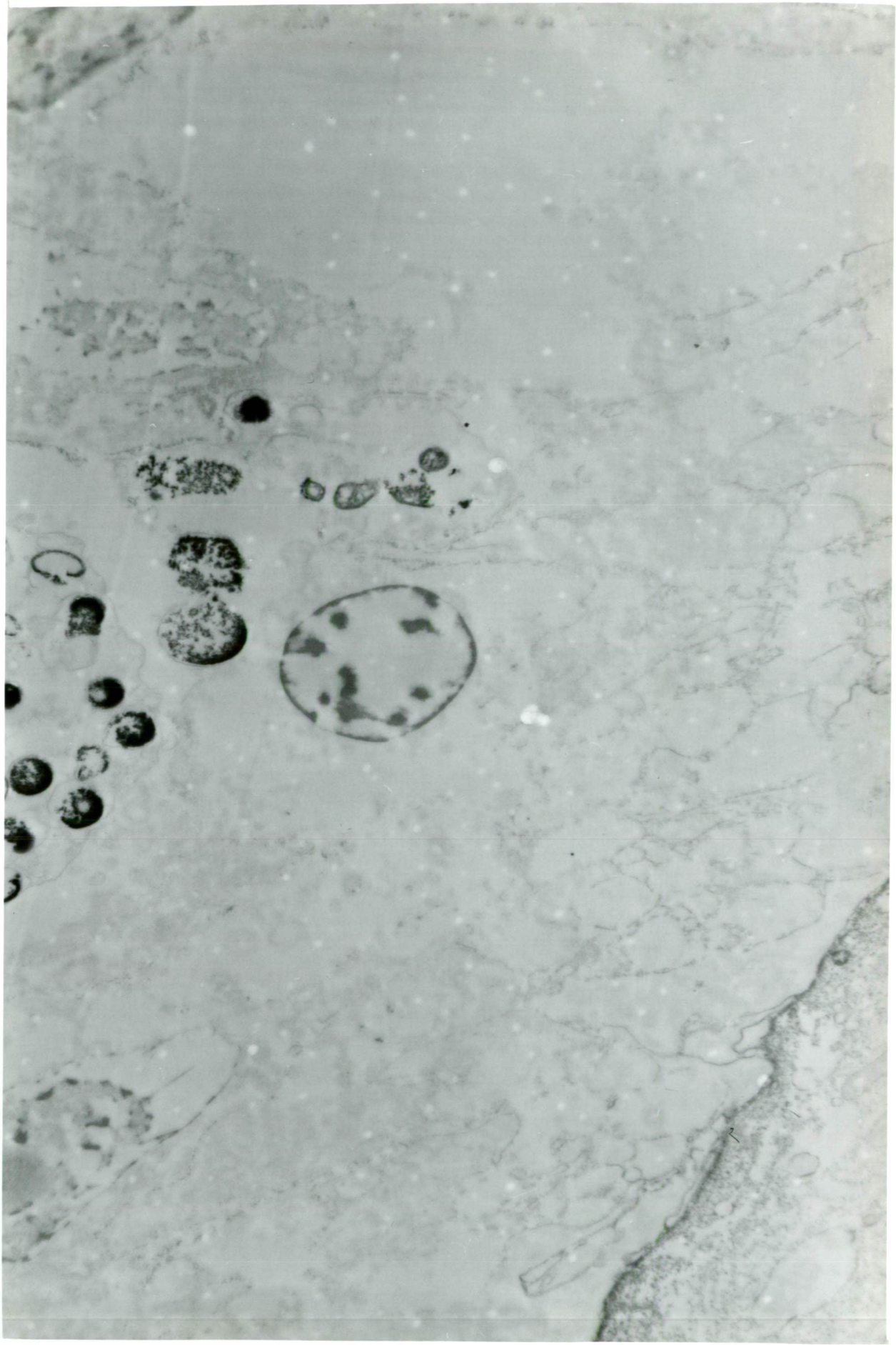

PLATE 46. TEM (04). Consecutive field to Plate 45. Basement membrane of mid-gut. Zinc granules are present in the ECF subjacent to the basement membrane.

Fixation: H_2S-glutaraldehyde.

Unstained.

Mag. X 10,000.

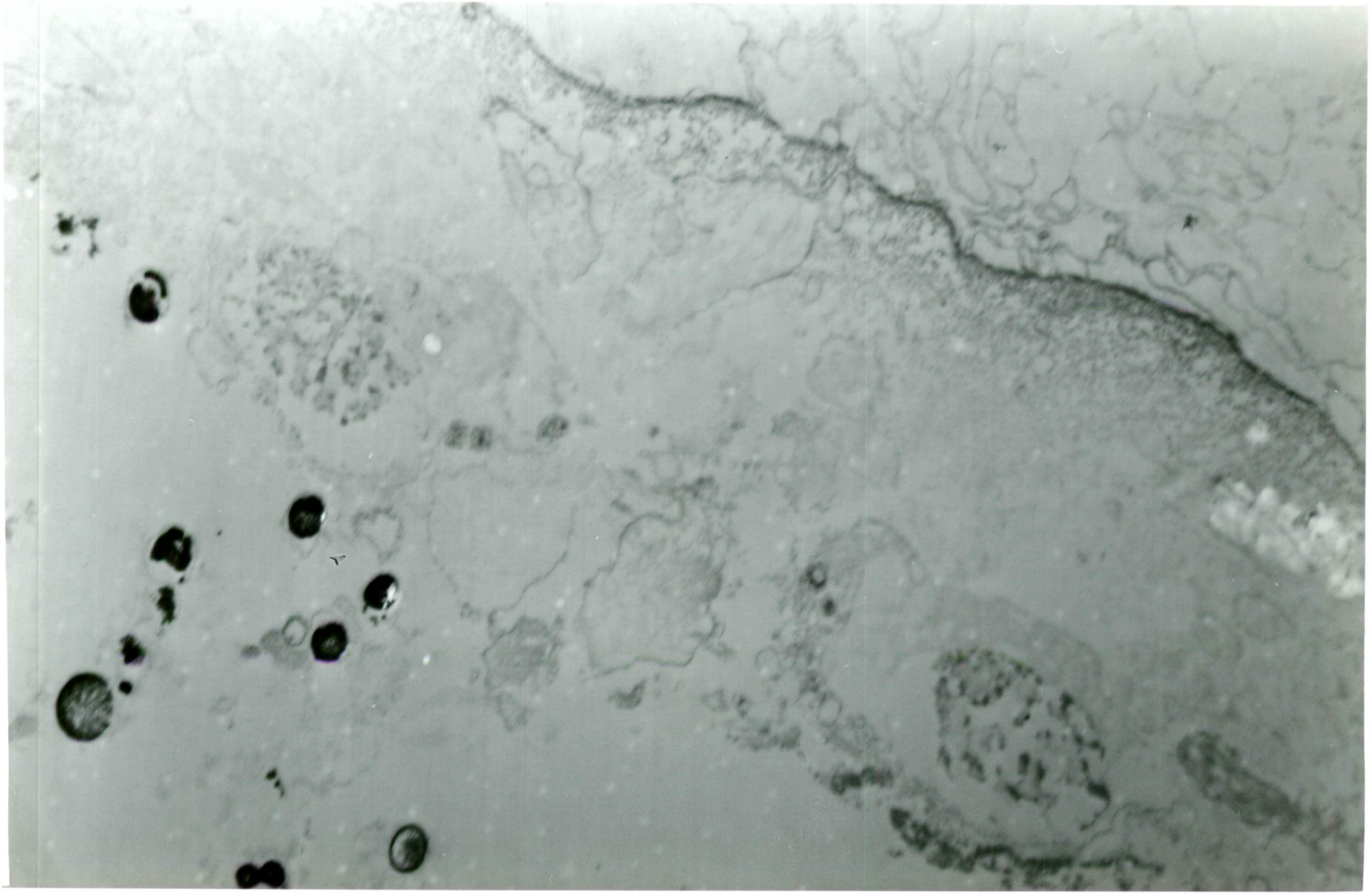

PLATE 47. TEM (04). Consecutive field to Plate 46.
Subepithelial zone of mid-gut. Part of
zinc granulocyte (bottom right).
Fixation: H_2S-glutaraldehyde.
Unstained.
Mag. X 10,000.

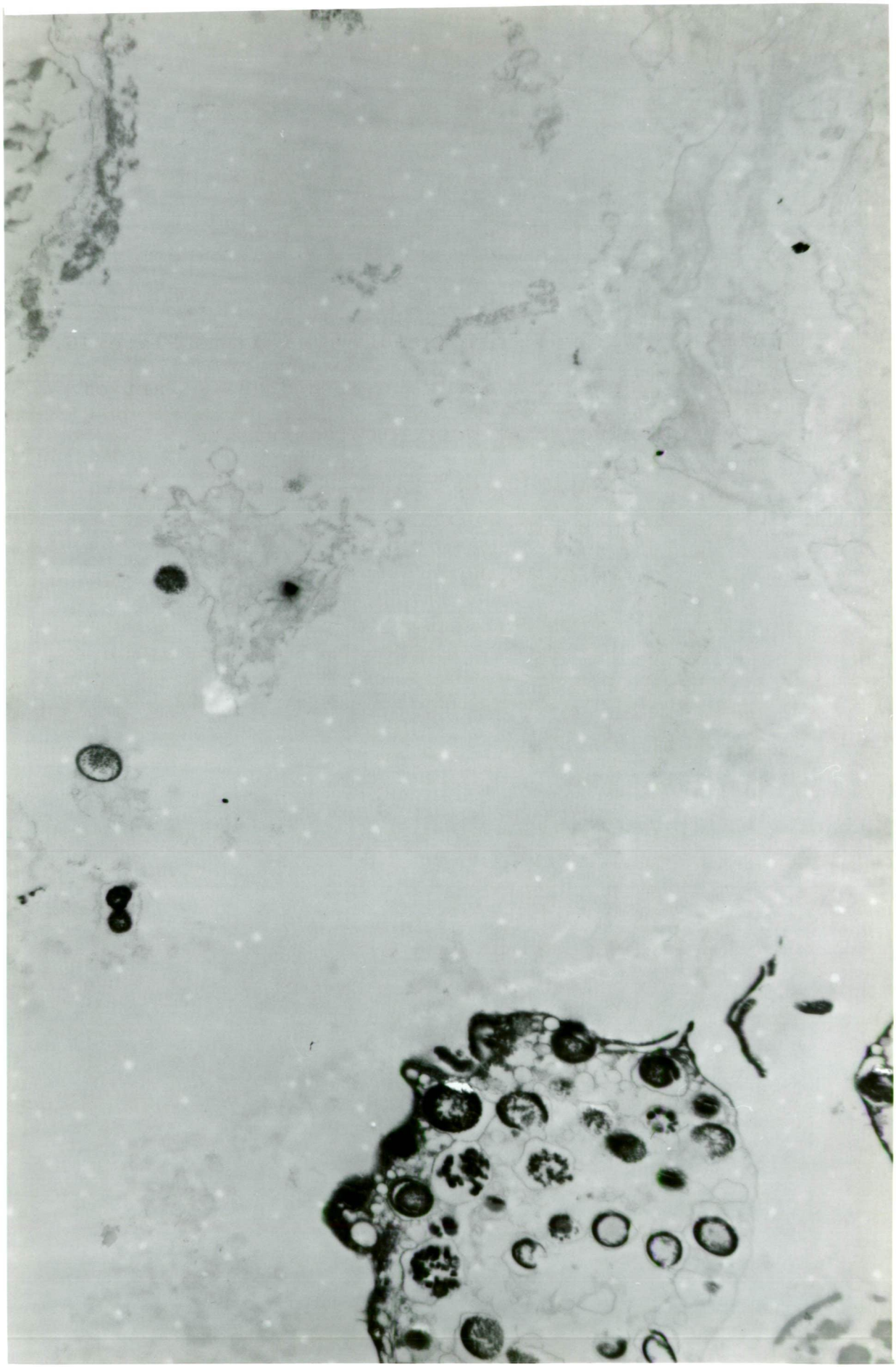

PLATE 48. TEM (04). Consecutive field to Plate 47.
Subepithelial zone of mid-gut. Zinc
granulocyte with heterogeneous granules.
Fixation: H_2S-glutaraldehyde.
Unstained.
Mag. X 10,000.

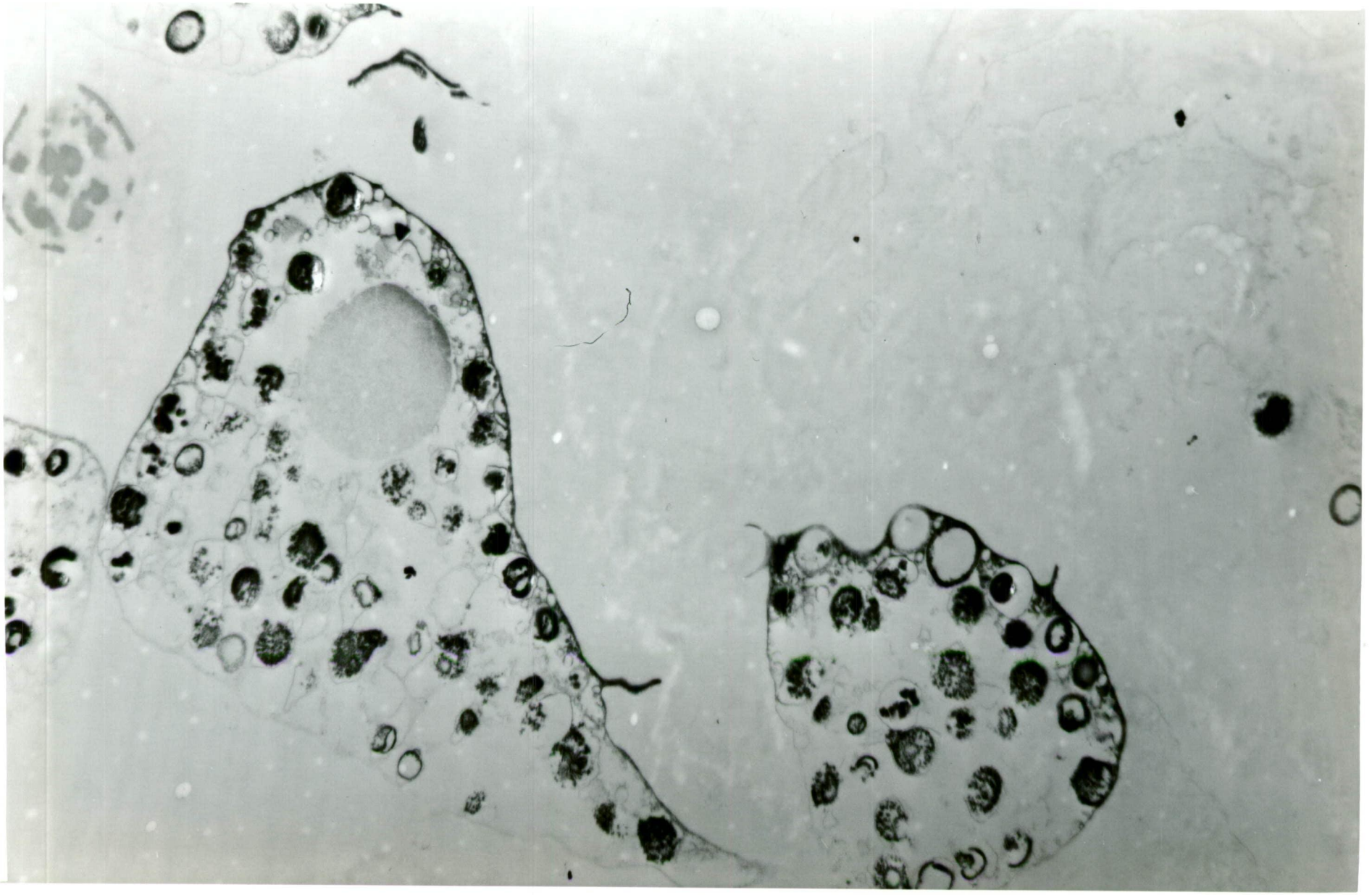

Correlative microscopy and X-ray analysis

The presence of zinc in the granulocyte was confirmed in each case by correlating the microscopic image with X-ray analysis. Thin sections on metal grids were used in the preliminary experiments (01) and (02), but the adventitious metals obscured the results and led to the abandonment of this technique.

In the first experiment (01), peri-intestinal tissue was located initially on the LM (Plate 49a) and two conspicuous Leydig cells used as markers. A serial thin section was placed on a copper grid and the two cells relocated in the TEM (Plate 49b, c). The grid was removed from the TEM, coated with carbon and gold and transferred to the SEM/EPMA. The Leydig cells were again relocated by the secondary electron image (Plate 50a, b) and an area between the two cells (Plate 50c) examined by EDAX in the spot mode (i.e. stationary beam, 5-25 nm diameter). The area probed had already been suspected in the TEM of containing zinc which was detected by EDAX (Plate 50d) along with silicon from the embedding medium, iron mainly derived from the specimen chamber and copper predominantly from the grid. The result was however obscured by the overlap of the (K) X-ray lines of Cu and Zn.

In a second experiment (02), a Formvar coated nickel grid replaced the copper one, as the (K) X-ray lines of Ni do not overlap those of Zn. The thin section was

developed by the sulphide-silver technique to enhance the secondary electron image (Plate 51a) and an individual granule was analysed by EDAX in the spot mode. Zn was detected (Plate 51b) together with Ni from the grid and iron from the specimen chamber. After analysis the section was transferred to the TEM and the analysed cell relocated, thereby confirming that the beam had been on a granule (Plate 51c).

Extraneous metals were entirely eliminated from the preparation of tissue (03) and (04) for X-ray analysis by placing epoxy resin embedded thick sections on a carbon block (Plate 52b). LM of a serial section (Plate 52a) enabled the same area to be located in the SEM (Plate 52c). Individual granulocytes stained up as 'bright' objects in the secondary electron image (Plate 53a) and the EDAX profile (Plate 53b) confirmed the presence of zinc within the cell. By moving the beam away from the cell it could be shown that the other elements present came either from the surrounding tissue (Plate 53c), or the embedding medium (Plate 53d).

EDAX maps of a single granulocyte showed that the zinc was localized to the cell (Plate 54a). Most of the sulphur was also confined to the cell (Plate 54b) although some was present in the background tissue. This was consistent with the use of H_2S in the fixative and confirmed that the dissolved gas had precipitated the metal as zinc sulphide. Maps for phosphorus (Plate 54c) and chlorine (Plate 54d) showed no difference

between the cell and background.

Intra-epithelial zinc granulocytes (03) were examined in the same way (Plate 55 & 56), except that it was found that the backscattered electron image (Plate 56b) gave improved resolution over the secondary electron image (Plate 56a). Zinc sulphide was located within the cells (Plate 56c, d) and identical results were obtained with (04), (Plates 57 & 58).

PLATE 49. LM & TEM correlation (01).

(a) LM. 1 μm section embedded in epoxy resin. Intestinal epithelium and subjacent connective tissue. Zinc granulocytes are interspersed between the more conspicuous Leydig cells. Area analysed by EPMA in centre of field.

Fixation: Glutaraldehyde in cacodylate buffer.

Stain: OsO_4, toluidine blue.

Mag. X 500.

(b) TEM montage. 80 nm serial section on a copper grid of Leydig cell (C_1) left of centre in (a). Note the electron dense osmophilic fat droplets within the cell. Zinc granules can be seen in the surrounding tissue (bottom left).

Mag. X 3000.

(c) TEM montage of Leydig cell (C_2), right of centre in (a). Note the zinc granules surrounding the cell (bottom left).

Mag. X 2300.

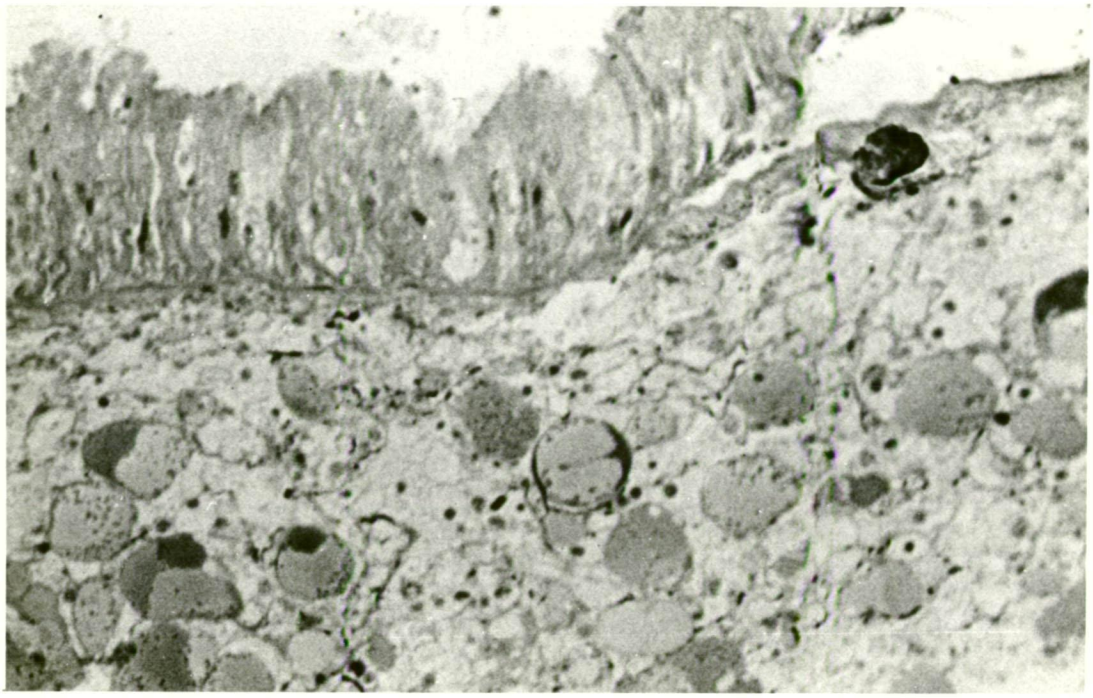

a

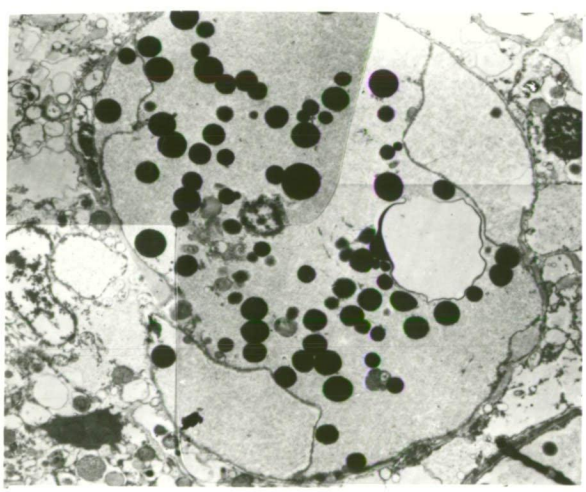

b

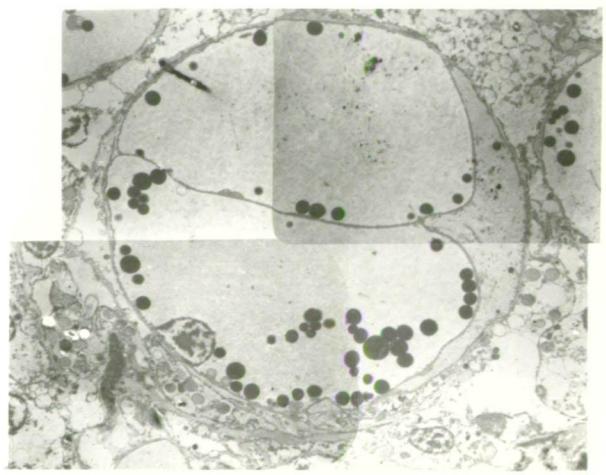

c

PLATE 50. SEM & EPMA correlation (01).

(a) SEM. Secondary electron image of Leydig cell (C_1) in Plate 49b after transfer of section to SEM/EPMA. The osmophilic fat droplets now appear as 'bright' electron-reflective spherules. The small rectangular area in the centre of the field has been damaged by the electron beam. Section coated with carbon, normal to the surface, and gold, 35° from normal.

Mag. X 1800.

(b) SEM. Secondary electron image of Leydig cell (C_2) in Plate 49c.

Mag. X 1800.

(c) SEM of area probed by EPMA, between cells (C_1) and (C_2).

Mag. X 4700.

(d) EDAX profile of (c). Elements detected:

Element	X-ray line	Energy (kV)	Source
Si	K_α	1.74	embedding medium
Fe	K_α	6.40	specimen chamber
Cu	K_α	8.05	copper grid
	K_β	8.90	
Zn	K_α	8.64	tissue
	K_β	9.57	

Vertical bar is through K_α line for Zn.

Operating conditions: spot mode; 15 kV; 20 nA; 80 s count; Zn count rate = 7 counts s^{-1}.

a

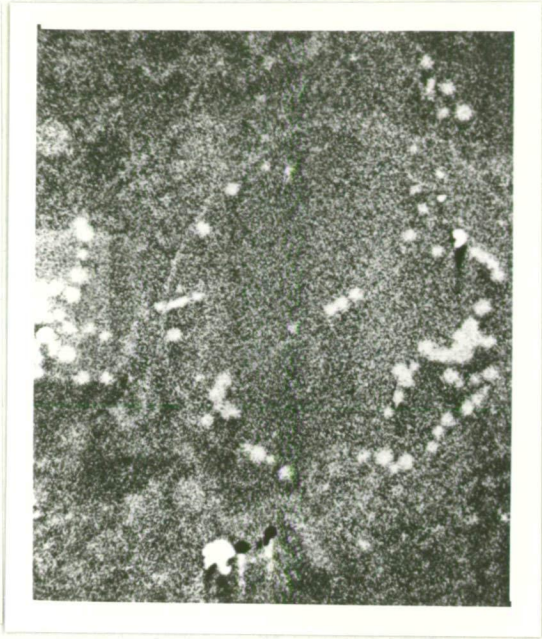

b

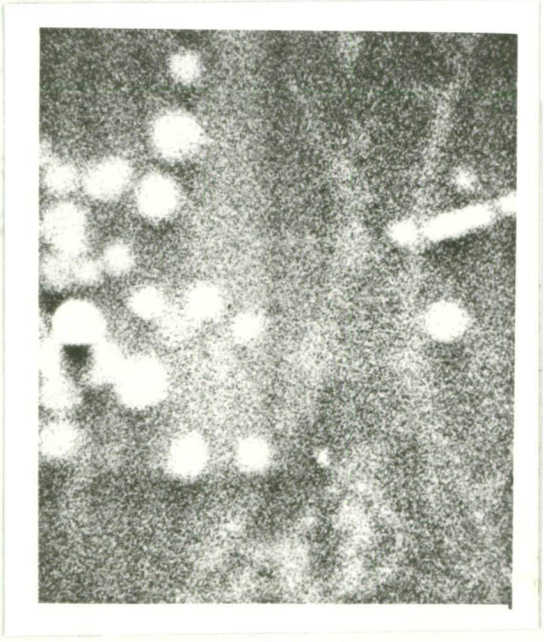

c

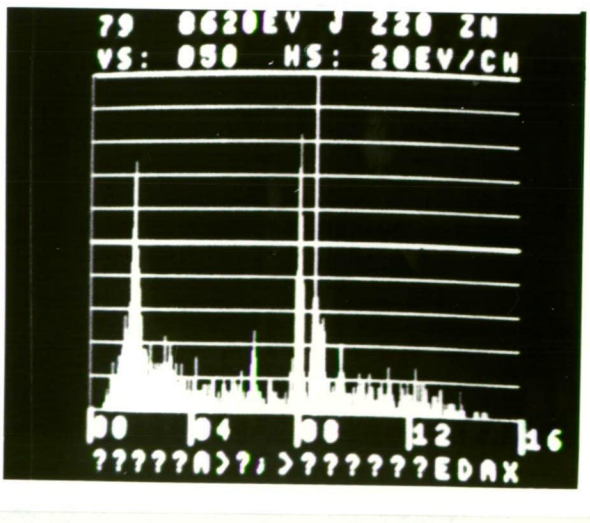

d

PLATE 51. TEM correlation post-SEM/EPMA (02).

(a) SEM 80 nm section of a zinc granulocyte in the peri-intestinal tissue embedded in epoxy resin. The section is on a Formvar coated nickel grid and developed by the sulphide-silver technique. The 'mulberry' effect is due to the strong secondary electron emission from the silver 'grains' deposited on the zinc sulphide granules. 15 nm gold coating.

Mag. X 4,700.

(b) EDAX profile of granule in centre of (a).

Elements detected:

Element	X-ray line	Energy (kV)	Source
Fe	K_α	6.40	specimen chamber
	K_β	7.06	
Ni	K_α	7.48	nickel grid
	K_β	8.33	
Zn	K_α	8.64	tissue

Operating conditions: Spot mode; 15 kV; 1 nA; 80 s count.

(c) TEM of zinc granulocyte probed in (a). The nucleus of the cell is surrounded by cytoplasmic, electron-dense zinc granules, with their deposited silver 'grains'. The dark triangle in the centre of the field, adjacent to the nucleus and over two zinc granules, is in the area probed by the electron beam which has 'burnt' the embedding medium.

Mag. X 4200.

a

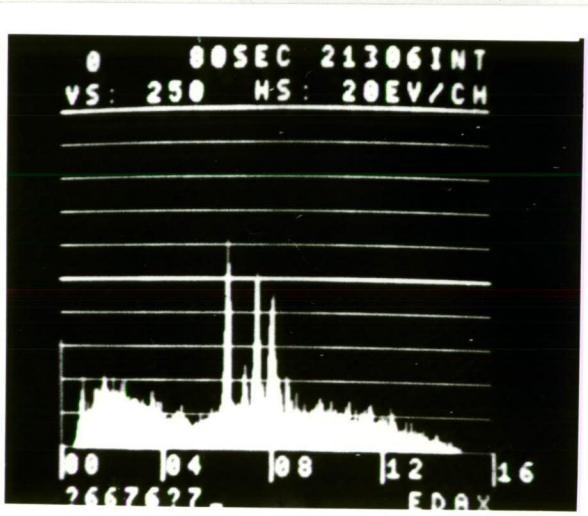

b

c

PLATE 52. LM & SEM correlation (03).

(a) LM. 1 μm section of mid-gut embedded in epoxy resin. Black staining zinc granulocytes are in the epithelium and subepithelial tissue. Probed area in centre of field just beneath the basement membrane.
Fixation: H_2S-glutaraldehyde.
Stain: Sulphide-silver.
Mag. X 200.

(b) SEM. Secondary electron image of 5 μm serial section, carbon coated on a carbon block. Probed area top left.
Mag. X 30.

(c) SEM. Secondary electron image of probed area, shown by the rectangular area of beam damage in the centre of the field. (cf. of (a) at same magnification.) Zinc granulocytes show up as electron-reflective bodies.
Mag. X 200.

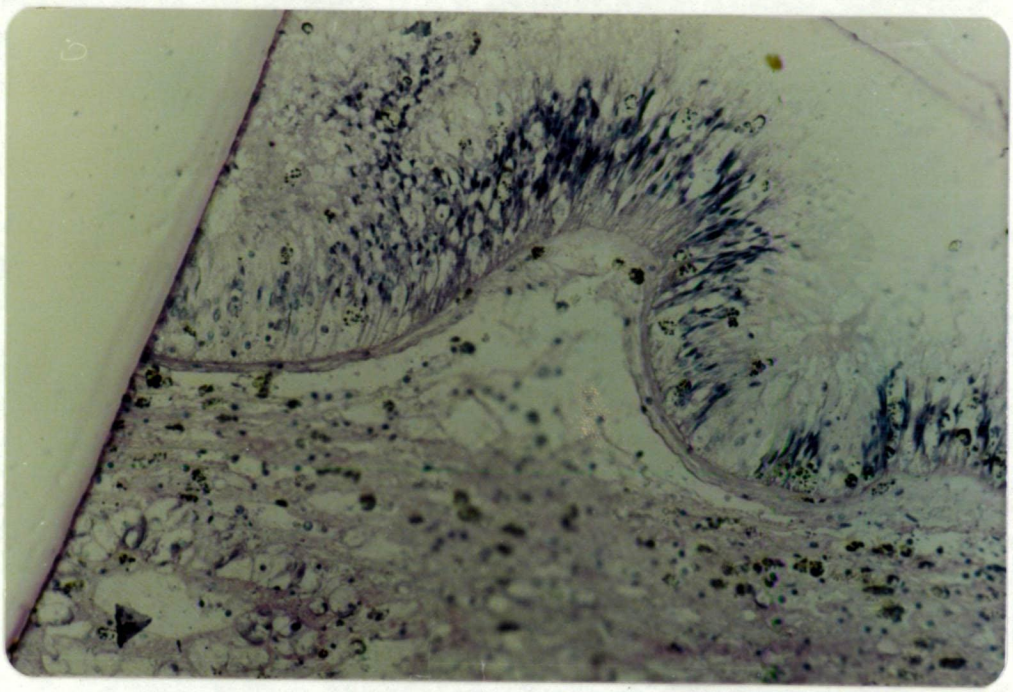

a

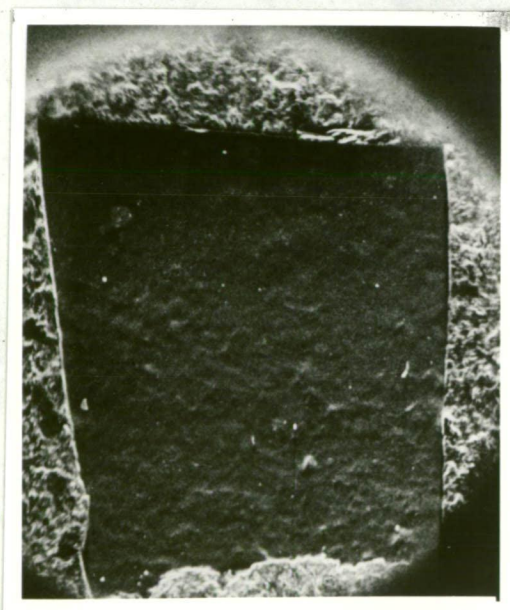

b

c

PLATE 53. SEM & EPMA correlation (03).

(a) SEM. Secondary electron image of zinc granulocyte in centre of Plate 52c. Individual granules appear as electron-reflective spherules. The nucleus is in the centre.

Mag. X 2,300.

(b) EDAX profile of granulocyte in (a), taken at the same magnification.

Element	X-ray line	Energy (kV)	Source
Zn	L_α	1.01	granule
	K_α	8.64	"
	K_β	9.57	"
S	K_α	2.31	granule & tissue
Si	K_α	1.74	embedding medium
Cl	K_α	2.62	"
Cu	K_α	8.05	"

Operating conditions; scanning mode; 15 kV; 2 nA; 80 s count.

(c) EDAX profile of tissue adjacent to zinc granulocyte in (a), taken under the same operating conditions as (b). Zinc peaks from the granules are absent. The sulphur peak is reduced, but still present due to the tissue contribution. Si, Cl and Cu peaks from the embedding medium are of the same intensity as (b).

a

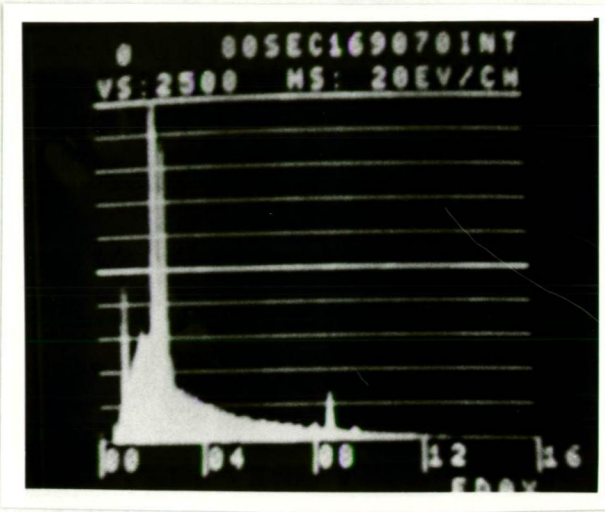

b

(d) EDAX profile of Spurr embedding medium, taken under the same operating conditions as (b, c). Zinc and sulphur peaks are completely absent. Si, Cl and Cu peaks are of the same intensity as (b, c). Note the clean profile (apart from a trace of Cu) of elements beyond Cl.

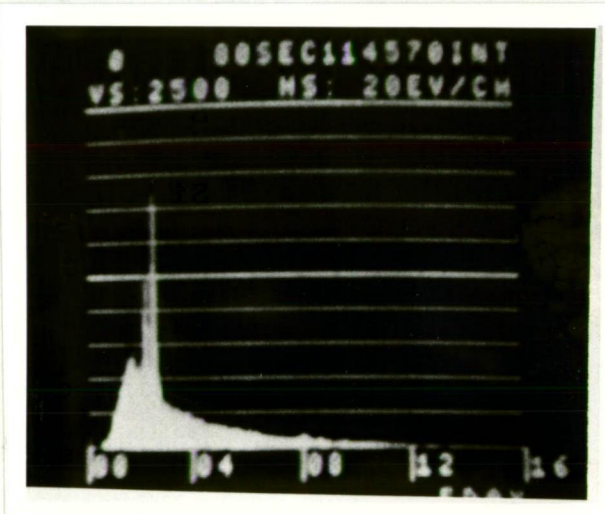

c

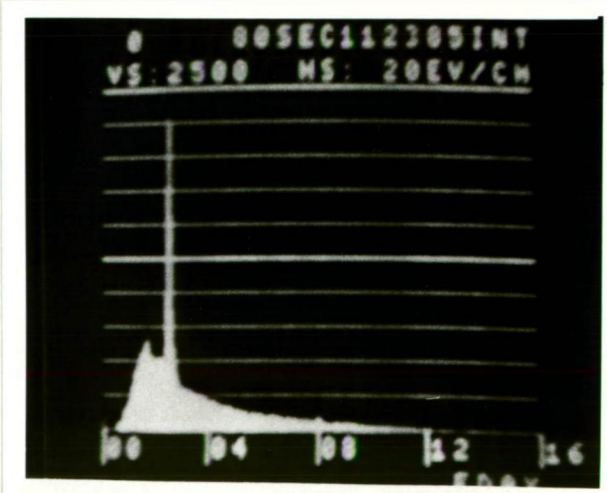

d

PLATE 54. EDAX maps of zinc granulocyte in Plate 53.

(a) Spectrometer set on K_α line for zinc. Note the greater X-ray emission from the cell (centre of the field). Operating conditions as in Plate 53. Window width 180 V; 400 s count.

(b) Spectrometer set on K_α line for sulphur. Note the stronger X-ray emission from the cell due to the zinc sulphide precipitated by H_2S in the fixative. Sulphur also present in the background tissue. 400 s count.

(c) Spectrometer set on K_α line for phosphorus. No differentiation between cell and background; phosphorus present in tissue. 250 s count.

(d) Spectrometer set on K_α line for chlorine. No differentiation between cell and background. Chlorine in embedding medium. 250 s count.

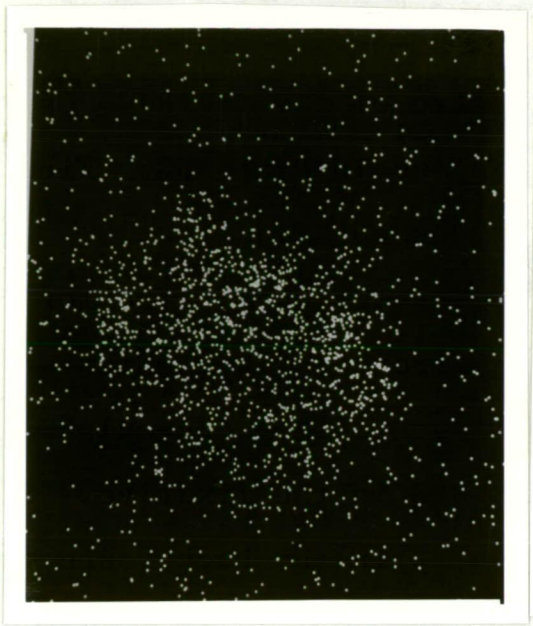

a

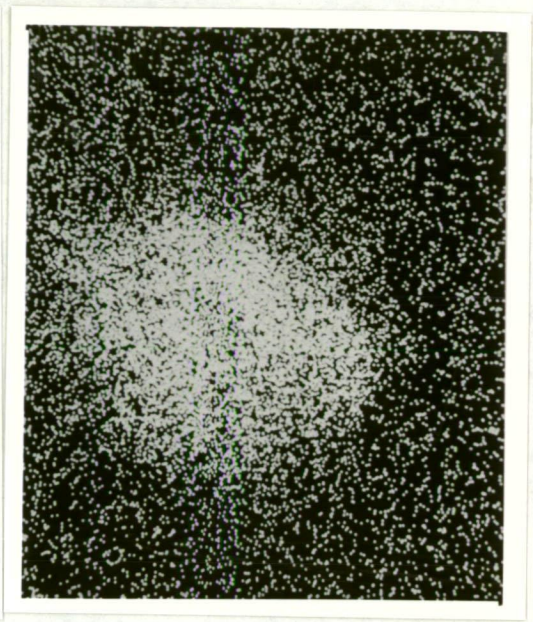

b

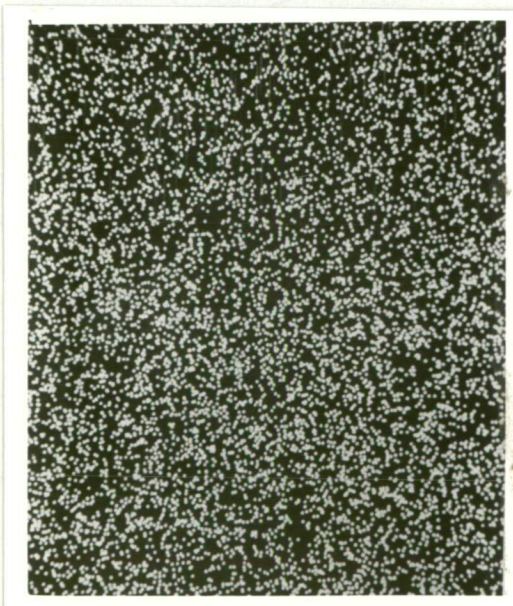

c

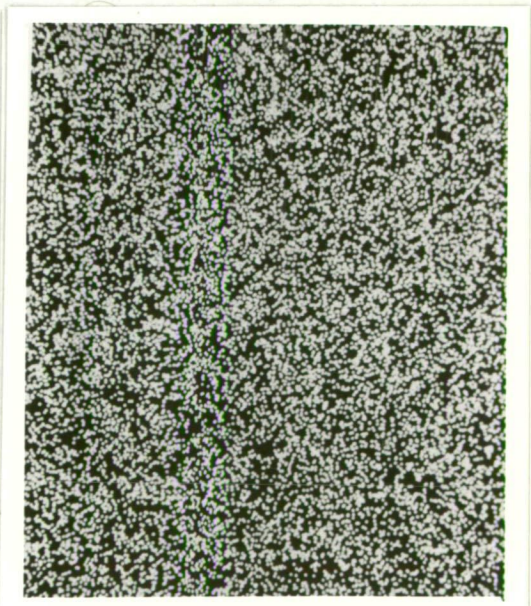

d

PLATE 55. LM & SEM correlation (03).

(a) LM of field to the right of Plate 52a. Probed area in the centre within the epithelium, just above the basement membrane. Mag. X 200.

(b) SEM. Backscattered electron image of area to the right of Plate 52c. Probed area (upper right) shown by the rectangle of beam damage. Zinc granulocytes on either side of the basement membrane show up as electron-reflective bodies. Operating conditions: 25 kV; 20 nA. Mag. X 240.

(c) SEM. Backscattered electron image of field to the right of (b). Basement membrane runs across the centre of the field. Mag. X 240.

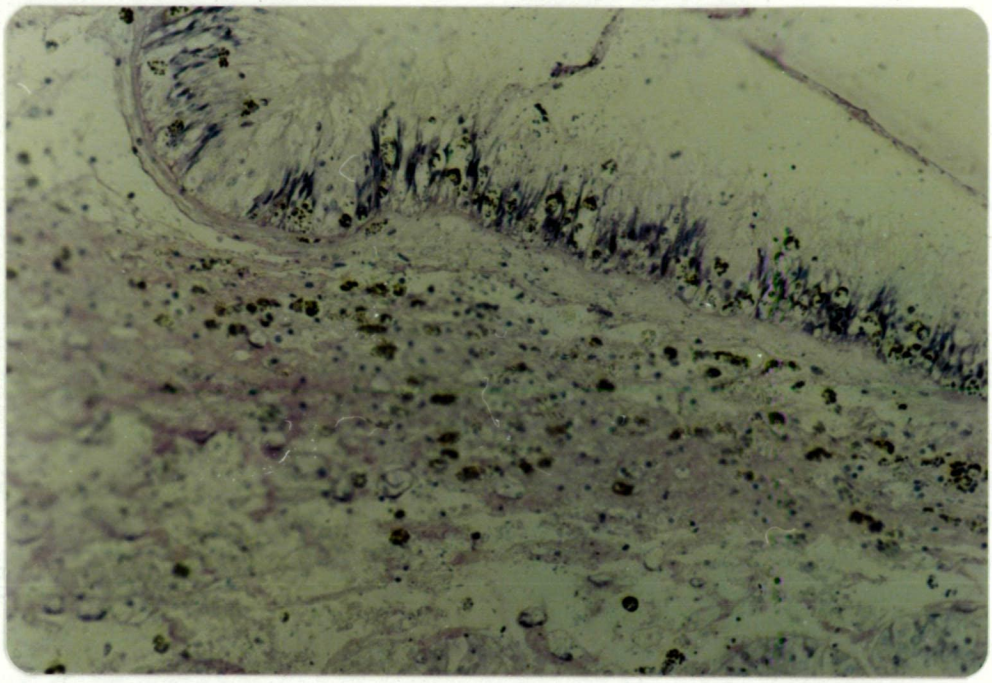

a

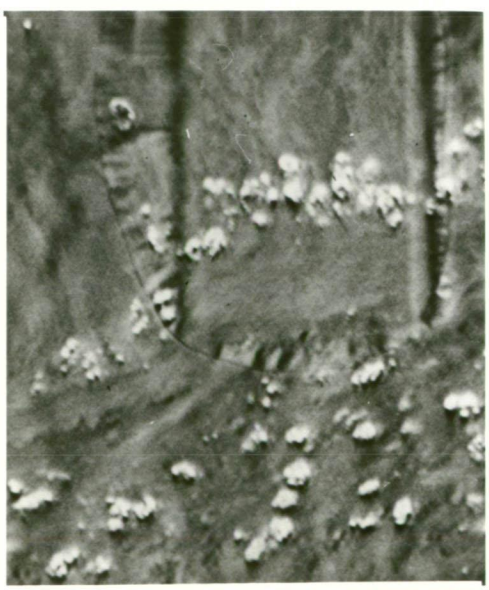

b

c

PLATE 56. SEM & EDAX correlation (03).

(a) SEM. Secondary electron image of intra-epithelial zinc granulocytes in the probed area (Plate 55b). Although the cells show up as electron-reflective bodies, the resolution is poor.
Operating conditions: 15 kV; 2 nA.
Mag. X 800.

(b) SEM. Backscattered electron image (with differentiation) of same field as (a). Note the improved resolution.
Operating conditions: 25 kV; 20 nA.

(c) EDAX map of (b) with spectrometer set on K_{α} line for zinc. The intensity of X-ray emission is greater from the cells.
500 s count.

(d) EDAX map of (b) with spectrometer set on K_{α} line for sulphur. The X-ray emission is more intense over the cells confirming the presence of zinc sulphide.
250 s count.

a

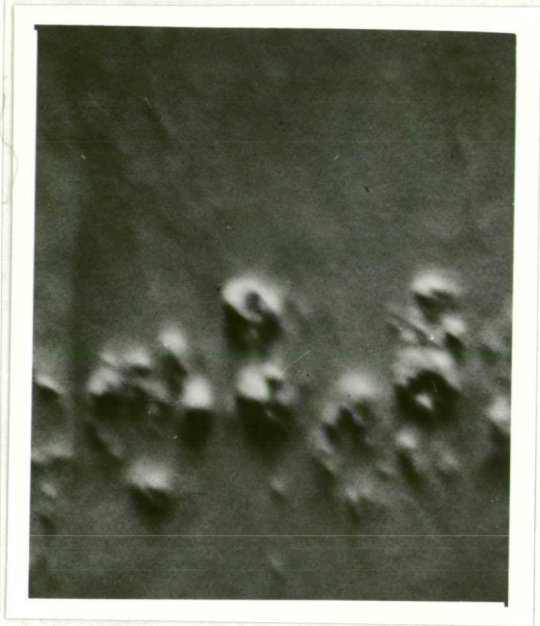

b

c

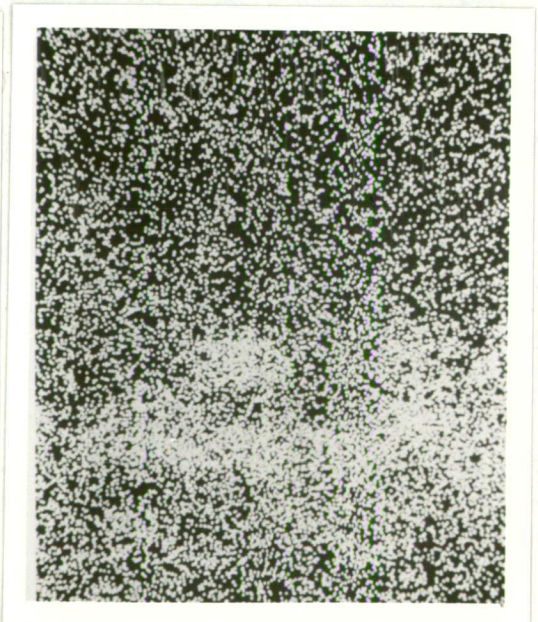

d

PLATE 57. LM, SEM & EDAX correlation (04).

(a) LM. 1 μm section of mid-gut epithelium embedded in epoxy resin. Yellow, refractile zinc sulphide granules are clearly seen within the granulocytes, both within the epithelium and beneath the basement membrane. Area probed in the centre of the field.
Fixation: H_2S-glutaraldehyde.
Stain: Toluidine blue (note that some of the granules have taken up the stain.
Mag. X 1000.

(b) SEM. Backscattered electron image of same field as (a). 5 μm serial section on carbon block.
Operating conditions: 20 kV; 6 nA.
Mag. X 700.

(c) EDAX map of (b) with spectrometer set on K_α line for zinc, confirming the presence of zinc within the granulocytes.
500 s count at 15-25 counts s^{-1}.

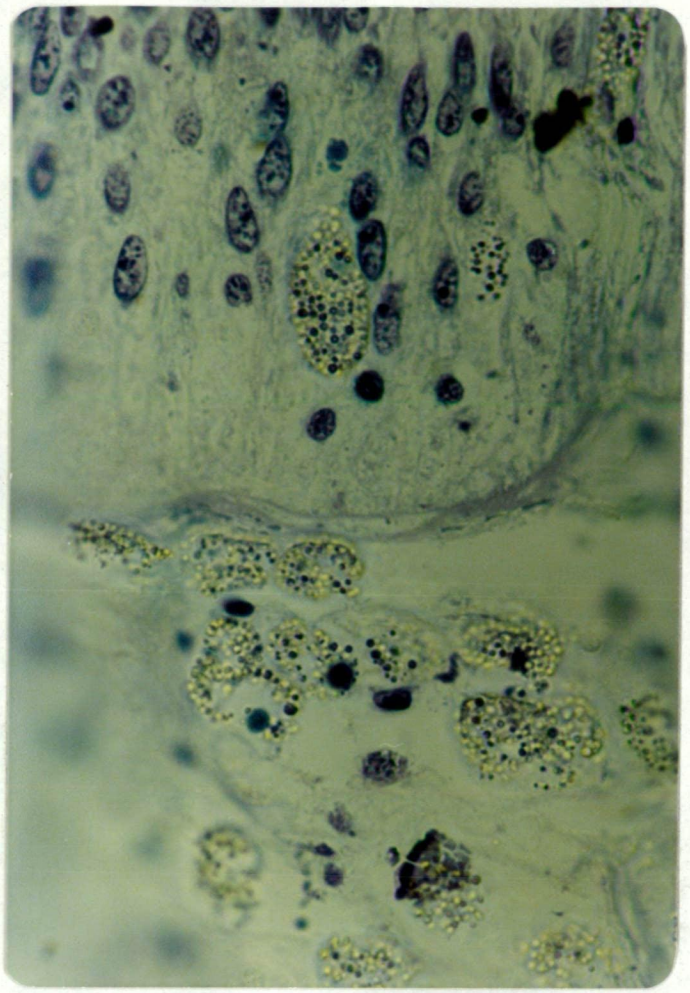

a

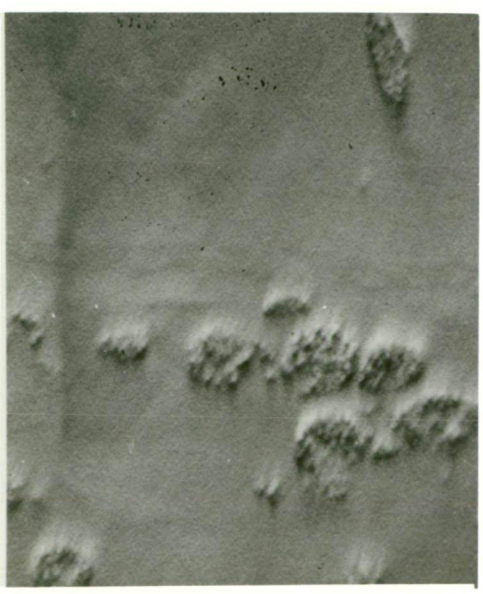

b

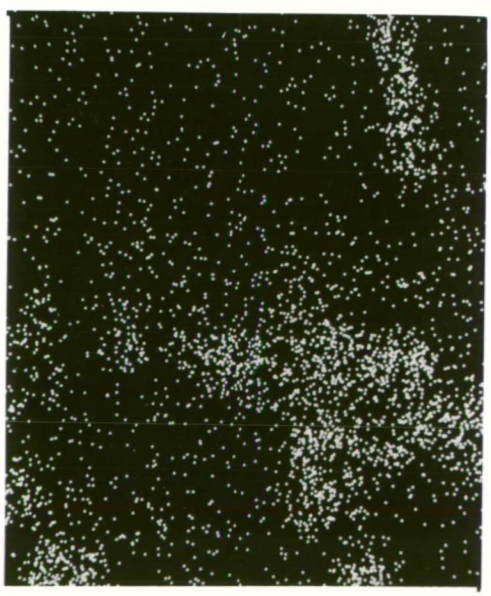

c

PLATE 58. SEM, EDAX profile and map correlation (04).

(a) SEM. Backscattered electron image of cell in Plate 57b, (bottom left hand corner). Note the absence of granules in the region of the nucleus.

Mag. X 2400.

(b) EDAX map of (a) with spectrometer set on K_α line for zinc. Note the strong X-ray emission from the cell.

150 s count.

(c) EDAX profile of (a), taken at the same magnification.

Element	X-ray line	Energy (kV)	Source
Zn	L_α	1.01	granule
	K_α	8.64	"
P	K_α	2.01	tissue
S	K_α	2.31	granule & tissue
Si	K_α	1.74	embedding medium
Cl	K_α	2.62	embedding medium

Operating conditions: Scanning mode; 20 kV; 6 nA.

a

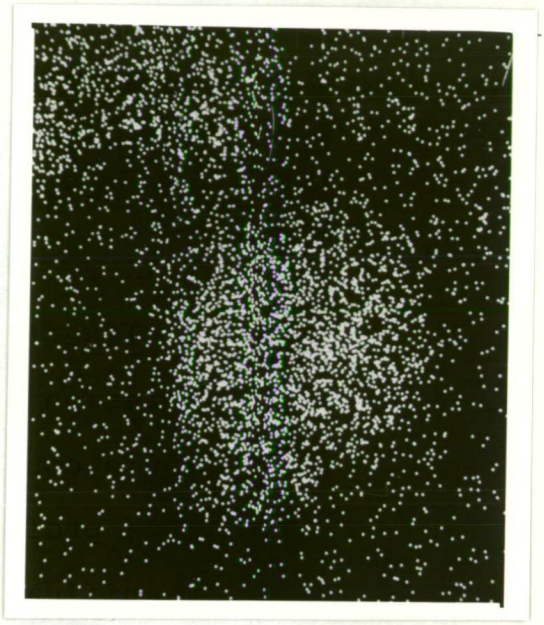

b

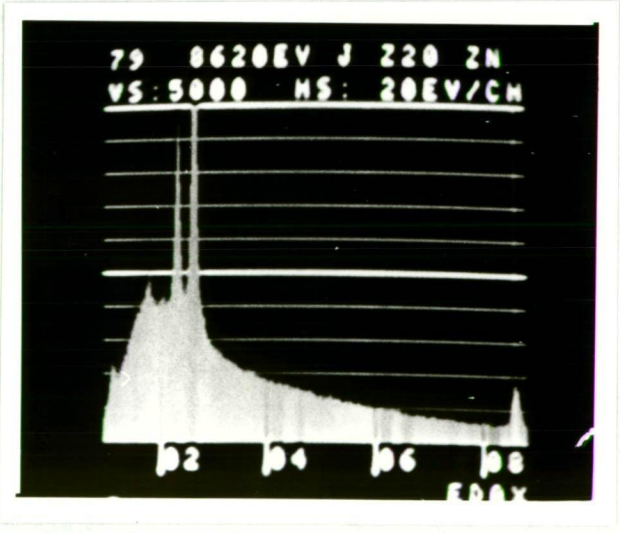

c

DISCUSSION AND CONCLUSIONS

Résumé of methods

The methods employed in this study ranged from the quantitative technique of AAS, through the semi-quantitative technique of electron probe microanalysis to the qualitative techniques of histochemistry. Each method has its own distinct set of advantages and disadvantages and can be assessed in terms of the information it can provide, its limitations, accuracy and ease of application. The efficacy of each method will be discussed from this point of view and the evaluation is summarized in Table 3.

(a) Atomic absorption spectrophotometry

AAS provides an accurate estimate of the concentration of specific elements in tissue, however its main limitation in this study was the destruction of tissue morphology during the preparative procedure. Although the method is both highly sensitive and highly selective for the detection of zinc in tissue, there are further limitations. There is some loss in precision due to contamination of the sample from external sources, most notably the presence of zinc in glassware. This necessitates a high degree of quality control in the laboratory if reproducible results are to be obtained. The need for absolute cleanliness in the preparation of glassware extends the preparation time and reduces the overall facility of the procedure, despite the short machine time. A further consideration is the capital cost of the equipment and its maintenance which is high in this instance.

TABLE III. EFFICACY OF METHODS

Parameters	AAS	SEM/EPMA	Histochemistry
Information	Tissue concentration Zn	Tissue localization Zn	Same as SEM/EPMA
Accuracy	High	High	High
Precision	Contamination from glassware	Contamination from specimen stage	High
Selectivity	High (Bandpass 0.1 nm[a])	High (Window width 180 eV)	Low
Sensitivity	High (0.01 $\mu g\ ml^{-1}$ [a])	Range 0.9-90 keV[b]	Uncertain
Detection limit	0.005 $\mu g\ ml^{-1}$ [a]	2000 μg g dry wt^{-1} [c]	Uncertain
Limitation	Destruction of tissue morphology	Poor detection limit	Poor selectivity
Facility			
(i) Preparation time	Long	Long	Short
(ii) Machine time	Short	Long	Short
Cost	High	High	Low

References: (a) Analytical Methods for Flame Spectroscopy, Varian Techtron, Australia 1972

(b) Edax International Service Manual, 1976

(c) Electron Microprobe Analysis, S.J.B. Reed, Cambridge University Press, 1975

The main concern in this study was the localization of zinc in tissue by a sensitive and selective method that retained the morphology of the sample. The technique of scanning electron microscopy coupled with X-ray analysis met these requirements.

(b) Scanning electron microscopy/electron probe microanalysis

EPMA provides information on the elemental composition of tissues. Point to point chemical analysis can be visualized in the intact tissue using the SEM mode of operation. The method is highly selective for individual elements and can be controlled by choosing the optimum 'window-width' of the X-ray spectrometers. In this way interference from other elements can be eliminated. The selectivity of this method is comparable to that of AAS. In the latter case the selectivity is attained by operating the spectrometer with a narrow spectral bandpass of 0.1 nm (see Table 3). Good resolution of the X-ray emission was achieved using a 'window-width' of 180 eV, ensuring a high accuracy for the method.

The main limitation of EPMA in determining the concentration of zinc in tissue lies in its detection limit. The detection limit for zinc is approximately 2000 $\mu g\ g\ \text{dry weight}^{-1}$ (see Table 3). Although the detection limit is well below the concentrations determined in this study, the detection limit curtails the versatility of the instrument in trace-element analysis of tissue. EPMA is also disadvantaged by a loss in precision due to the 'penumbra' effect of

X-ray sources extraneous to the sample. The most common sources of spurious X-ray emission are the metals in the specimen stage and metal contamination of the embedding medium. For example the strength of signal from a copper grid would 'swamp' any signal from the tissue (see Plate 50 d). However even with the copper grid eliminated from the system, copper was still detected in the embedding medium (Plate 53 d), some distance from where the tissue was situated. The preparation of tissue for EPMA developed in this study has reduced possible contamination of samples from external metals, thereby improving the facility of the method.

A further drawback to EPMA as a routine method is the time taken to prepare and examine the specimen. Preparation time is three to four days and although machine time is half a day, in actual practice the demands on the SEM/EPMA are so heavy that results cannot be obtained in under a fortnight. Again the high capital cost of the equipment and the expertize required for its maintanance is a disadvantage for environmental monitoring, where it is desirable to be able to process a large number of samples from different sites in a short time.

In studies such as this on trace-elements in marine invertebrates there is a need for a simple laboratory technique that is non-destructive of tissue, selective for the metal concerned, sensitive and quick to perform at low cost. The histochemical

techniques described here go some way towards meeting these requirements.

(c) Histochemical techniques

Histochemistry has been bedevilled by its qualitative nature, lack of standardization and uncertainty regarding specificity and sensitivity of the method. The two histochemical techniques employed in this study will be reviewed in this light.

(i) Sulphide-silver method for heavy metals

This test provided information on the morphology of the zinc granulcoyte and its distribution within the tissue of the oyster. Depending as it does on the argyrophilic properties of heavy metal sulphides, the method is non-specific. However some estimate of its precision was obtained by visualizing the silver 'grains' deposited on the zinc sulphide granules (Plate 42). This physico-chemical interaction between silver and zinc sulphide was confirmed in the series of correlative microscopy experiments illustrated in Plates 51 to 56 and EPMA in this instance provided additional evidence of the bonding of silver to the zinc sulphide.

(ii) Alkaline dithizone method for zinc

The alkaline dithizone method complemented the sulphide-silver technique and gave the same information. The precision of both methods was the same (cf. Plates 20 & 21), the dye being taken up by individual zinc granules (Plates 13 & 27). In a series of preliminary experiments the sensitivity and detection limit of

the method was assessed by examining dithizone stained sections in the SEM/EPMA, where the zinc peaks on EDAX corresponded to the dithizone positive material.

The specificity of this method is debatable. Dithizone, or diphenyl thiocarbazone chelates heavy metals non-specifically by forming inner complex salts (Pearse, 1972). Dithizone forms a deep red inner complex salt with zinc ions, especially in alkaline solutions:

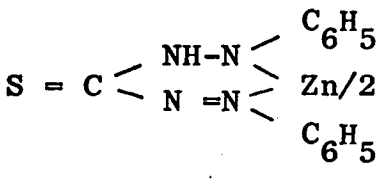

(Pearse, 1972).

The work of Midorikawa & Eder (1962) suggests that the magenta colour of a metal-dithizone complex in alkaline solution is highly specific for zinc. Uncertaintly about specificity constitutes the main drawback in the histochemical determination of zinc in tissue.

The histochemical approach has distinct advantages over the other methods. With proper laboratory facilities results can be obtained within two to three days at low cost and with minimum training of personnel. The techniques are comparatively simple and can be adapted to the processing of a large number of samples. This is particularly important in the field of environmental monitoring where samples may have to be obtained from a large number of sites in order to assess the relative pollution in an area.

Correlative microscopy and X-ray analysis have confirmed the efficacy of the histochemical techniques as rapid and simple laboratory screening tests for the localization of heavy metals in tissue. It should be emphasized however that the limitations of each method mean that for a throoughgoing analysis different techniques have to be used in combination, each one acting as a control on the other.

The evaluation of techniques discussed above constituted the primary objective of the study. The secondary objectives (2-6), listed on Page 9, were also achieved. The final objective (7), to establish any abnormal tissue reaction associated with the presence of zinc in oyster tissue was not satisfactorily resolved. The presence of zinc granulocytes in the tissue may be a normal feature, but to prove the point oysters would have to be raised in a 'low-zinc' environment. This would necessitate the measurement of environmental zinc levels at the site and time of collection. As already intimated the evaluation of a complex methodology placed the measurement of environmental zinc levels outside the scope of the study. Indirect evidence suggests that all four specimens may have come from a 'high-zinc' environment (see Table 4).

Prospectus

Further studies would have to be carried out to achieve the final objective and establish whether or not zinc is acting as a pollutant in oyster tissue. Further specimens, remote from man's activities, would have to be examined and the zinc levels in sediment, water and phytoplankton measured at the same time. In the first instance both oysters and phytoplankton should be examined by the histochemical methods described here, in conjunction with AAS. It would be desirable to refine the sulphide-silver technique into a semi-quantitative method by conducting micro-densitometry experiments on the stained tissue.

Functional studies will have to be carried out on the relative importance of the different uptake pathways of zinc in oysters before the histological appearances can be interpreted correctly. The current thinking on this aspect is reviewed in the appendix. The most interesting question raised by the study is the relationship between the zinc granulocytes and pollution. This relationship is conjectural at present, but discussed briefly in the following section.

Zinc granulocytes and pollution

The morphology of the zinc granulocyte demonstrated in this study is the same as that of the Type B amoebocyte described by George *et al.*,(1978). Furthermore the fine structure of the granule is the same; both authors independently employing almost identical techniques to oyster tissue treated with hydrogen sulphide.

There is a further parallel between the two studies in terms of the environments from which the oysters were taken. George *et al.*, compared "green-sick" oysters *Ostrea edulis* from a "polluted" environment with specimens taken from a "non-polluted" area. The parameters which they used to define these two environments are not given, but a comparison can be drawn if certain assumptions are made.

Their "polluted" oysters came from Restronguet Creek in Falmouth Harbour, Cornwall, previously shown to be contaminated with zinc and copper as a result of mining (Thornton *et al.*, 1975). These latter authors had shown heavy-metal contamination of sediments in the creek, with mean concentrations of Zn (1540 μg g dry weight^{-1}) and Cu (1690 μg g dry weight^{-1}). The mean zinc content in the filtered surface water of the creek was 570 μg l^{-1}.

The "non-polluted" oysters came from Tal-y-foel Estuary, Anglesey and the concentrations of zinc in sediment and filtered water are likely to be similar to those in Conway Bay (sediment 59 μg g dry weight^{-1}Zn, filtered water 20 μg l^{-1}Zn; Thornton et al., 1975).

A similar problem was encountered in this study since direct measurements of environmental zinc concentrations were not made on site at the time of collection. However, the estimated values from secondary sources are presented in Table 4. If zinc concentrations in sediment and filtered water are taken as indices of "pollution", then the Derwent Estuary can be regarded as a 'high-zinc' environment and sites 3 & 4, outside the estuary as a 'low-zinc' environment; comparable to the "polluted" and "non-polluted" areas of George et al.

If, on the other hand, the concentration of zinc in suspended particles, such as phytoplankton, is an important determinant of the oyster's environment, then the difference in the two environments is not so great (Table 4).

George et al. found high concentrations of zinc in the viscera of oysters from both environments:

	μg g wet weight^{-1}	μg g dry weight^{-1}*
Anglesey	2,988	15,000
Cornwall	5,817	30,000

* Calculated assuming a 20% dry matter content.

TABLE IV. ESTIMATED ENVIRONMENTAL ZINC CONCENTRATIONS AT THE FOUR COLLECTION SITES

Collection Site	Particulate Zinc			Filtered Water
	Sediment	Suspended particles (Phytoplankton)		
	$\mu g\ g\ dry\ wt^{-1}$	$\mu g\ g\ dry\ wt^{-1}$	$\mu g\ l^{-1}$	$\mu g\ l^{-1}$
(1) Ralphs Bay	107[a]	-	-	100-300[b]
(2) Crayfish Point	178[a]	615[a]	3.2[a]	210[a]
(3) Limekiln Point	-	-	-	10[c]
(4) Mickeys Bay	30[d]	348[d]	-	12[d]

(a) Bloom, H., 1975.

(b) Bloom & Ayling, 1977.

(c) De Forest et al., 1978.

(d) Electrolytic Zinc Co., 1979.

This present study supports the findings of George et al. that the concentration of zinc in the viscera of "polluted" and "non-polluted" oysters is the same order of magnitude, there being only a two fold increase in the concentration of zinc for "polluted" oysters. Furthermore both studies have shown that the distribution of the zinc in the tissues is the same in oysters from both environments. George et al. found the greatest mass of zinc in the viscera (45% of total zinc), which confirms the LM observations in this study.

There are several possible explanations for these findings:

1. The zinc from the Derwent Estuary is more widely dispersed than previously thought.
2. The accumulation of zinc in the granulocytes is a natural phenomenon and not a pathological response to pollution.
3. The oysters remote from the estuary were larger and may have accumulated zinc over a longer period.

The correct interpretation is only forthcoming through a knowledge of zinc metabolism and the interchange of zinc between the oyster and its aquatic environment. At present these processes are poorly understood.

The unequivocal demonstration of a specific metal-bearing cell in the tissues of the oyster Ostrea angasi has raised many physiological and biochemical questions. The function of the zinc granulocyte is unknown. The

origin and migration of the cell through the tissue is uncertain. These questions will have to be answered before the histological features can be interpreted correctly.

REFERENCES

AYLING, G.M., 1974; Uptake of cadmium, zinc, copper lead and chromium in the pacific oyster, Crassostrea gigas, grown in the Tamar River, Tasmania. Water Research, 8, 729.

BARROS, J. & JOHNSTON, D.M., 1974; The internatiinal law of pollution. The Free Press, New York.

BLOOM, H., 1975; Heavy metals in the Derwent Estuary. University of Tasmania. (Internal publication).

BLOOM, H. & AYLING, G.M., 1977; Heavy metals in the Derwent Estuary. Environmental Geology, 2, 3.

BOYCE, R. & HERDMAN, W.A., 1897; On a green leucocytosis in oysters associated with the presence of copper in the leucocytes. Proceedings of the Royal Society, 62B, 30.

COOMBS, T.L., 1972; The distribution of zinc in the oyster Ostrea edulis and its relation to enzymic activity and to other metals. Marine Biology, 12, 170.

COOMBS, T.L., 1974; The nature of zinc and copper complexes in the oyster Ostrea edulis. Marine Biology, 28, 1.

CULLING, C.F.A., 1974; Handbook of histopathological and histochemical techniques, 3rd. edition, Butterworth & Co. Ltd., London.

DE FOREST, A., PETTIS, R.W. & FABRIS, G., 1978; Analytical acceptability of trace metal levels found in oceanic waters around Australia. Australian Journal of Marine & Freshwater Research, 29, 193.

DREW, G.H., 1910; Some points in the physiology of Lamellibranch blood-corpuscles. Quarterly Journal of microscopical Science, 54, 605.

DREW, G.H. & DE MORGAN, W. 1910; The origin and formation of fibrous tissue produced as a reaction to injury in Pecten maximus, as a type of the Lamellibranchiata. Quarterly Journal of Microscopical Science, 55, 595.

GEORGE, S.G., PIRIE, B.J.S., CHEYNE, A.R., COOMBS, T.L. & GRANT, P.T., 1978; Detoxification of metals by marine bivalves; an ultrastructural study of the compartmentation of copper and zinc in the oyster Ostrea edulis. Marine Biology, 45, 147.

LANKESTER, E.R., 1885; On green oysters. Quarterly Journal of microscopical Science, 26, 71.

MACPHERSON, J.H. & GABRIEL, C.J., 1962; Marine molluscs in Victoria. Melbourne University Press.

METSCHNIKOFF, VON E., 1884; Ueber eine Sprosspilzkrankheit der Daphnien. Beitrag zur Lehre über ken Kampf der Phagocyten gegen Krankheitserreger. Archiv für pathologische Anatomie und Physiologie und für klinische Medicin, 96, 177.

MIDDLETON, G.J. & PATTERSON, I.G., 1977; Energy analysis of zinc production. Environmental Studies working paper 5, University of Tasmania.

MIDORIKAWA, O. & EDER, M., 1962; Vergleichende histochemische Untersuchungen über Zink im Darm. Histochemie, 2, 444.

ORTON, J.H., 1923; Summary of an account of investigations into the cause or causes of the unusual mortality among oysters in English Oyster Beds during 1920 and 1921. Journal of the marine biological Association, United Kingdom, 13, 1.

PEARSE, A.G.E., 1972; Histochemistry, theoretical and applied, 3rd. edition v. 2, Churchill Livingstone, London.

PHILLIPS, D.J.H., 1977; The use of biological indicator organisms to monitor trace metal pollution in marine and estuarine environments - a review. Environmental Pollution, 13, 281.

PIHL, E. & FALKMER, S., 1967; Trials to modify the sulphide-silver method for ultrastructural tissue localization of heavy metals. Acta histochemica, 27, 34.

RATKOWSKY, D.A., THROWER, S.J., EUSTACE, I.J. & OLLEY, J., 1974; A numerical study of the concentration of some heavy metals in Tasmanian Oysters. Journal of the Fisheries Research Board, Canada, 31, 1165.

REED, S.J.B., 1975; Electron Microprobe Analysis. Cambridge University Press.

RUDDELL, C.L., 1971; Elucidation of the nature and function of the granular oyster amoebocytes through histochemical studies of normal and traumatized oyster tissues. Histochemie, 26, 98.

RUDDELL, C.L. & RAINS, D.W., 1975; The relationship between zinc, copper and the basophils of two crassostreid oysters, C. gigas and C. virginica. Comparative Biochemistry and Physiology, 51A, 585.

STAUBER, L.A., 1950; The fate of India ink injected intracardially into the oyster, Ostrea virginica Gmelin. Biological Bulletin, 98, 227.

TAKATSUKI, S., 1934; On the nature and functions of the amoebocytes of Ostrea edulis. Quarterly Journal of Microscopical Science, 76, 379.

TASMANIA. ENVIRONMENT PROTECTION ACT, No. 34 of 1973; Government Printer.

THORNTON, I., WATLING, H. & DARRACOTT, A., 1975; Geochemical studies in several rivers and estuaries used for oyster rearing. The Science of the Total Environment, 4, 325.

THROWER, S.J. & EUSTACE, I.J., 1973; Heavy metal accumulation in oysters grown in Tasmanian waters. Food Technology in Australia, 25, 546.

TIMM, F., 1958; Zur Histochemie der Schwermetalle Das Sulphid-silberverfahren. Deutsche Zeitschrift für gerichtliche Medizin, 46, 706.

TIMM, F., 1960; Der histochemische Nachweis der normalen Schwermetalle der Leber. Histochemie, 2, 150.

TRIPP, M.R., 1960; Mechanisms of removal of injected microorganisms from the American oyster Crassostrea virginica Gmelin. Biological Bulletin, 119, 273.

WOLFE, D.A., 1970b; Zinc enzymes in Crassostrea virginica. Journal of the Fisheries Research Board, Canada, 27, 59.

APPENDIX

An ecological model of zinc accumulation in the oyster

Zinc metabolism in the oyster has three main components,

(i) the uptake pathway

(ii) tissue utilization

(iii) the excretion pathway

The distribution of zinc granulocytes within the tissue affords some evidence for the efferent pathway of zinc, but to complete the model, it is necessary to examine the afferent limb of zinc uptake as well as its metabolic role in the tissue.

Zinc can be taken up by the oyster from three sources:

(i) absorbed directly from seawater

(ii) ingested with food

(iii) ingestion of contaminated particles

The relative importance of these uptake pathways in the natural environment has not been satisfactorily measured (George, pers. comm.), most of the evidence being experimental.

The oyster is so placed ecologically that it depends for its food supply on microorganisms and small organic particles. The whole feeding mechanism of the oyster is designed to select from the water minute food particles in suspension. There is a clear distinction in vertebrates between the ingestion and digestion of foreign material and the normal digestive process, but

within the oyster, which is dependent on microorganisms as foodstuff, the distinction is not so clear cut. Yonge (1926) has suggested that the amoebocyte has a digestive function, apart from the elimination of pathogenic microorganisms and unwanted inorganic material.

Yonge (1926) conducted experiments with the oyster, Ostrea edulis that demonstrated the uptake pathway for metals in solution, by feeding adult oysters with a suspension of iron saccharate in seawater. The iron saccharate is a soluble organic-metal complex and probably similar to the zinc-organic complexes in the aquatic environment. Iron was ingested by the epithelial cells of the digestive diverticula and accumulated in the cells as small particles, some of which had a structure similar to the zinc granules seen in this study.

Within the epithelium Yonge observed amoebocytes that had phagocytosed particles of iron. Four days after feeding there was no trace of iron within the epithelial cells, but beneath the epithelium there were many amoebocytes full of minute granules of iron. The iron-laden amoebocytes illustrated in Yonge's paper resemble zinc granulocytes, suggesting a similar origin.

Metals in particulate form are also phagocytosed by the epithelial cells of the digestive diverticula as shown by the experiments of Owen (1955). Ostrea edulis

was fed a suspension of titanium dioxide in filtered seawater. Particles of titanium dioxide, concentrated into spherules, were identified in the epithelial cells within three hours. In another experiment Cardium edule was fed a mixture of titanium dioxide and Aquadag (colloidal graphite) and formed similar spherules 3-5 μm in diameter. Six hours after feeding 'excretory' spheres, 12-18 μm in diameter, containing spherules of titanium dioxide and colloidal graphite, were present in the lumen of the digestive diverticula. They were formed by fragmentation of the epithelial cells and served to convey indigestible material out of the diverticula.

Direct evidence of zinc uptake in the oyster is afforded by experiments with ^{65}Zn, which is a neutron activation product found in the effluent from nuclear power stations and in fallout from the atmospheric testing of nuclear weapons. It has a half-life of 276 days and was detected in Crassostrea virginica from North Carolina (Wolfe, 1970a). He also showed that tissues with exposed surfaces (gills, mantle, labial palps and digestive diverticula) contain more zinc than do internal tissues.

The exposed epithelia may serve as uptake sites as suggested by the experiments of Romeril (1971), who examined the uptake and distribution of ^{65}Zn in the

Portuguese oyster *Crassostrea angulata* and *Ostrea edulis*. He showed that ^{65}Zn, added to unfiltered seawater as zinc chloride accumulated to the greatest extent in the mantle, gills and visceral mass. The biological half-life of zinc in the visceral mass was much longer (79.8 days) than that in the mantle (16.7 days) and gills (13.5 days), suggesting that zinc granulocytes reside longer in the peri-intestinal connective tissue and are lost slowly into the gut lumen.

The metabolic role of zinc has been examined by Wolfe (1970b) and Coombs (1972). Zinc is an integral component of many enzymes, some of which have been demonstrated in oyster tissue, but both workers found that zinc enzymes only account for a small portion (5%) of the total zinc in oysters. The remaining zinc is presumably sequestered in the zinc granulocytes. This dialysable zinc is exchangeable with the zinc required for enzyme activity and Coombs, 1974, has suggested that the excess zinc acts as a mobile reserve to ensure constant saturation of zinc-dependent enzymes operating under adverse environments.

The ecologial model, based on the experimental evidence above and the findings of this study, is presented in Fig. 3.

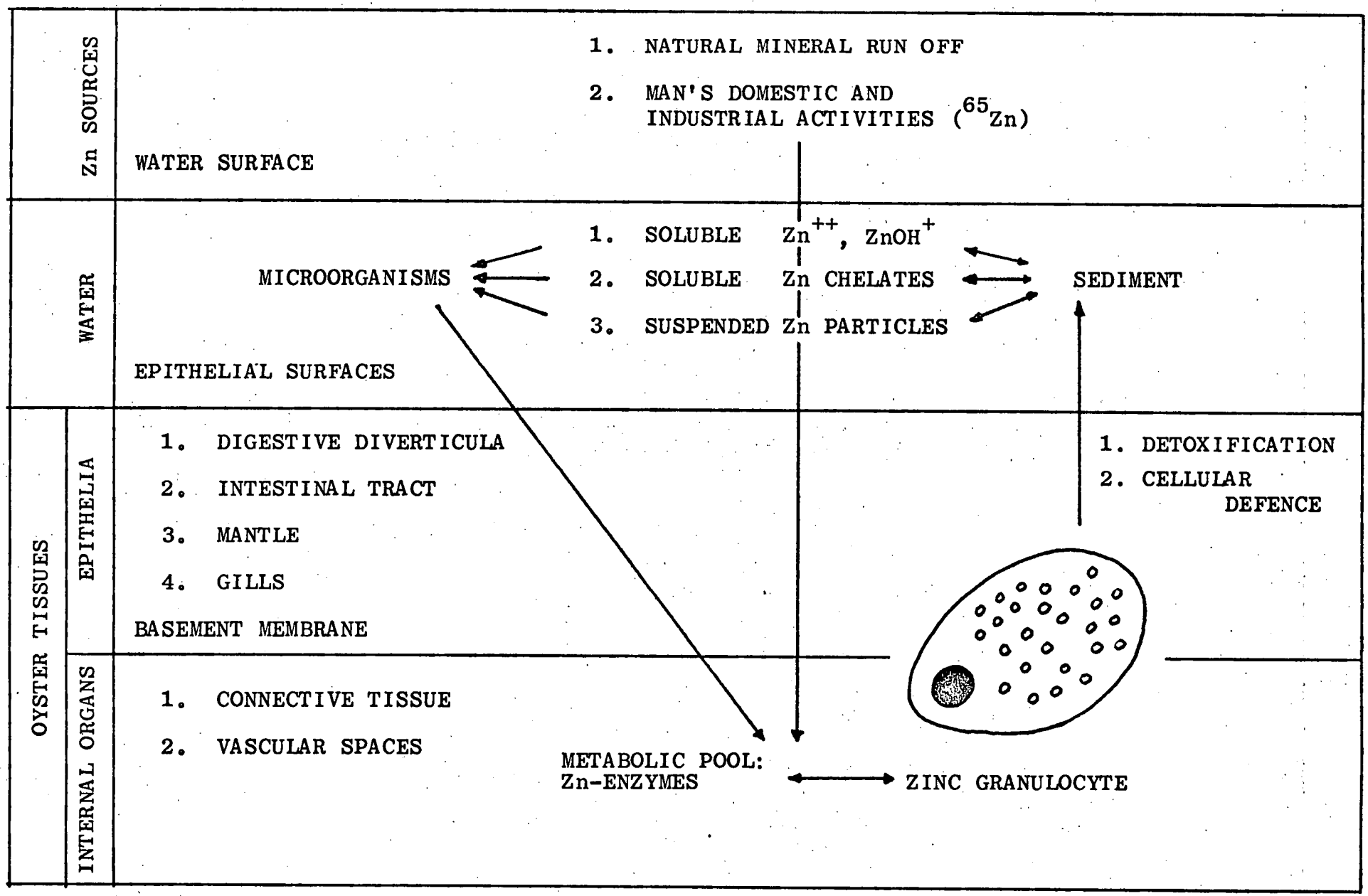

FIG. 3. HYPOTHETICAL MODEL OF ZINC ECOLOGY AND METABOLISM IN THE OYSTER

Microorganisms and zinc uptake in the oyster

There is indirect evidence that microorganisms in the estuarine environment play an important role in the transfer of zinc to the oyster (Fig. 3).

Phytoplankton are ingested by oysters (Yonge, 1926), but their nutritional function has been debated by Korringa, (1952) and Galstoff (1964). Other microorganisms, such as bacteria, may play an important part in oyster nutrition. Oysters maintained for several months on an exclusive diet of bacteria (Kincaid, quoted in Zobell & Feltham, 1937) developed normally and increased their glycogen content.

Other lamellibranchs can gain weight on a bacterial diet. Zobell & Feltham, (1937) fed the sea mussel Mytilus californianus a diet of Rhodococcus agilis, a motile Gram-positive coccus only 1 μm in diameter. The mussels were able to remove most of the bacterial suspension within two hours of feeding and over the ensuing 9 months gained weight (mean 12.4%).

Zinc can be taken up by aquatic microorganisms. Coliform bacilli, isolated from sewage effluent in the Derwent Estuary, accumulated zinc to a concentration of 107,000 μg g dry weight $^{-1}$ when grown on a medium containing 100 μg g Zn (Hughes, 1975). The zinc was diffusely distributed in the cell wall.

Phytoplankton also take up zinc (Parry & Hayward, 1973), which is firmly bound to living cells. The

uptake is dependent on temperature, pH and salinity, the latter causing considerable variation in concentrating ability ranging from 1 to 2.2 X 10^4 ^{65}Zn (Styron et al., 1976). The concentration factor for zinc is larger than that for other heavy metals as determined by culturing Ditylum brightwellii on media containing the elements Zn, Pb, Cu, and Cd. (Canterford et al., 1978). The uptake of zinc (150 μg g dry weight^{-1}) depended on the concentration of zinc in the medium.

Under experimental conditions, heavy metals can be taken up by the oyster via the food chain (Preston, 1971). He compared the direct uptake of metal from seawater with the indirect uptake via the food chain using ^{51}Cr. Crassostrea virginica was exposed to either a suspension of Chlamydomonas species, labelled with ^{51}Cr, or to $Na_2{}^{51}Cr\ O_4$ dissolved in sea water. The tissue distribution of the radionuclide was the same in both cases over the duration of the experiment (110 h), the accumulation being in the tissues with exposed epithelial surfaces, namely gills, mantle and visceral mass. The rate of accumulation by the direct uptake pathway was more rapid, but the important point is that both pathways were involved. The problem remains of extrapolating these results to the uptake of zinc in a natural setting.

Phytoplankton may play a role in the dissemination of zinc in the estuarine environment (Abdullah et al.,

1972). Although zooplankton tend to remain in specific zones within the Derwent Estuary (Taw & Ritz, 1978) phytoplankton may be less able to resist the continual exchange between oceanic, coastal and inshore waters.

The function of the zinc granulocyte

It would be important to determine the function of the zinc granulocyte in the oyster. Ruddell, (1971) has made the interesting suggestion that zinc granulocytes are analogous to basophils (mast cells) of vertebrate tissue. The mammalian basophil plays a role in the inflammatory response to injury by releasing heparin and histamine into the injured part; the heparin and histamine being bound together as a heparin-zinc-histamine complex (Kerp, 1963).

Zinc granules have been described in a number of marine Mollusca and Arthropoda (Coombs & George, 1977). For example intracellular zinc granules have been found in the parenchymal cells surrounding the mid-gut epithelium of the barnacle, Balanus balanoides (Walker et al., 1975a). The barnacle zinc granules were composed mainly of zinc phosphate, as determined by electron probe microanalysis (Walker et al., 1975b) and other elements such as iron and magnesium were minor constituents only. If the zinc granules were purely the result of a detoxification process then other trace

elements might be expected to be incorporated into the granules. It is noteworthy that both oyster and barnacle occupy very similar niches in the intertidal zone of the estuarine ecosystem and the possibility remains that the zinc granules are there for some specific physiological purpose.

REFERENCES

ABDULLAH, M.I., ROYLE, L.G. & MORRIS, A.W., 1972; Heavy metal concentration in coastal waters. Nature, 235, 158.

CANTERFORD, G.S., BUCHANAN, A.S. & DUCKER, S.C., 1978; Accumulation of heavy metals by the marine diatom Ditylum brightwellii (West) Grunow. Australian Journal of Marine & Freshwater Research, 29, 613.

COOMBS, T.L. & GEORGE, S.G., 1977; Mechanisms of immobilization and detoxification of metals in marine organisms. Proceedings of the 12 th European Symposium on Marine Biology, Stirling, Scotland, p.179.

GALTSOFF, P.S., 1964; The American oyster Crossostrea virginica Gmelin. Fishery Bulletin, v. 64, United States Government Printing Office, Washington, D.C.

HUGHES, J.P., 1975; Zinc and cadmium accumulation by sewage microorganisms. B.Sc. Thesis (Hons.), University of Tasmania.

KERP, VON L., 1963; Bedeutung von Zink für die Histaminspeicherung in Mastzellen, International Archives for Allergy and Applied Immunology, 22, 112.

KORRINGA, P., 1952; Recent advances in oyster biology. The Quarterly Review of Biology, 27, 266.

OWEN, G., 1955; Observations on the stomach and digestive diverticula of the lamellibranchia. Quarterly Journal of Microscopical Science, 96, 517.

PARRY, G.D.R. & HAYWARD, J., 1973; The uptake of ^{65}Zn by Dunaliella tertiolecta Butcher. Journal of the marine biological Association, United Kingdon, 53, 915.

PRESTON, E.M., 1971; The importance of ingestion in chromium-51 accumulation by Crassostrea virginica Gmelin. Journal of experimental marine Biology and Ecology, 6, 47.

ROMERIL, M.G., 1971; The uptake and distribution of ^{65}Zn in oysters. Marine Biology, 9, 347.

STYRON, C.E., HAGAN, T.M., CAMPBELL, D.R., HARVIN, J., WHITTENBURG, N.K., BAUGHMAN, G.A., BRANSFORD, M.E., SAUNDERS, W.H., WILLIAMS, D.C., WOODLE, C., DIXON, N.K. & McNEILL, C.R., 1976; Effects of temperature and salinity on growth and uptake of ^{65}Zn and ^{137}Cs for six marine algae. Journal of the marine biological Association, United Kingdom, 56, 13.

TAW, N. & RITZ, D.A., 1978; Zooplankton distribution in relation to the hydrology of the Derwent River estuary. Australian Journal of Marine & Freshwater Research, 29, 763.

WALKER, G., RAINBOW, P.S., FOSTER, P. & CRISP, D.J., 1975a; Barnacles: Possible indicators of zinc pollution? Marine Biology, 30, 57.

WALKER, G., RAINBOW, P.S., FOSTER P. & HOLLAND, D.L., 1975b; Zinc phosphate granules in tissue surrounding the midgut of the barnacle Balanus balanoides. Marine Biology, 33, 161.

WOLFE, D.A., 1970a; Levels of stable Zn and ^{65}Zn in Crassostrea virginica from North Carolina. Journal of the Fisheries Research Board, Canada, 27, 47.

YONGE, C.M., 1926; Structure and physiology of the organs of feeding and digestion in Ostrea edulis. Journal of the marine biological Association, United Kingdom, 14, 295

ZOBELL, C.E. & FELTHAM, C.B., 1938; Bacteria as food for certain marine invertebrates. Journal of Marine Research, 1, 312.